A Performance Based Approach for Seismic Design with Hysteretic Dampers

by

Sinan Keten

B.S. in Civil Engineering, Boğaziçi University (2005)
Istanbul, Turkey

Submitted to the Department of Civil and Environmental Engineering
in Partial Fulfillment of the Requirements for the Degree of
Master of Engineering in Civil and Environmental Engineering

at the

Massachusetts Institute of Technology

June 2006

Signature of Author.....
Department of Civil and Environmental Engineering
May 12, 2006

Certified by .....
Jerome J. Connor
Professor, Civil and Environmental Engineering
Thesis Supervisor

Accepted by .....
Andrew J. Whittle
Chairman, Departmental Committee for Graduate Students

A Performance Based Approach for Seismic Design with Hysteretic Dampers

by

Sinan Keten

Submitted to the Department of Civil and Environmental Engineering
on May 12, 2006 in partial fulfillment of the
requirements for the Degree of Master of Engineering in
Civil and Environmental Engineering

Abstract:

Current trends in structural engineering call for strict performance requirements from buildings prone to extreme earthquakes. Energy dissipation devices are known to be effective in reducing a building's response to earthquake induced vibrations. A promising strategy for controlling damage due to strong ground motion is the use of buckling restrained braces that dissipate energy by hysteretic behavior. Research conducted in the past reveals that devices such as The Unbonded Brace™ provide stiffness and damping to the structure, two key parameters that characterize a building's performance. The focus of this thesis is the development of a preliminary motion-based design methodology for the use of these devices in mitigating damage to structural and non-structural elements. In this regard, a shear beam idealization for a typical 10-story steel building is adopted and nonlinear dynamic response of the building for a set of earthquakes is simulated. Optimal ductility ratio and stiffness contribution of the bracing system is determined based on the inter-story drift values obtained from simulation results.

Thesis Supervisor: Jerome J. Connor

Title: Professor, Civil and Environmental Engineering

Acknowledgments

I would like to thank my advisor, Prof. Connor, for his help and guidance throughout the year. I am also grateful to Prof. Kausel for his encouragement and patience, as well as his contributions to the MATLAB routine used in this project. I consider myself lucky to have had the opportunity to study under their supervision.

Finally, I would like to thank my family for their love and their continuous support in my academic endeavors.

TABLE OF CONTENTS

List of Figures 6

List of Tables 8

Chapter 1 Introduction 9

Chapter 2 Performance Based Design Philosophy 13

2.1 Economic Significance of Damage Control in Buildings 13

2.2 Current Design Standards 16

Chapter 3 The Concept of Damping 22

3.1 Energy Dissipation in Structures 22

3.2 Passive Motion Control Devices 23

3.2.1 Viscous Dampers 24

3.2.2 Friction Dampers 25

3.2.3 Viscoelastic Dampers 27

3.2.4 Other Damping Mechanisms 28

Chapter 4 Hysteretic Damping 29

4.1 Introduction 29

4.2 Description of Hysteretic Dampers 30

4.3 Applications 34

Chapter 5 The Design Methodology 39

5.1 The Strategy 39

5.2 Motion Based Design Formulations 42

5.3 The MATLAB Algorithm 46

5.3.1 Procedure 46

5.3.2 Simulation of the Response 48

Chapter 6 Analysis Results 51

6.1 Description of the Study 51

6.2 Simulation Results 52

6.2.1 Stiffness Calibration 52

6.2.2 Yield Force and Stiffness Allocation Optimization 57

6.2.3 Alternative Solutions 62

Chapter 7 Concluding Remarks 64

References 66

Appendix A – Earthquake Records 68

Appendix B – Matlab Codes 70

Appendix C – Matlab Outputs 80

LIST OF FIGURES

Figure 1.1 Relationship between Dynamic Response Amplification and System Properties..... 10

Figure 2.1 Repair Cost versus Damage Intensity 14

Figure 2.2 Relationship Between Interstory Drift and Damage for Steel Buildings..... 16

Figure 3.1 Taylor Devices Viscous Damper 25

Figure 3.2 Pall Friction Damper 26

Figure 3.3 Stress Strain Relationship for Elastic, Viscous and Viscoelastic Materials..... 27

Figure 4.1 Hysteretic Behavior of an Elastoplastic Material 32

Figure 4.2 The Unbonded Brace – Configuration and Behavior 33

Figure 4.3 Hysteresis Loop for the Unbonded Brace Specimen 34

Figure 4.4 Timeline for US Implementation of Hysteretic Dampers..... 35

Figure 4.5 Unbonded Braces used for Kaiser Santa Clara Project 35

Figure 4.6 UC Davis Plant & Environmental Sciences Facility 36

Figure 4.7 Braces Used in the Rehabilitation of two Office Buildings in San Francisco 37

Figure 4.8 Braces Installed by Degenkolb Engineers – San Francisco 37

Figure 4.9 List of U.S. Buildings Utilizing the Unbonded Brace 38

Figure 5.1 Breakdown of the Structure into Primary and Secondary Systems 40

Figure 5.2 Stress-Strain Curves for Various Steels Available..... 41

Figure 5.3 Cantilever Beam Model..... 43

Figure 5.4 Discrete Shear Beam Model..... 44

Figure 5.5 Schematic Representation of a 3 Degree of Freedom (DOF) System 44

Figure 5.6 Flowchart for the Dynamic Analysis of Damage Controlled Structures 46

Figure 6.1 Stiffness Calibration Results for BSE-1 Earthquake 54

Figure 6.2 Convergence Plot for Stiffness Calibration based on BSE-1 54

Figure 6.3 Displacement Profiles at Peak Response 55

Figure 6.4 Response of the Calibrated System to Imperial Valley (BSE-1) Earthquake 56

Figure 6.5 Response of the Calibrated System to Loma Prieta (BSE-1) Earthquake 56

Figure 6.6 Response of the Calibrated System to Northridge (BSE-1) Earthquake 57

Figure 6.7 Response Time History of the Selected System 61

LIST OF TABLES

Table 2.1 Associating Damage and Performance for Conventional Braces Steel Frames 20

Table 6.1 Scaled Peak Ground Accelerations for the Earthquakes 51

Table 6.2 Earthquake Records Used for the Analysis 53

Table 6.3 Spatial Distributions of Characteristics for the Selected System 61

Chapter 1

INTRODUCTION

The early professionals dealing with structures used a combination of mathematical tools and rules of thumb derived from experience to make sure that their masterpieces would have minimal chance of failure within its lifetime. Compared with his predecessors, the contemporary engineer is well-armed against the uncertainties that concern his work, such as those pertaining to material properties, structural behavior, and the nature of the loads.

The modern era of engineering is influenced greatly by the rapid development of computational power, which facilitates a better fundamental understanding of building materials and structural systems. In this regard, the development of computer aided design tools brought about a paradigm shift in the practice. Until recently, design loads and the associated analyses did not take into account the time-variant nature of the loads and the dynamic nature of the structural response. Traditional strength based design procedures involve the calculation of forces in structural members based on a static analysis, with time-invariant, equivalent loads. Finding the most economic member sections that can accommodate these loads without exceeding specified stress limits is the key objective in this design scheme. It is a well established fact, however, that strength alone may not be the governing criteria to evaluate a building's performance. In this regard, current trends in structural engineering call for strict strength, serviceability and human comfort requirements from buildings prone to strong winds and ground motion.

These forces are as such time-dependant, and so is the response of a building due to these excitations. The recently developed codes such as the FEMA *Guidelines* [1] take these time dependant effects into consideration, which have been incorporated into a design scheme called performance based design, or equivalently motion based design originally proposed by Jerome J. Connor[1]. Hence, the design methodology presented in this thesis employs the motion based design philosophy, which will be further explained in the following section. Before proceeding to the methodology, however, it is considered somewhat useful by the author to dwell on the concept of dynamic response; as it provides the basis for the methodology adopted.

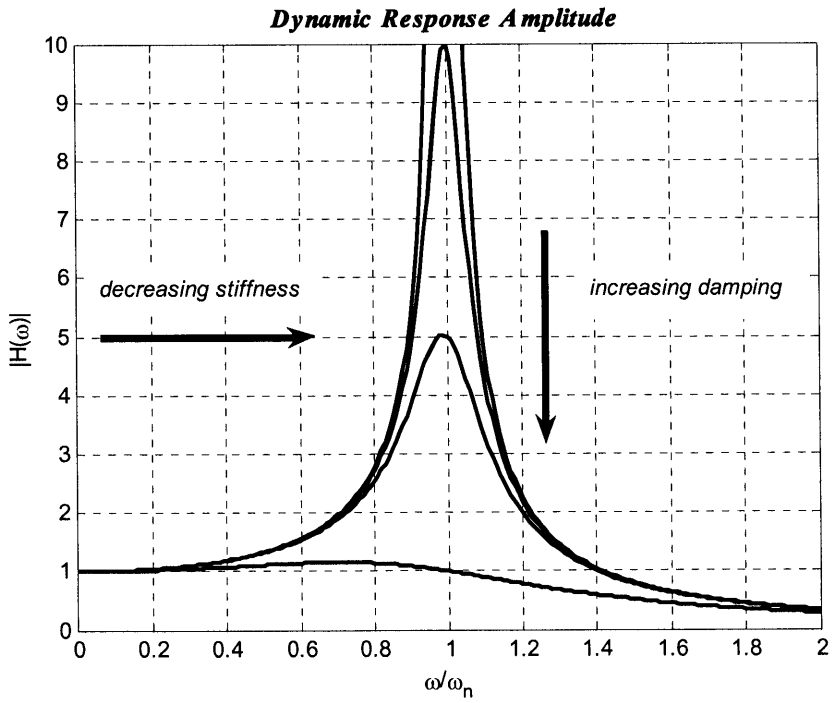

Figure 1.1 Relationship between Dynamic Response Amplification and System Properties

[1] Professor, Dept. of Civil and Environmental Engineering, Massachusetts Institute of Technology

Structural response is characterized by three key parameters; mass, stiffness and damping. Mass distribution in a building influences the behavior of the building, but is rarely a design parameter. For design purposes, stiffness is often the primary "tuning" variable available to the engineer. For earthquake and wind loads, the lateral stiffness of a building provided by the rigidity of its structural members is of utmost importance. For steel structures, lateral resistance to wind and earthquake loads is generally achieved either by moment resisting connections between beams and columns or by a braced frame. The energy transferred to the structure by the loads is either dissipated through various mechanisms or stored in the members as strain energy, which is observed as deformation, or displacement. The measure of energy dissipation capacity of a system is called damping. Damping in a structural system happens due to internal friction, inelastic deformation, material viscosity or interaction with the environment as in the precedence of a drag force. A more in depth discussion of damping mechanisms will be provided in Chapter 3. Figure 1.1 illustrates the effects of stiffness and damping on the dynamic response amplification of a typical system.

Over the years, numerous damping enhancement mechanisms have been proposed to be used in buildings subject to dynamic excitations, such as earthquakes. Hysteretic damping is one such mechanism. Several devices, such as the Unbonded Brace™ developed by Nippon Steel have been used in buildings as hysteretic dampers for their stiffness contribution and energy dissipation capacity. These braces provide damping to a structure by yielding and going through cyclic inelastic deformation. Primarily used in Japan, these devices have been considered as a promising technology for seismic damage

mitigation. However, although research on such devices has been well-received in academia, there has been a lag in the development of a robust design methodology for the widespread application of these devices in the practice. In this regard, the scope of this thesis is to aid the development of preliminary seismic design guidelines for the use of hysteretic dampers in steel structures.

For this purpose, a motion based design methodology with hysteretic dampers is proposed for mitigating damage in structural and non-structural elements in a building. This research is focused primarily on mid-rise buildings situated in regions with high seismic risk. In this procedure, a shear beam idealization for a typical 10-story steel building is adopted and non-linear dynamic response of the building for a set of earthquakes is simulated using a MATLAB algorithm. Optimal yielding ratio and stiffness contribution of the bracing system is determined based on the inter-story drift and ductility demand values obtained from simulation results.

Chapter 2

PERFORMANCE BASED DESIGN PHILOSOPHY

2.1 Economic Significance of Damage Control in Buildings

Structural behavior due to an earthquake can be complex and unpredictable. When a building is experiences a severe earthquake, the flexibility of the building and the presence of redundant structural members would be very important for the safety of the structure and its contents. Until recently, however, building codes included only strength considerations. This design philosophy, which considers only elastic behavior of the building and assumes limited inelastic deformation in an extreme event, may be adequate for life safety concerns. Indeed, both 1994 Northridge and 1989 Loma Prieta Earthquakes caused minimal loss of life, which validates this point. On the other hand, the economic impact of these two earthquakes was tremendous, with at least $20 billion of damage just resulting from Northridge Earthquake [2]. In response to these findings, numerous studies have stated the need to control damage in buildings for economic considerations. This has lead to a new perception of cost, a key design variable.

From a project management perspective, the initial development and maintenance cost of a facility roughly makes up the total cost of the project. From a structural perspective, the initial cost includes material, workmanship, erection and equipment costs. Maintenance on the other hand is primarily related to the damage and deterioration of structural elements. In most projects, cost estimation for maintenance is not taken into

consideration. It is also ambiguous, in most cases, who should bear the costs in case of partial or total failure of the building. Consequently, adding in a premium cost for controlling damage may become difficult to justify both from the designers and owners perspective, mainly because the benefits attained by the premium may be difficult to validate accurately by the stakeholders. However, it has been shown that controlling the damage of a building due to seismic hazard is an effective way to reduce the total lifetime cost of the building and its impact in the local economy.

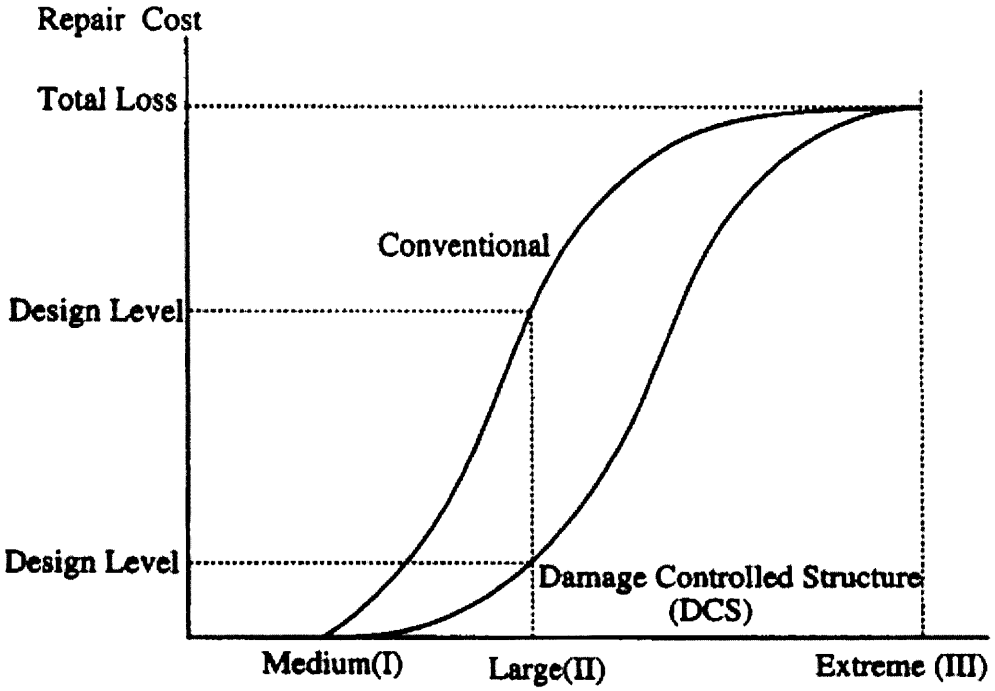

Figure 2.1 Repair Cost versus Damage Intensity [3]

This idea of damage controlled structures dates back to early 90's and was introduced by Connor et al [3]. Figure 2.1 illustrates the benefits associated with this concept. In light of this research, as well as others, the new building rehabilitation and design codes such as the *Guidelines* are based on the life-cycle performance assessment of a building. These

new codes call for stricter performance requirements that are based on motion control of a building to mitigate damage due to earthquakes. These recent trends have accelerated the use of performance based design methods not only on the West Coast and Japan but around the globe.

Quantifying damage in structures is a difficult task, since it depends on various factors that have both structural and non-structural components. Many damage indices that quantify damage based on peak floor acceleration or velocity, spectrum intensity, soil properties, ductility ratio, increase in period, or degradation of stiffness have been proposed. Reference [4] discusses the state of the art of damage indices and proposes a new index based on ductility demand compared to ultimate ductility of the building at collapse. For the purposes of this thesis, damage is assumed to be directly related to inter-story drift. Figure 2.2 shows a representative damage and inter-story drift relationship for steel structures:

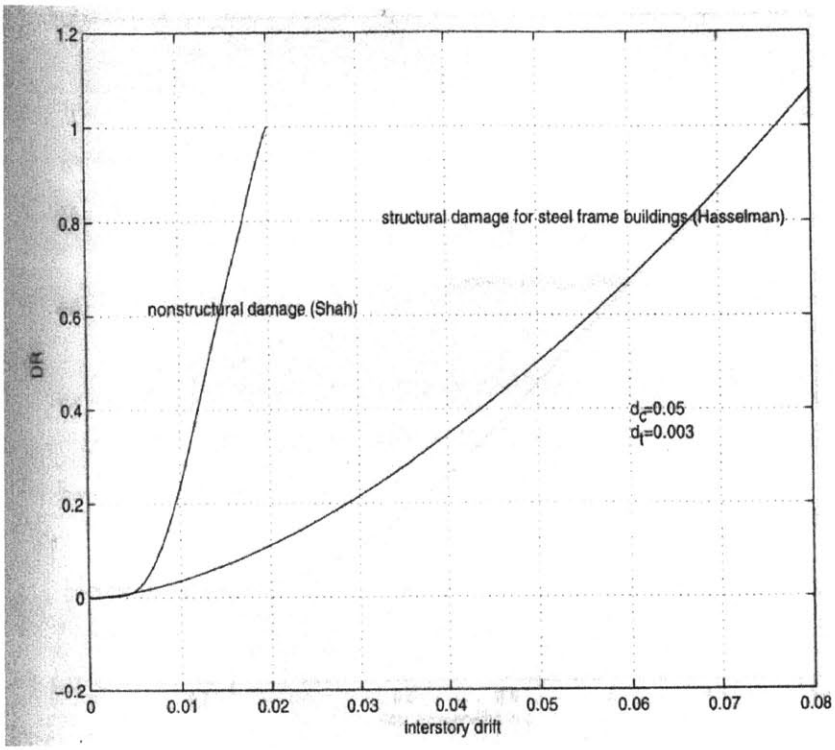

Figure 2.2 Relationship Between Interstory Drift and Damage for Steel Buildings [2]

2.2 Current Design Standards

As mentioned in the previous section, the FEMA *Guidelines*, established in 1997 was the first of a series of documents which serve the purpose of providing the basic guidelines for seismic rehabilitation of buildings. The intended audience is a technical community of design professionals, which include engineers, architects and building officials. FEMA - 273, the original document, has been the basis for the more recent pre-standards and standards for both new buildings and rehabilitation of existing structures, which includes the latest pre-standard FEMA 450, NEHRP Recommended Provisions For Seismic Regulations For New Buildings And Other Structures, 2003.

Although the *Guidelines* have been developed originally for the rehabilitation of existing buildings, a lot of the ideas derived from this work have been incorporated into the design of new buildings. One of the key concepts introduced was that of structural performance levels, defined as the expected behavior of the building in the design earthquakes in terms of limiting levels of damage to the structural and non-structural components. These performance levels are used to evaluate whether the desired rehabilitation objectives are achieved. A Rehabilitation Objective relates a specified hazard, or earthquake intensity level to a corresponding damage condition, or performance level. The *Guidelines* present a Basic Safety Objective (BSO), which has performance and hazard levels consistent with seismic risk traditionally considered acceptable in the United States. Alternative objectives that provide lower levels or higher levels of performance are also defined in the *Guidelines* as Limited Objectives or Enhanced Objectives respectively. A short description of the seismic performance levels and rehabilitation objectives is shown in Figure 2.3.

For hazard levels, the Guidelines take into account 4 different seismic excitation levels. Two of these earthquake hazard levels are especially useful for evaluating the performance of the building in moderate and extreme events. These are represented by BSE-1 and BSE-2 earthquakes respectively. The BSE-1 and BSE-2 earthquakes are typically taken as 10%/50 and 2%/50 year events as shown in Figure 2.3. On the other hand, levels of performance have been considered both separately from structural and non-structural perspectives and have also been incorporated into combined criteria that are named as Building Performance Levels.

Another vital point addressed in the *Guidelines* is the differentiation of structural components as being primary and secondary. The primary system provides the main load bearing capacity of the structure. Failure of this system must be avoided at all times, since failure of the primary system results in collapse. The secondary system consists of all other members that contribute to the lateral stiffness but are not essential in terms of life safety and collapse prevention. In summary, the concept of primary and secondary elements allows the structural engineer to differentiate between the performance required of elements that are critical to the building's ability to resist collapse and of those that are not. The proposed design methodology that will be presented in Chapter 5 builds upon this concept to bring about a new strategy for design with hysteretic dampers.

		Building Performance Levels			
		Operational Performance Level (1-A)	Immediate Occupancy Performance Level (1-B)	Life Safety Performance Level (3-C)	Collapse Prevention Performance Level (5-E)
Earthquake Hazard Level	50%/50 year	a	b	c	d
	20%/50 year	e	f	g	h
	BSE-1 (~10%/50 year)	i	j	k	l
	BSE-2 (~2%/50 year)	m	n	o	p

k – p = BSO
k – p + any of a, e, i, m, or b, f, j, or n = Enhanced Objectives
o = Enhanced Objective
k alone or p alone = Limited Objectives
c, g, d, h = Limited Objectives

Figure 2.3 Rehabilitation Objectives [1]

Based on the above definitions of seismic hazard and corresponding performance levels, we can now establish the design criteria for the purposes of this thesis. According to the *Guidelines*, a building has to sustain Life Safety Performance Level for a moderate earthquake and Collapse Prevention Level under an extreme event to achieve the Basic Safety Objective. As mentioned before, the moderate and extreme events are represented by BSE-1 and BSE-2 earthquakes respectively. Considering the results illustrated by Wada and Connor's work on damage controlled structures, a more conservative approach

that yields lower damage levels is taken as the design objective for this thesis. As a result, the proposed scheme aims for Immediate Occupancy Level for BSE-1 and satisfies Collapse Prevention Level for BSE-2. As defined previously, this objective may be considered an Enhanced Rehabilitation Objective.

As shown in Table 2.1, a typical building designed for this objective would have 0.5% transient and negligible permanent drift for BSE-1 and would have 2% transient or permanent drift for BSE-2. Although these values are not proposed as displacement goals for design, it is a sound methodology to employ these values in a motion based design scheme to achieve the target design objectives.

Structural Performance Levels and Damage for Conventional Braced Steel Frames			
	Collapse Prevention (S-5)	**Life Safety (S-3)**	**Immediate Occupancy (S-1)**
Primary	Extensive yielding and buckling of braces. Many braces and their connections may fail.	Many braces yield or buckle but do not totally fail. Many connections may fail.	Minor yielding or buckling of braces
Secondary	Same as primary.	Same as primary.	Same as primary.
Drift	2% transient or permanent.	1.5% transient, 0.5 % permanent.	0.5% transient, negligible permanent.

Table 2.1 Associating Damage and Performance for Conventional Braces Steel Frames [1]

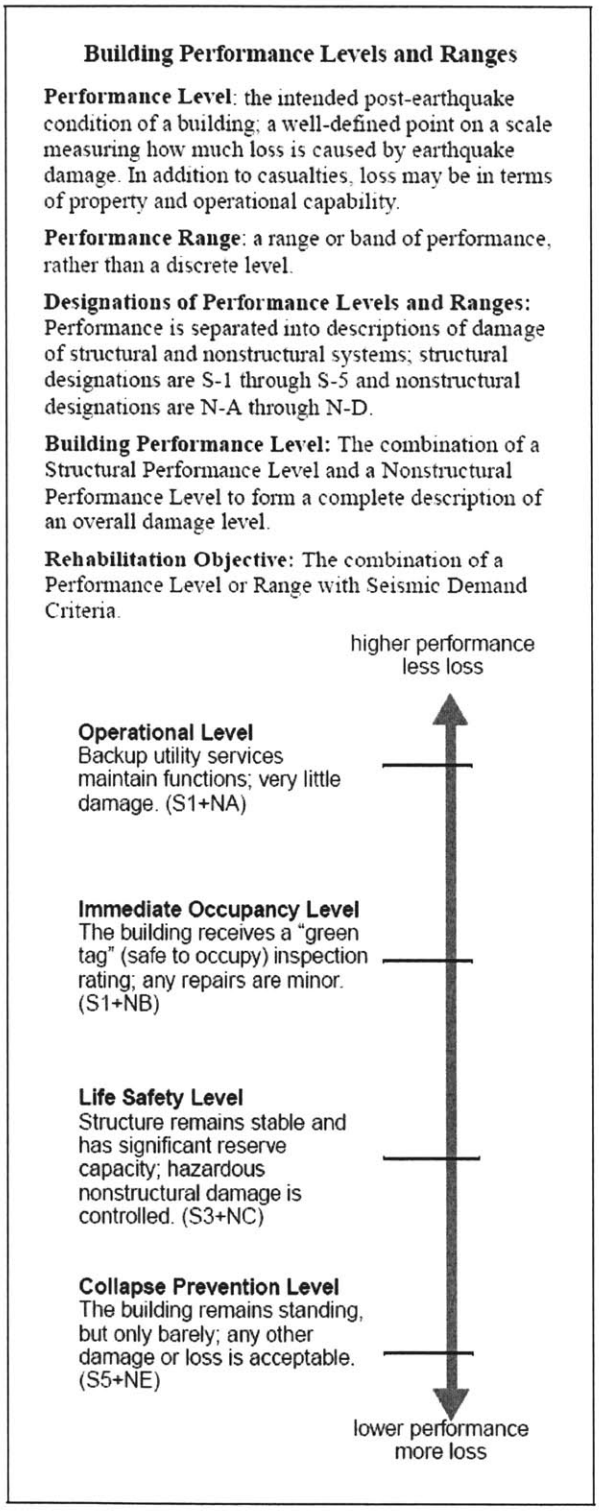

Figure 2.4 Building Performance Levels [1]

Chapter 3

THE CONCEPT OF DAMPING

3.1 Energy Dissipation in Structures

All buildings vibrate when they are subjected to lateral loads such as wind and earthquakes. Such excitations can be thought of as an energy input to the structural system considered. When a building deforms elastically, it stores some of this energy input as strain energy and begins to oscillate around its equilibrium point. What keeps a building from oscillating forever is its internal damping, or equivalently its energy dissipation capacity. Damping not only kills off sustained oscillation of the building but it also affects the amplitude of the oscillations throughout the time history of the building's response. Since damage to structures is primarily determined by displacements, specifically inter-story drifts, one can easily conclude that by increasing damping in a structure, energy stored as strain in members can be reduced, and hence total structural and non-structural damage can be mitigated. Several sources of energy dissipation in a structure have been mentioned in [5]:

- Dissipation due to material viscosity, as in viscoelastic dampers
- Dissipation and absorption caused by cyclic inelastic deformation or hysteresis
- Energy dissipation resulting from interaction with the environment, as in drag forces
- Dissipation due to external devices with dissipation/absorption capacity, such as inertial dampers like tuned mass dampers or active control systems.

The beneficial aspects of energy dissipation have been well-addressed in the literature. For this reason, efforts have been made both from the academia and also from the industry to develop devices that can enhance the energy dissipation capacity of buildings. A market for passive dissipation systems has emerged in this sense, and has contributed to the fruitful efforts for mitigating damage due to earthquakes. The next section will briefly describe some of the novel technologies proven effective in the market for structural motion control and damage mitigation.

3.2 Passive Motion Control Devices

Passive control differs from active control in the sense that it doesn't impart any external energy into the building. All the forces generated by these devices derive from the motion of the building rather than an actuator or a mechanical system driven by external energy. Although one can easily say that active control provides more power and flexibility as a dissipative system for vibration reduction, passive control is considered to be more practical and advantageous for several reasons. The first reason is the well-addressed issue of cost. An active system, when employed for a building, significantly increases the initial costs of the project; a key consideration for developers and designers alike. From a reliability perspective, the external energy dependence of these systems becomes a key limiting aspect of their applicability. Furthermore, controlling and predicting the behavior of active control devices still poses some important questions. An important thing to note here is that since these devices input energy into the system, special attention must be paid to make sure that the stability of the system is ensured at all times. Considering that instability may lead to irreparable damage and collapse of the building, using passive and

hence inherently stable devices with lower cost is favorable from a design perspective. The trend in the market has been observed to follow this. Consequently, the goal of this section is to provide some insight into the reader on how different passive damping devices work and their comparative advantages and disadvantages.

3.2.1 Viscous Dampers

Viscous damping refers to all types of damping mechanisms which create a dissipative force that is a function of velocity, or time rate of change of displacement. Assuming a linear relationship between force and velocity, the damping force of a viscous damper can be formulated as:

$$F_d = c\dot{u} \tag{3.1}$$

The energy dissipated by a viscous damper subjected to periodic motion can be given as:

$$W_{viscous} = c\pi\Omega\hat{u}^2 \tag{3.2}$$

where Ω is the frequency of the sinusoidal wave and $\hat{u}$ is its magnitude.

The concept of viscous damping is very important in the dynamic analysis of structures, since it provides a mathematically simple, linear way of including energy dissipation in the equations of motion. For this reason, formulations to relate other, nonlinear types of damping into an equivalent viscous damping coefficient, c, have been proposed. Such an

idealization usually works well for periodic excitations, but may be more subjective in case of random excitations such as earthquakes. In dynamic analysis, this coefficient c is converted into a modal damping ratio of ξ, which ranges from 0.01 up to 0.2 for typical civil structures. A higher damping ratio indicates greater energy dissipation capacity and less need to store energy input as strain in structural members. Another aspect of viscous damping that derives from dynamic analysis is the fact that the dissipative forces generated by these devices are 90° out of phase with the displacements in the building.

Viscous dampers such as the one shown in Figure 3.1 have gained global acceptance in the market for passive energy dissipation systems for buildings. In US, Taylor Devices [6] has been the dominant manufacturer for such systems. In Europe, companies like GERB [7] and FIP Industriele [8] have been providing viscous dampers solutions for both seismic protection and other vibration isolation applications.

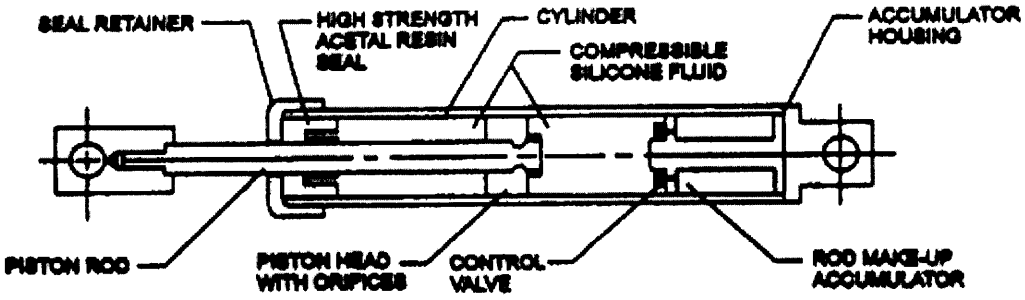

Figure 3.1 Taylor Devices Viscous Damper [9]

3.2.2 Friction Dampers

Friction is a dissipation mechanism that derives from the contact forces between adjacent surfaces. They have been used as the primary system for breaks in the automotive industry. Two types of friction have to be defined in terms of structural design

considerations, one is coulomb friction, or dry friction, and the other is structural damping. Coulomb friction in motion generates a constant magnitude force whose direction depends on the motion of the system, such that:

$$F = \overline{F}\,\mathrm{sgn}(\dot{u}) \tag{3.3}$$

On the other hand, structural damping has a magnitude that is allowed to change with the magnitude of displacement. Friction dampers such as the one shown Figure 3.2 utilize sliding surfaces that dissipate energy as heat. These surfaces are usually designed such that they only slip under a severe earthquake before the primary structure yields.

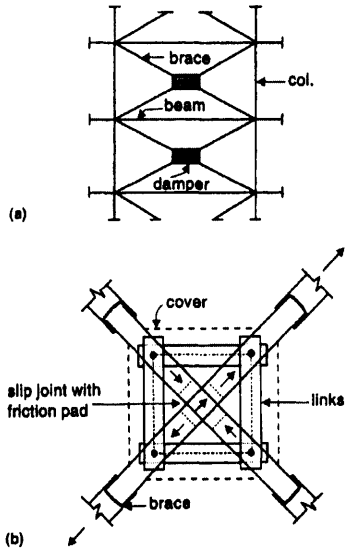

Figure 3.2 Pall Friction Damper [9]

3.2.3 Viscoelastic Dampers

Viscoelastic dampers are devices that behave in a manner that has both viscous damping and elastic spring characteristics. The elastic component has a linear relationship with deformation, whereas the viscous force has a phase difference as mentioned in the relevant section. The corresponding stress strain relationship is shown in Figure 3.3.

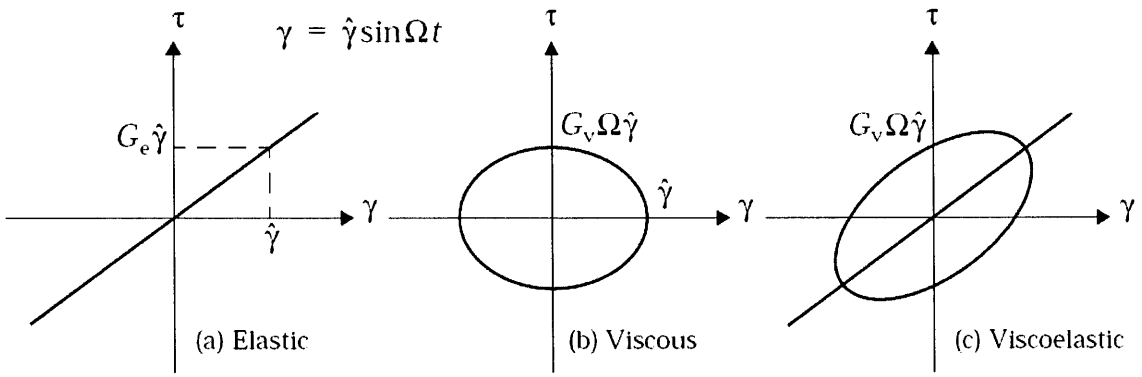

Figure 3.3 Stress Strain Relationship for Elastic, Viscous and Viscoelastic Materials [5]

The use of viscoelastic materials has been common in the aerospace industry for nearly half a century. The first civil engineering application has been in the twin towers of the World Trade Center, New York in 1969, when roughly 10,000 viscoelastic dampers were installed in each tower to reduce wind induced vibrations. In general, viscoelastic materials such as copolymers and glassy substances have been found to be somewhat effective against seismic vibrations as well. This, along with the linear behavior of these materials over a wide range of strain, has made viscoelastic dampers a useful tool for structural engineers. However, the material properties of these devices have been found to be dependant on temperature and excitation frequency, which complicates the design of passive damping systems that employ these devices.

3.2.4 Other Damping Mechanisms

The primary purpose of this chapter was to introduce different damping devices that can be used as or in combination with primary load bearing system of a building to enhance its energy dissipation capacity. A brief discussion of these different technologies is adequate within the scope of this thesis. Presenting this material is essential since these passive devices provide alternatives for hysteretic damping, the subject matter of this work. The concept of hysteresis and hysteretic damping requires a more in depth discussion within the scope of this thesis; hence they will be treated individually in Chapter 4.

There are a myriad of other devices and methodologies employed in buildings to mitigate damage due to seismic or wind excitation. These devices include base isolation systems that allow a building to move as nearly a rigid body when a very flexible isolation system reduces earthquake loads imparted on the structure. Another scheme frequently employed for reducing wind induced vibration is that of Tuned Mass Dampers, originally proposed by Den Hartog. TMD's utilize the inertia of an additional mass that moves out of phase with the building to limit the vibrations of a structure. More advanced motion control devices include active mass dampers or hybrid systems that employ both active and passive components. The references [5], [9] provide a more in depth description of damping devices.

Chapter 4

HYSTERETIC DAMPING

4.1 Introduction

As mentioned previously, traditional strength based design is usually based on the assumption that a structure behaves linearly under moderate excitations. In the case of an extreme event, it is assumed that the inelastic deformation of the structural members come into play to deal with the intense energy input to the building. Most conventional structures are designed with the strong-column-weak-beam approach, which utilizes plastic deformation at the beam-ends to dissipate energy input from the ground motion. In this regard, structural members are designed to have some inelastic deformation capacity, which contributes to the ductility of the building. A ductile system is more favorable than a brittle one, since brittle failure happens suddenly; that is without any warning or extensive deformation. In the case of a severe earthquake, the yielding of primary load bearing members in a ductile structure allows for energy dissipation. On the other hand, this behavior also causes permanent deformation and extensive structural and non-structural damage.

The idea of primary and secondary structures, introduced by Wada and Connor's work, and also mentioned in the *Guidelines*, is an important concept for understanding how hysteretic dampers work. Having stated the significance of ductile design, we mentioned that yielding of a primary lateral load bearing system is acceptable from a collapse

prevention perspective, but not optimal economically. On the other hand, if the building was supplemented with a secondary lateral resistance system that would be capable of undergoing inelastic deformation before the yielding of the primary system, then the design would be both economical and safe. In other words, under an extreme event, lateral stiffness of the system would not be altogether lost, and energy would still be dissipated by the inelastic action of the secondary system. Hence, a secondary structure consisting of braces that provide both lateral stiffness and inelastic deformation capability could be a very useful tool for seismic damage mitigation. As it will be explained in the following section, hysteretic dampers have been proven to be reliable devices that have both of these desirable characteristics.

4.2 Description of Hysteretic Dampers

As mentioned before, most steel buildings are designed with either a moment resisting frame or a brace system to carry lateral loads. Performance issues related to moment resisting frames have been well-addressed by the academia after the 1994 Northridge Earthquake. On the other hand, using braced frames is not by itself a perfect solution either. Conventional braces are usually susceptible to buckling and have a lower capacity in compression than in tension. Buckling causes a significant loss of stiffness. Furthermore, when these braces yield under cyclic loading, their capacity can be degraded rapidly. In this regard, an ideal brace would have a predictable, preferably elasto-plastic stress strain relationship like the one shown in Figure 4.1. The force-displacement curve shown is an example for a hysteresis loop. The energy dissipation capacity of an ideal brace exhibiting this type of hysteretic behavior can be given as:

$$W_{hysteretic} = 4F_y \bar{u}\left[\frac{\mu - 1}{\mu}\right] \tag{4.1}$$

where F_y stands for the yield force of the member, μ is the ductility ratio defined as the ratio of the maximum displacement to the yield displacement, and $\bar{u}$ is the maximum displacement observed. As described in [5], energy dissipation of an ideal hysteretic damper can be equated to that of a viscous damper to get an equivalent viscous damping coefficient given as:

$$c_{eq} = \frac{4F_y}{\pi \Omega \hat{u}}\left[\frac{\mu - 1}{\mu}\right] \tag{4.2}$$

Although this equivalent damping coefficient is useful for analysis of systems subjected to periodic excitation, it is not directly applicable for random excitations, such as earthquakes. This is mainly because the yielding of the element would not take place at every cycle and the force-displacement curve in reality would be more irregular, having different loops and elastic reloading and unloading cycles. For random excitations and non-ideal braces, the energy dissipated is equal to the area enclosed within the hysteresis loop.

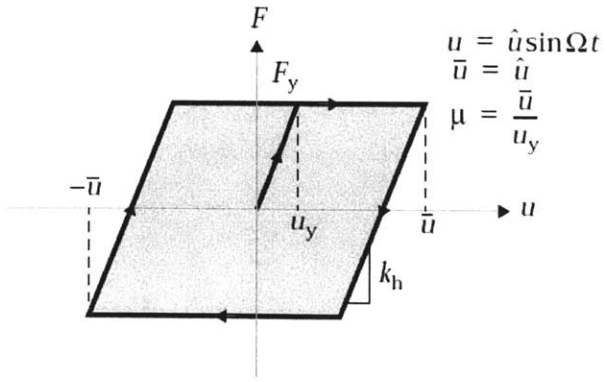

Figure 4.1 Hysteretic Behavior of an Elastoplastic Material [5]

The research effort invested in engineering high performing braces has lead to the development of the unbonded brace scheme, or equivalently buckling restrained braces. These devices consist of a highly ductile low-strength steel core encased in a concrete filled steel tube. The core and the concrete encasing are separated by an unbonding material which allows the yielding core to deform independently from the outer component. The sections and materials of the composite system are selected such that the buckling load of the brace equals the yield force of the core. Hence, consistent and similar loading and unloading curves for compression and tension of the member can be achieved. According to experimental results [10], the braces may have even more capacity in compression than in tension (up to 10% according to some studies). The ductility capacity of the braces are remarkable; some tests show results that exceed 300 times the initial yield deformation of the brace before failure.

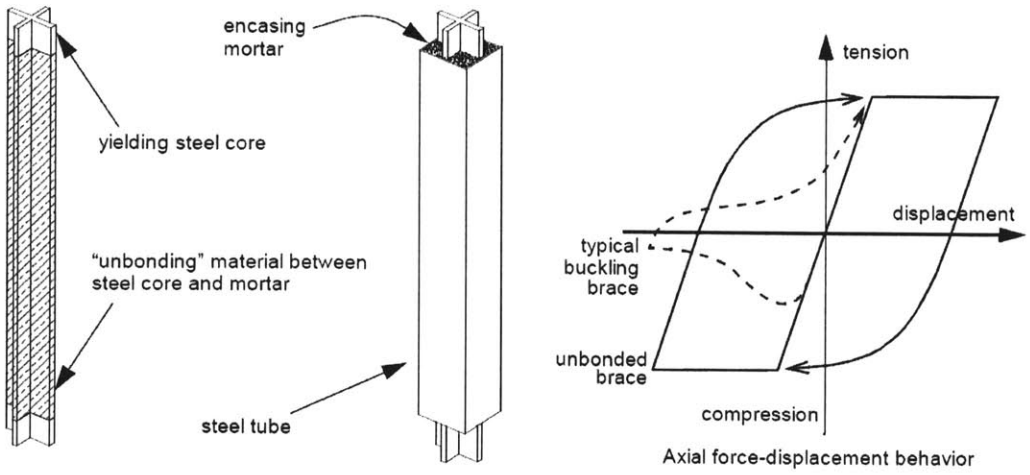

Figure 4.2 The Unbonded Brace – Configuration and Behavior [13]

Most of the buildings that feature hysteretic dampers employ braces manufactured in Japan. Working closely with Prof. Wada's team at Tokyo Institute of Technology, Nippon Steel Corporation [11] has been successful in developing the Unbonded Brace™, which has gained wide acceptance in Japan as a device for passive energy dissipation. Kazak Composites Incorporated (KCI) of Woburn, MA, has also developed a similar product in collaboration with the Department of Civil and Environmental Engineering at MIT. The design approach adopted by KCI was to develop light-weight, low yield force braces for application in civil engineering structures. References [10], [12], [13] provide more information on the development, testing and characteristics of both KCI and Nippon Steel Braces.

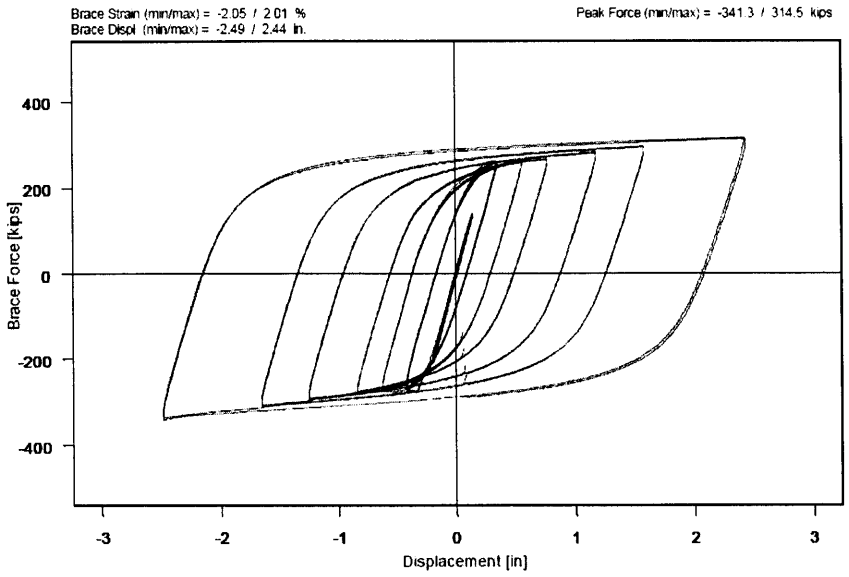

Figure 4.3 Hysteresis Loop for the Unbonded Brace Specimen [13]

4.3 Applications

The idea of hysteretic dampers was originally proposed in 1970'ies. [14]. The first prototypes for yielding metallic dampers were built in early 80'ies and implementation in Japan began soon after the 1995 Kobe Earthquake. The Unbonded Brace^{TM} has been used in nearly 200 buildings in Japan since 1997. According to the Building Center of Japan, for the year 1997, roughly two-thirds of all tall buildings (greater than 60 meters) approved for design that year incorporate some form of passive damping system, and most of these use hysteretic dampers [13]. Implementation of this technology in US happened at a much slower rate. A timeline for initial invention of the technology and its adoption in US has been provided in Figure 4.4.

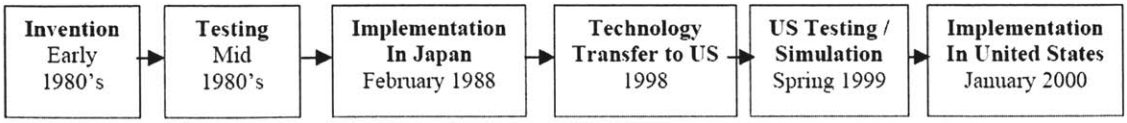

Figure 4.4 Timeline for US Implementation of Hysteretic Dampers [15]

The first building in US that employed hysteretic dampers was the Plant & Environmental Sciences Building of University of California, Davis. It is reported that the easy installation of the dampers in this project lead to a one month reduction in the total steel erection time. Figure 4.5 and Figure 4.6 show the installed braces in the UC Davis and Kaiser Santa Clara Medical Center Projects, both designed by Ove Arup & Partners, California [15].

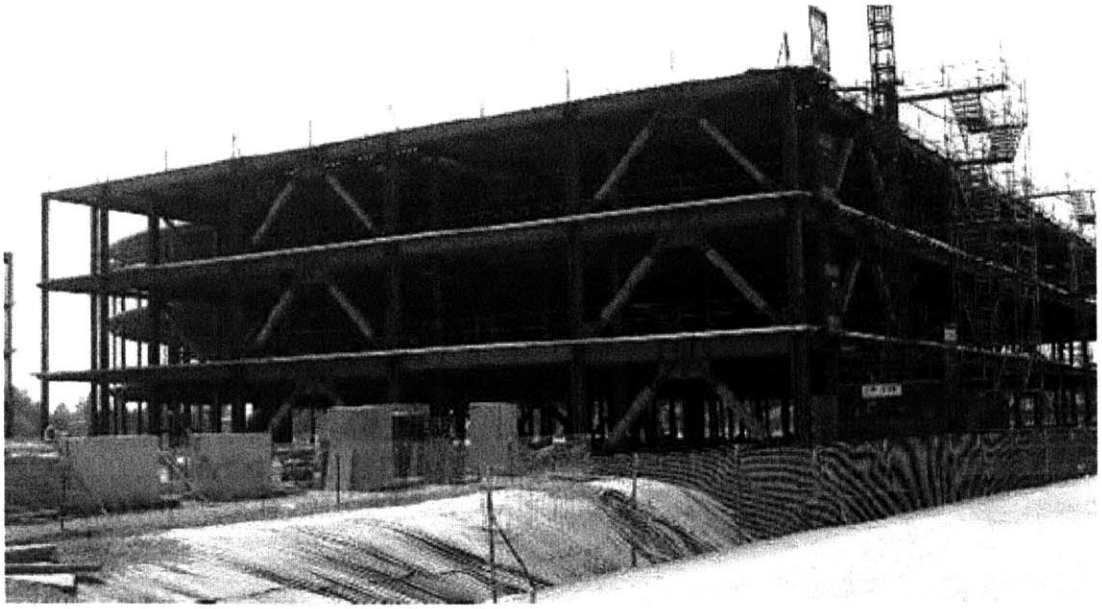

Figure 4.5 Unbonded Braces used for Kaiser Santa Clara Project [15]

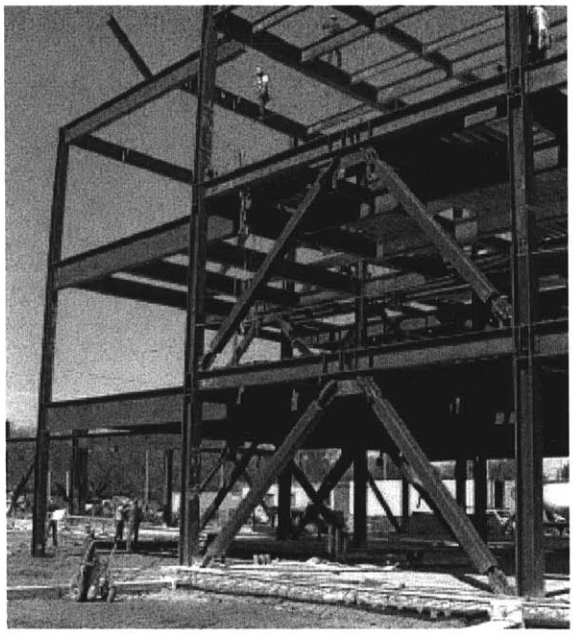

Figure 4.6 UC Davis Plant & Environmental Sciences Facility [15]

Another interesting US application was the retrofitting of two office buildings in the San Francisco Bay Area in accordance with FEMA-356, which is a newer edition of the *Guidelines*. An external splayed brace design that employed buckling restrained braces were used to attain the owner's established rehabilitation objective, which corresponded to a level set halfway between Collapse Prevention and Life-Safety Performance Levels for the BSE-1 Earthquake. System designed by the San Francisco office Degenkolb Engineers [16] reduced earthquake risk on other system components such as connections, collectors as well as gravity columns. Before rehabilitation, most of these components had deficiencies and the building wasn't in compliance with the performance levels. The cost effective nature of the technology was also mentioned in the study [17]. The details of the bracing system used in this project are shown in Figure 4.7. As a summary, Figure 4.9 shows some of the buildings in US that have incorporated the Unbonded Brace™.

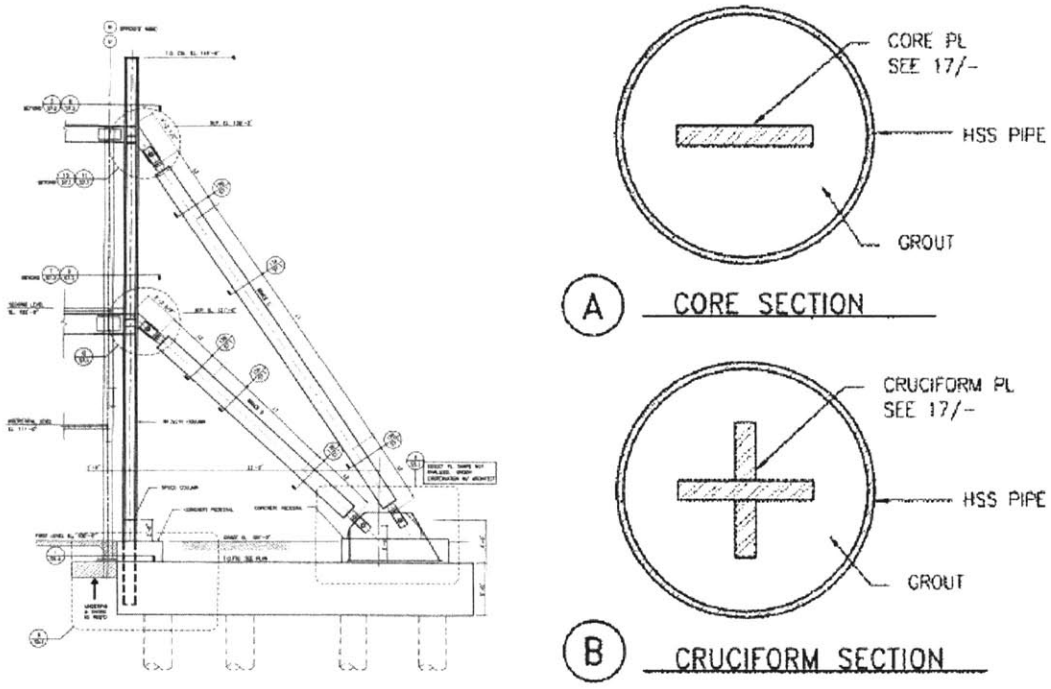

Figure 4.7 Braces Used in the Rehabilitation of two Office Buildings in San Francisco [17]

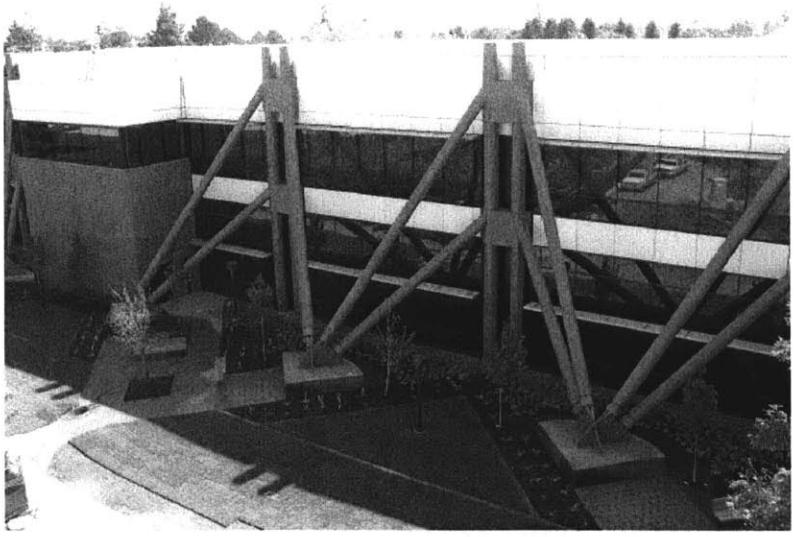

Figure 4.8 Braces Installed by Degenkolb Engineers – San Francisco [17]

Building, owner and location	Type of construction and building size	Unbonded braces
Plant & Environmental Sciences Building University of California, Davis, Calif.	New, Steel 3 stories+basement, 125,000 ft^2	132 Braces, Py = 115-550 kips Core: JIS SM490A
Marin County Civic Center Hall of Justice County of Marin, Calif.	Retrofit, RCa, 3–6 stories 600,000 ft^2	44 braces, Py = 400– 600 kips Core: JIS SN400B
Broad Center for the Biological Sciences California Institute of Technology, Calif.	New, Steel 3 stories+basement, 118,000 gross ft^2	84 braces, Py = 285– 660 kips Core: JIS SN490B
Hildebrand Hall University of California, Berkeley, Calif.	Retrofit, RC 3 stories+basement, 138,000 ft^2	36 braces, Py = 200– 400 kips Core: JIS SN400B
Wallace F. Bennett Federal Building Federal General Services Administration Salt Lake City, Utah	Retrofit, RC 8 stories, 300,000 ft^2	344 braces, Py = 205– 1,905 kips Core: JIS SN490B
Building 5, HP Corvallis Campus Hewlett-Packard, Corvallis, Ore.	Retrofit, Steel 2 stories, 160,000 ft^2	60 braces, Py = 110– 130 kips Core: JIS LYP235
Centralized Dining & Student Services Building University of California, Berkeley, Calif.	New, Steel 4 stories, 90,000 ft^2	95 braces, Py = 210– 705 kips Core: JIS SN490B
King County Courthouse, King County, Seattle, Wash.	Retrofit, RC 12 stories, 500,000 ft^2	50 braces, Py = 200– 500 kips Core: JIS SN400B
Genome & Biomedical Sciences Building University of California, Davis, Calif.	New, Steel 6 stories+basement, 211,000 ft^2	97 braces, Py = 150– 520 kips Core: JIS SN400B
Physical Sciences Building University of California at Santa Cruz, Calif.	New, Steel 5 stories, 136,500 net ft^2	74 braces, Py = 150– 500 kips Core: JIS SN400B
Second Research Building (Building 19B) University of California, San Francisco, Calif.	New, Steel 5 stories, 171,000 ft^2	132 braces, Py = 150– 675 kips Core: JIS SN400B
Kaiser Santa Clara Medical Center Hospital Building Phase I, Kaiser Permanente Santa Clara, Calif.	New, Steel 3 stories+basement, 266,000 ft^2	120 braces, Py = 265– 545 kips Core: JIS SN400B

Figure 4.9 List of U.S. Buildings Utilizing the Unbonded Brace [10]

Chapter 5

THE DESIGN METHODOLOGY

5.1 The Strategy

The first two chapters described the importance of damage controlled structures and the necessity to come up with preliminary performance based design tools for using hysteretic dampers in buildings that are designed based on performance levels. In this chapter, we propose a strategy for achieving the enhanced rehabilitation objective defined in Chapter 2.

The first step in the proposed methodology is to consider the building as two separate systems, namely the primary and the secondary system as described in [18] an shown in Figure 5.1. The primary system carries the vertical service loads and also contributes to the lateral resistance of the system. This system is supposed to remain elastic at all times, including both moderate and severe earthquakes. On the other hand, the secondary system, which consists of the hysteretic dampers, is designed to remain elastic in a moderate earthquake but should yield and undergo inelastic deformation in the case of a severe earthquake. The two cases considered, namely moderate and severe ground motions, are represented by BSE-1 and BSE-2 earthquakes as defined in the *Guidelines*.

This strategy allows the secondary system to have significant inelastic deformation but restricts the primary system to elastic behavior. From a damage control perspective, this

methodology is very desirable since damage is constrained only to the secondary system. In other words, these sacrificial elements can be thought of as a "fuse" for preventing extensive damage. Generally, replacing this secondary system consisting of the dampers is much more convenient and cost effective than rehabilitating a conventional structure with damaged connections or load bearing members. Furthermore, the collapse of the building is prevented at all times since the primary load bearing members are designed for elastic behavior.

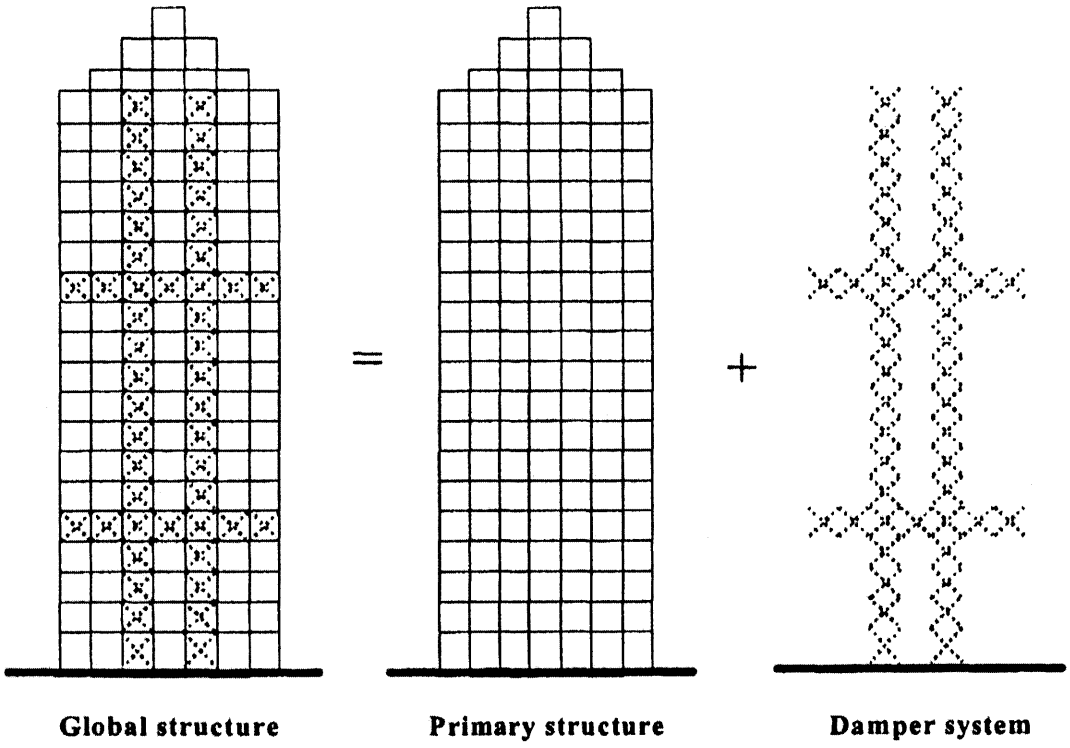

Figure 5.1 Breakdown of the Structure into Primary and Secondary Systems [18]

The only way to achieve elastic behavior in the primary structure and yielding in the secondary structure for steel frames is to use a very low-strength steel for the braces and

high strength steel for the primary members. Figure 5.2 shows some typical steels used for this purpose.

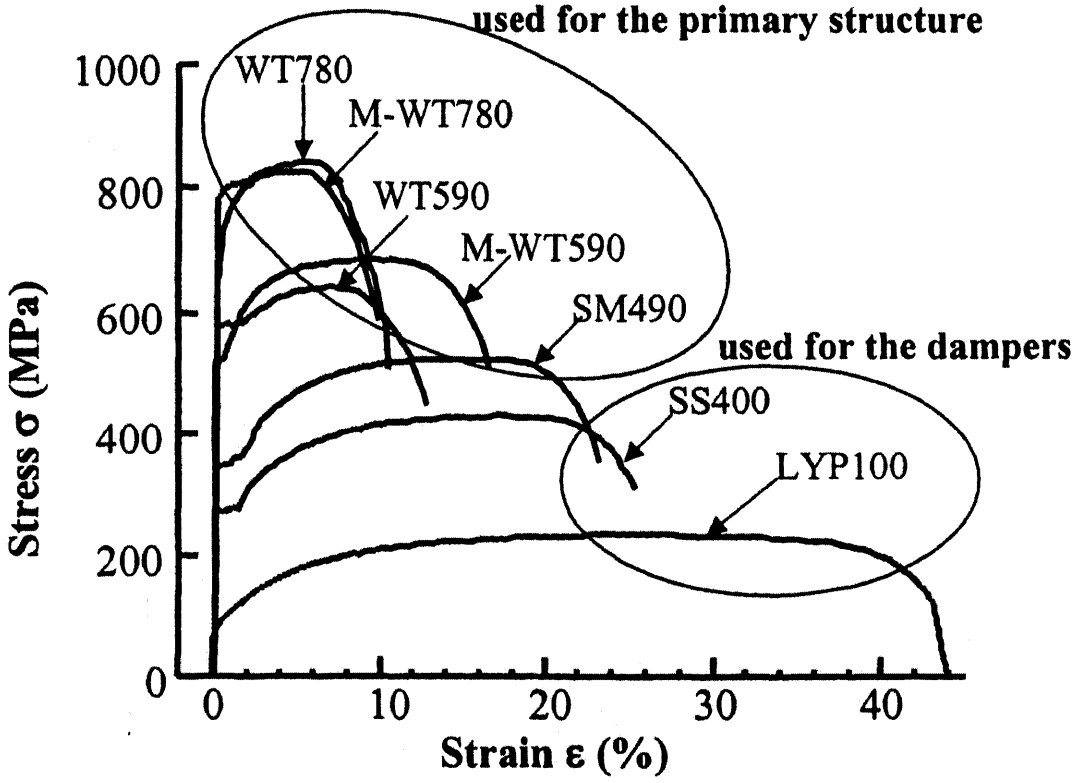

Figure 5.2 Stress-Strain Curves for Various Steels Available [18]

The first phase of any structural design is conceptual and broad. Even though a specific layout or building geometry is not considered in this thesis, the discussion up to this point may be thought of as the conceptualization of a basic design idea. So far, the load carrying system and performance expectations have been set as part of this phase. The next step in the process would be to determine stiffness distribution throughout the building height, set up deformation criteria and calculate building response and seismic demands based on a set of earthquake records. This would be done by simplifying the building to a discrete shear beam model, as it will be explained in the following section.

In the final phase, section detailing and three-dimensional computer models of the building would be created to come up with the actual design that will be implemented on the site. This final phase is beyond the scope of this thesis. The primary goal of this work is to come up with rules of thumb for preliminary design with hysteretic dampers for steel structures.

5.2 Motion Based Design Formulations

A key assumption in motion based design is the idea that buildings usually respond to earthquake excitation in their fundamental mode, which can be roughly approximated as a triangular displacement distribution over the floors, with the top floor having the largest absolute displacements. In this regard, for most structures, optimal design from a motion perspective corresponds to a state of uniform shear and bending deformation under the design loading. For a given excitation, this motion in such a fashion is natural for a structure, as it relates to the displacement profile which minimizes the strain energy stored in the structure. This consequently reduces the overall damage in the building. Such a design objective would be formulated as follows:

$$\gamma = \gamma^* \tag{5.1}$$

$$\chi = \chi^* \tag{5.2}$$

where we have introduced the shear and bending deformation parameters γ and χ respectively. Idealizing the building as a cantilever beam as shown in Figure 5.3, the deflection profile of the building becomes:

$$u = \gamma * x + \chi * \frac{x^2}{2} \tag{5.3}$$

where x stands for the distance from the base of the cantilever beam. In general, a building can be modeled as a discrete shear beam with lumped masses at floors, which can be further idealized as a mass-spring-dashpot system as shown in Figure 5.5. Under earthquake excitation, the equation of motion for this system in linear behavior becomes:

$$M\ddot{u}(t) + C\dot{u}(t) + Ku(t) = -m_i a_g(t) \tag{5.4}$$

where the variable u is the vector of relative displacements of the building with respect to the ground, m_i are the nodal masses, and a_g is the ground acceleration record for the earthquake. Matrices M , C , and K are the mass, damping and stiffness matrices of the system.

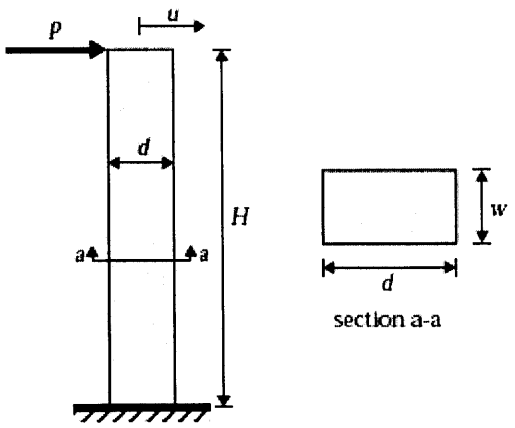

Figure 5.3 Cantilever Beam Model [5]

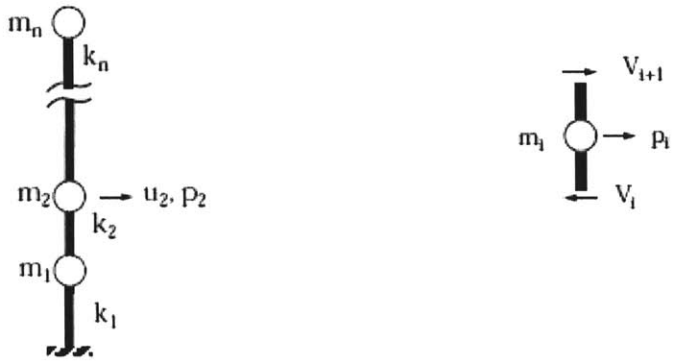

Figure 5.4 Discrete Shear Beam Model [5]

In reality, when analyzing high rise buildings, the bending deformation of the system must also be taken into account. However, since the systems considered for the purposes of this thesis are low to mid-rise buildings with low aspect ratios and high bending rigidities, only shear deformation will be considered.

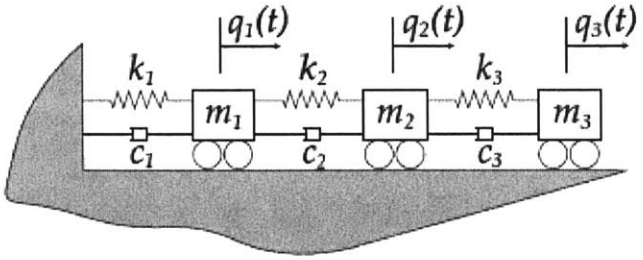

Figure 5.5 Schematic Representation of a 3 Degree of Freedom (DOF) System [19]

These formulations can be generalized to include material non-linearity as well. Considering the primary system to be linear at all times and the secondary system to have elasto-plastic stress strain behavior, the equation of motion can be written as:

$$M\ddot{u}(t) + C\dot{u}(t) + K_p u(t) + f_b(t) = -m_i a_g(t) \tag{5.5}$$

where K_p stands for the stiffness matrix of the linear primary frame and f_b represents the non-linear brace force. Based on the shear beam model defined above and shown in Figure 5.4, the brace force f_b can be given as:

$$f_b = V_i(t) - V_{i-1}(t) \tag{5.6}$$

where V_i stands for the shear force provided by the braces situated on the i^{th} story. At any time step, the non-linear brace force depends not only on the displacement at that time step but also on the yielding history of the braces. In other words, at any time, the brace may be virgin, in which case it has experienced no inelastic deformation yet, it may be unloading or reloading in an elastic manner or it may be flowing plastically in either direction. Hence the non-linear force is calculated at each time step by considering the change in the displacement of the brace and then adding the effect of this change to the force from the previous time step. As it will be explained in the next section, this procedure requires some iteration at any time step, since the force in the brace depends on the displacement and vice versa.

Based on these formulations, the response of the system can be simulated in MATLAB using numerical methods. The following section describes the MATLAB algorithm developed and used for this thesis.

5.3 The MATLAB Algorithm

5.3.1 Procedure

Huang et al. have proposed a convenient algorithm for dynamic analysis for a damage controlled structure. The flowchart for this methodology is given in Figure 5.6. The algorithm presented in this thesis is similar to the approach described in [18], but includes a strategy for finding feasible solutions for the performance levels described in Chapter 2.

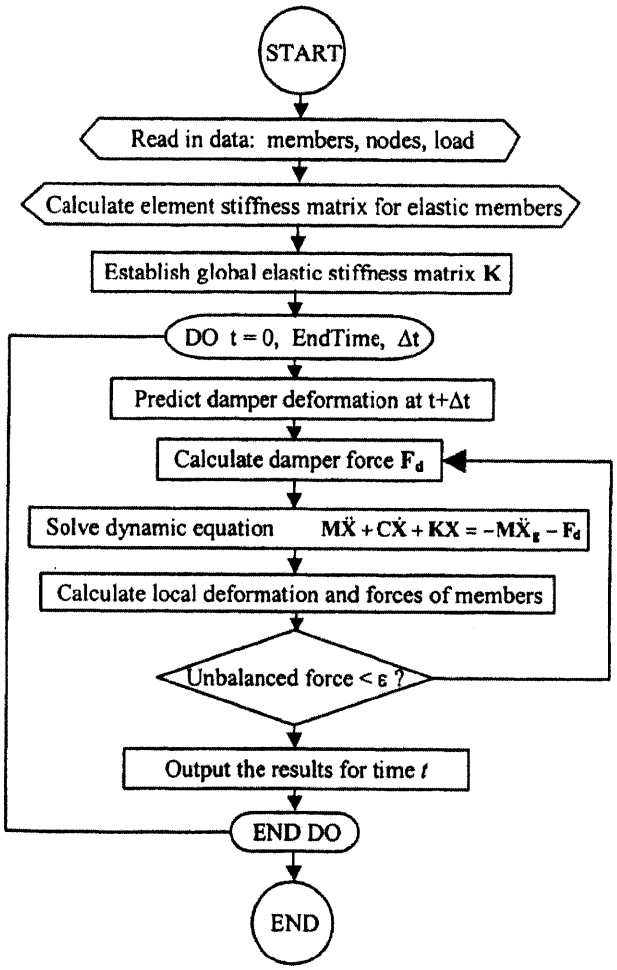

Figure 5.6 Flowchart for the Dynamic Analysis of Damage Controlled Structures [18]

The first step in the analysis is to determine the acceleration records to be used in the analysis. These are scaled up to BSE-1 and BSE-2 earthquakes based on FEMA-355 Peak Ground Acceleration values. Following this, the structural properties such as stiffness, damping and mass are determined. The stiffness and damping of the system are calibrated based on the BSE-1 earthquake and the maximum allowable inter-story drift. This requires calculating the response of the system iteratively until the inter-story drifts converge to the allowable drift. The initial guess for stiffness has to be reasonably close to guarantee fast convergence.

Once the system is calibrated, the response of the system is calculated for the BSE-2 earthquake. This part requires non-linear analysis due to the yielding of the hysteretic dampers. The ductility demand on the braces and the maximum inter-story drift is calculated.

The routine is repeated for varying design parameters. There are two key design parameters for designing with hysteretic dampers for any case, be it a new building or a rehabilitation project. The first parameter is the stiffness allocation to the braces; the second is the yielding point of the braces. The algorithm presented here calibrates the braces such that they are on the verge of yielding for the BSE-1 earthquake. The tuning parameter then states whether the braces should yield at a higher or lower point than this. In the MATLAB algorithm, these two variables are defined as *kratio* and *yratio* respectively. The variable *kratio* is the ratio of stiffness allocation to the primary system. For instance, if *kratio* is equal to 1, this means that the primary system is

providing all of the lateral stiffness, an extreme case that will not be considered in this study. The variable *yratio* is the yielding point of the braces compared to the BSE-1 calibration. For instance, if *yratio* is equal to 1, this means that the braces are on the verge of yielding when subjected to BSE-1 earthquake.

Using an external MATLAB routine, the simulations are repeated for varying *kratio* and *yratio* values and the ductility demand and maximum inter-story drifts are plotted for each case. From these plots, one can easily conclude which cases satisfy the performance objectives. Furthermore, if a large number of simulations for different earthquakes can be run, rules of thumb for designing with hysteretic braces can be derived with the help of this program.

5.3.2 Simulation of the Response

This section briefly treats the numerical procedure implemented for finding the dynamic response of the system. The method described involves the integration of the equations of motion using numerical methods. Starting from the initial conditions of the system, which are set to zero for both displacements and velocities, the state of the system is computed incrementally in the time domain.

The method used in the algorithm is known as the Newmark - β method. This is one of the most commonly used numerical integration methods in structural dynamics. This method approximates the displacements and velocities by marching forward in time. The formulations can be given as follows [20]:

$$u_{i+1} = u_i + \dot{u}_i \Delta t + \left(\frac{1}{2} - \beta\right)\Delta t^2 M^{-1}[p_i - C\dot{u}_i - f_i] + \beta \Delta t^2 M^{-1}[p_{i+1} - C\dot{u}_{i+1} - f_{i+1}] \quad (5.7)$$

$$\dot{u}_{i+1} = \dot{u}_i + +(1-\alpha)\Delta t\, M^{-1}[p_i - C\dot{u}_i - f_i] + \alpha \Delta t M^{-1}[p_{i+1} - C\dot{u}_{i+1} - f_{i+1}] \quad (5.8)$$

For $\alpha = \frac{1}{2}$ and $\beta = \frac{1}{4}$, which are the values used in this analysis, this method becomes the trapezoidal rule, or the constant acceleration method. As it is, this method is implicit. For linear systems, the system can be changed to an explicit form with state space formulations. If the method is used in this form, the time step for the integration needs to be smaller than the critical time step, given as:

$$\Delta t_{cr} = \frac{T_N}{\pi} \quad (5.9)$$

where T_N would be the shortest natural period of the system. When using the linear formulations for simulating BSE-1, the MATLAB algorithm checks for this case and interpolates the acceleration time history of the earthquake so that the sampling time of the earthquake satisfies this limit. For the cases studied thus far, the sampling time was below the critical time step, hence stability was ensured.

For the nonlinear case, the implicit formulation is used. The brace force is initially assumed to be the same as the force from the previous step. The displacements and velocities are found based on this initial assumption. Then, the force on the brace based on this new displacement is found, and the procedure is repeated within the time step.

The iterations converge to the actual force that equates the right and left sides of the non linear equation of motion. Convergence is checked by comparing the change in the iterated velocities, displacements and forces to a tolerance value. Once the values are accepted, the procedure is repeated for the next time step. The non-linear time history analysis of the system is carried out proceeding in this fashion.

Chapter 6

ANALYSIS RESULTS

6.1 Description of the Study

In these numerical simulations, a feasible, preferably optimal solution for achieving the stated performance objectives is sought after. The system considered is a ten story building modeled as a discrete shear beam. Each story is assumed to be 500,000 kg and the story height is specified as 4 meters. Considering the 0.5 % drift ratio limit for BSE-1, the allowable inter-story drift becomes 0.02 meters. The stiffness calibration is done using iterations on an initial guess, which is taken as a parabolic decreasing distribution over the height with a linear projection at the top 2 floors. This calibration has been done for three earthquakes, namely 1979 Imperial Valley, 1989 Loma Prieta and 1994 Northridge earthquakes. FEMA-355 gives the following peak ground acceleration values for these earthquakes for BSE-1:

BSE - 1	IMPERIAL VALLEY	LOMA PRIETA	NORTHRIDGE
PGA (m/s^2)	6.63	6.53	6.44

Table 6.1 Scaled Peak Ground Accelerations for the Earthquakes

Instead of the PGA values provided for BSE-2, a more conservative scaling factor of 1.5 is used for the non-linear analysis.

Apart from hysteretic damping, the system is considered to have structural damping. The damping matrix is constructed using Rayleigh Damping parameters $\alpha = 0$ and $\beta = 0.003$ which gives:

$$C = 0.003K_T \tag{6.1}$$

where K_T is the total linear stiffness matrix of the system. Once calibration is complete, the yielding shear and displacements are computed based on the yield ratio and stiffness allocation for the braces. This finalizes the characteristics of the system, which is then hit with the BSE-2 earthquake.

6.2 Simulation Results

6.2.1 Stiffness Calibration

The results of stiffness calibration are provided below. As it can be observed from the graphs, a parabolic distribution, similar to the initial guess is yields optimal results. The figures illustrate the uniform displacement profile of the system at the time of peak response. It is clear that the goal to keep inter-story displacements constant and equal to a threshold value has been achieved. It must be noted that with a decent initial guess, a few iterations are needed to achieve approximate convergence. Figure shows the error in maximum drift with increasing iterations. The purely elastic response of the system is also shown below.

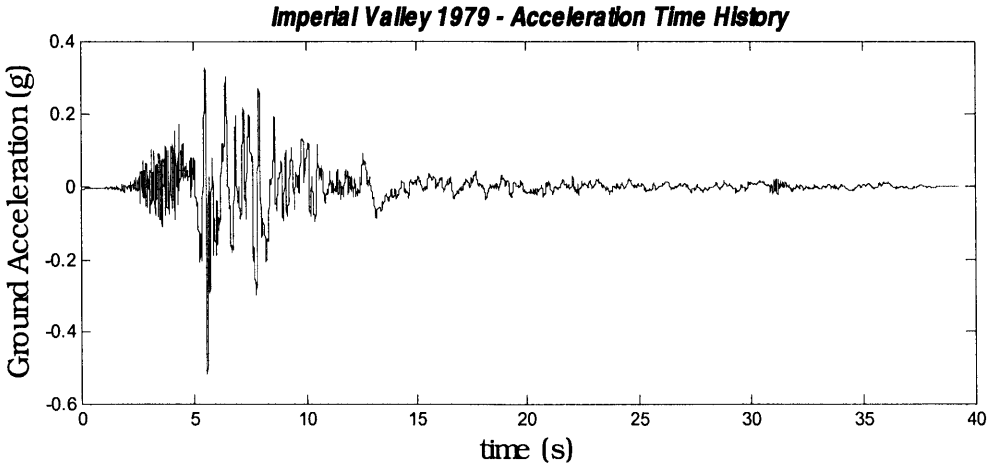

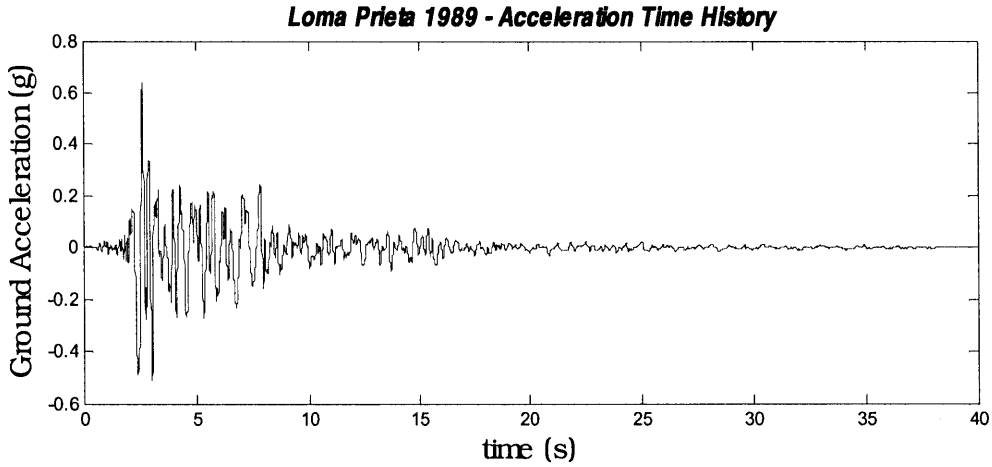

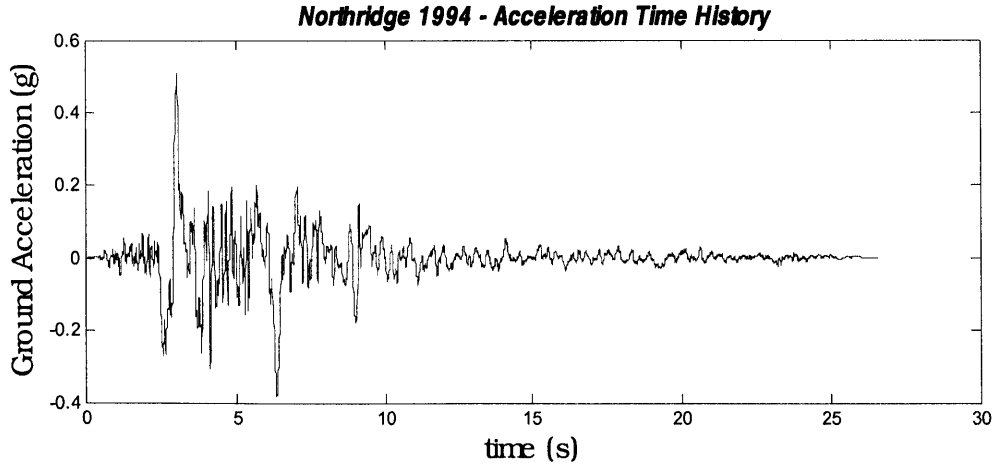

Table 6.2 Earthquake Records Used for the Analysis

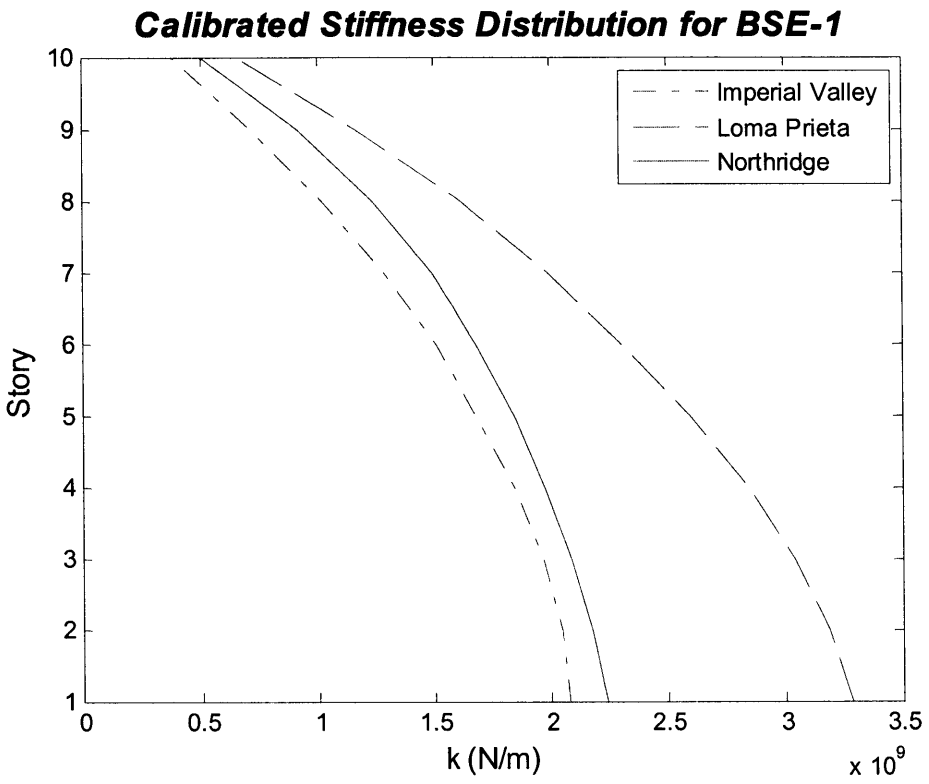

Figure 6.1 Stiffness Calibration Results for BSE-1 Earthquake

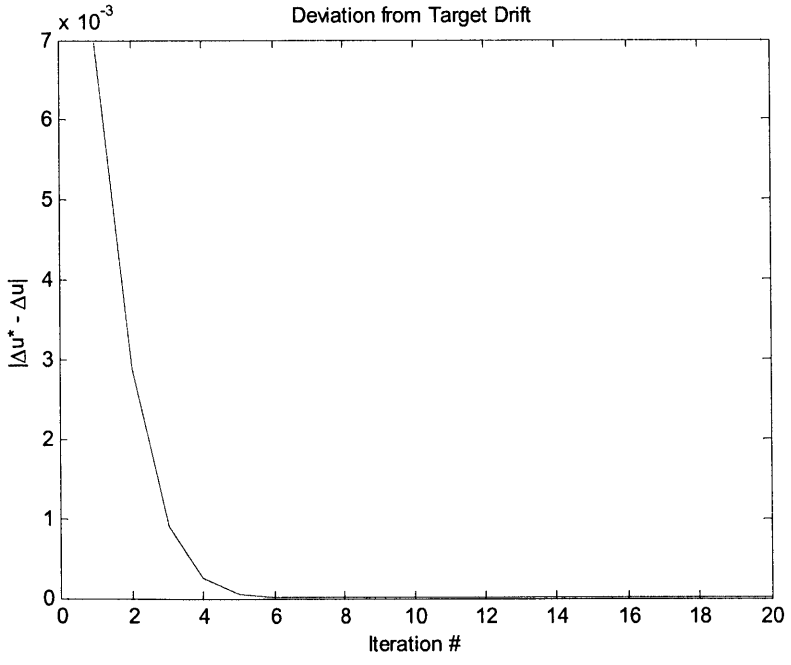

Figure 6.2 Convergence Plot for Stiffness Calibration based on BSE-1

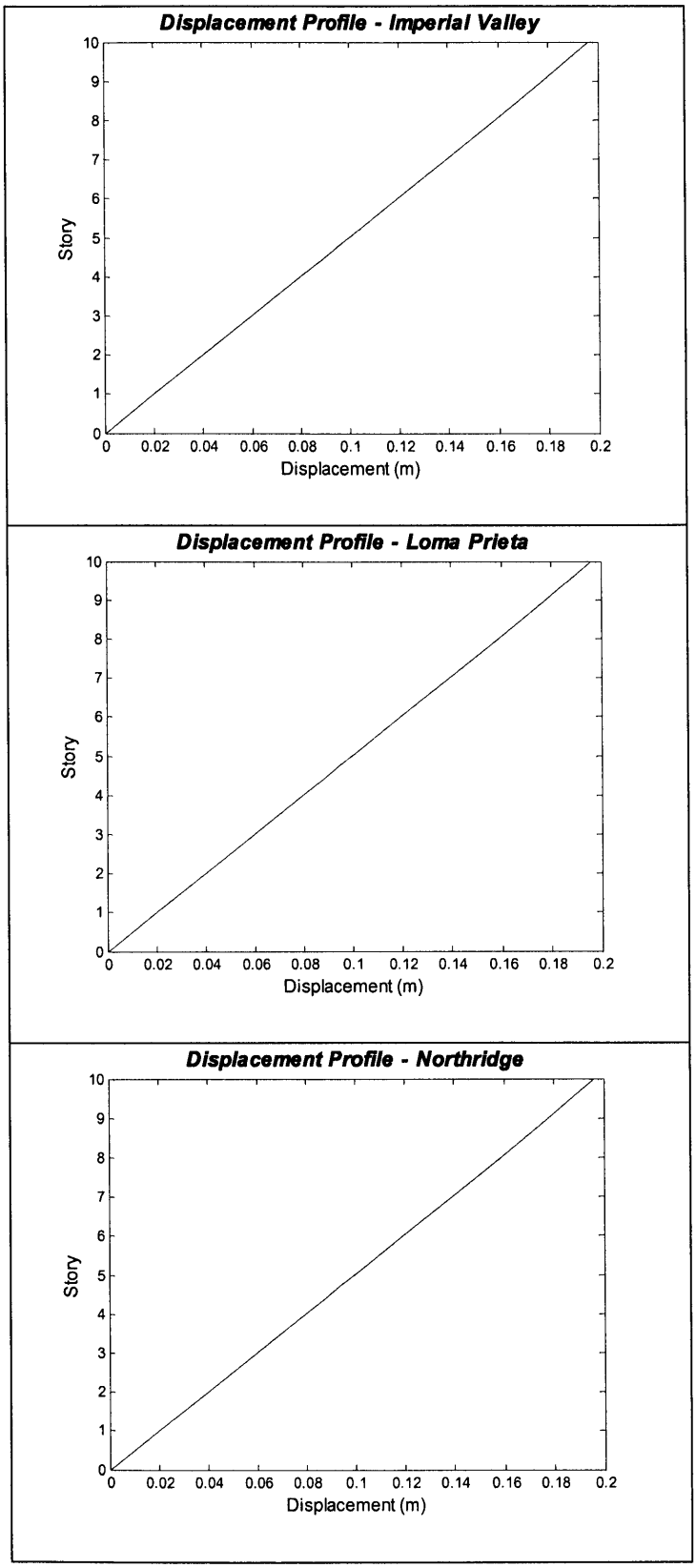

Figure 6.3 Displacement Profiles at Peak Response

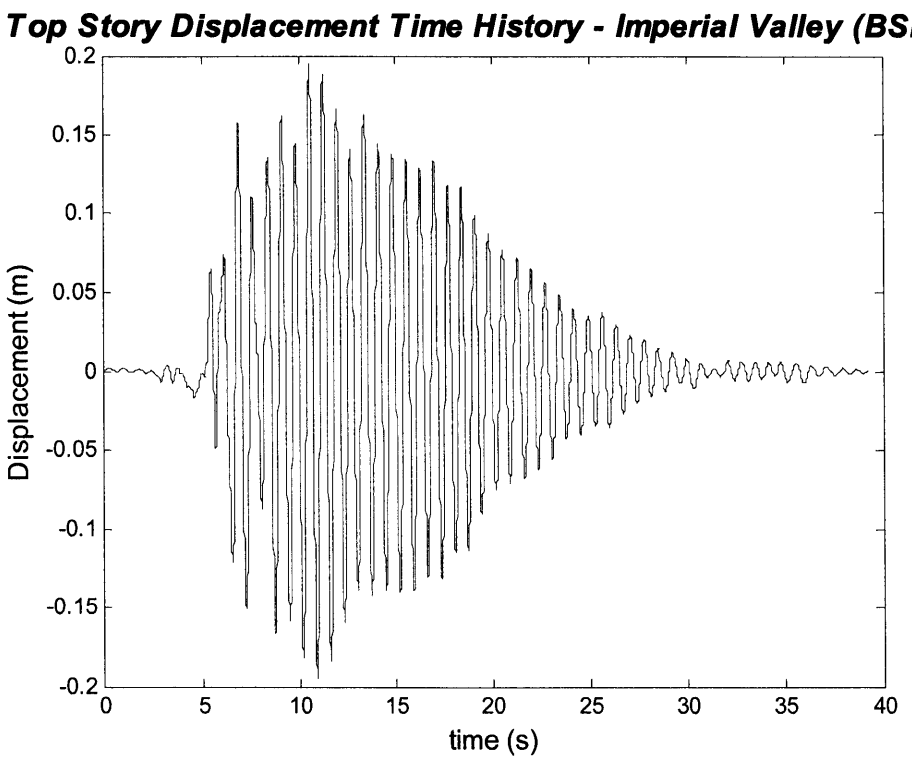

Figure 6.4 Response of the Calibrated System to Imperial Valley (BSE-1) Earthquake

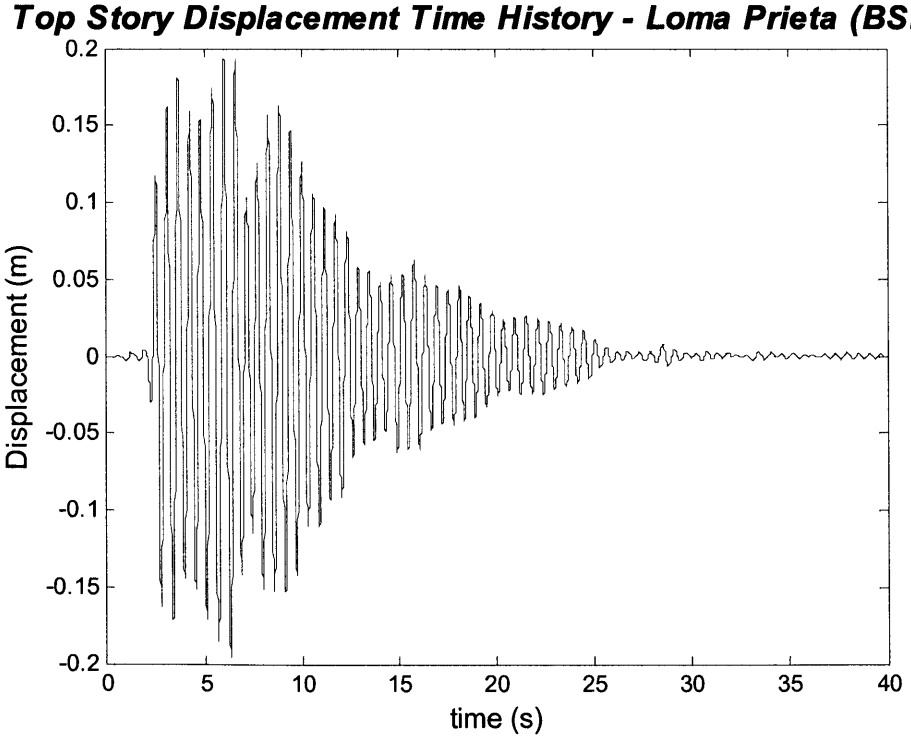

Figure 6.5 Response of the Calibrated System to Loma Prieta (BSE-1) Earthquake

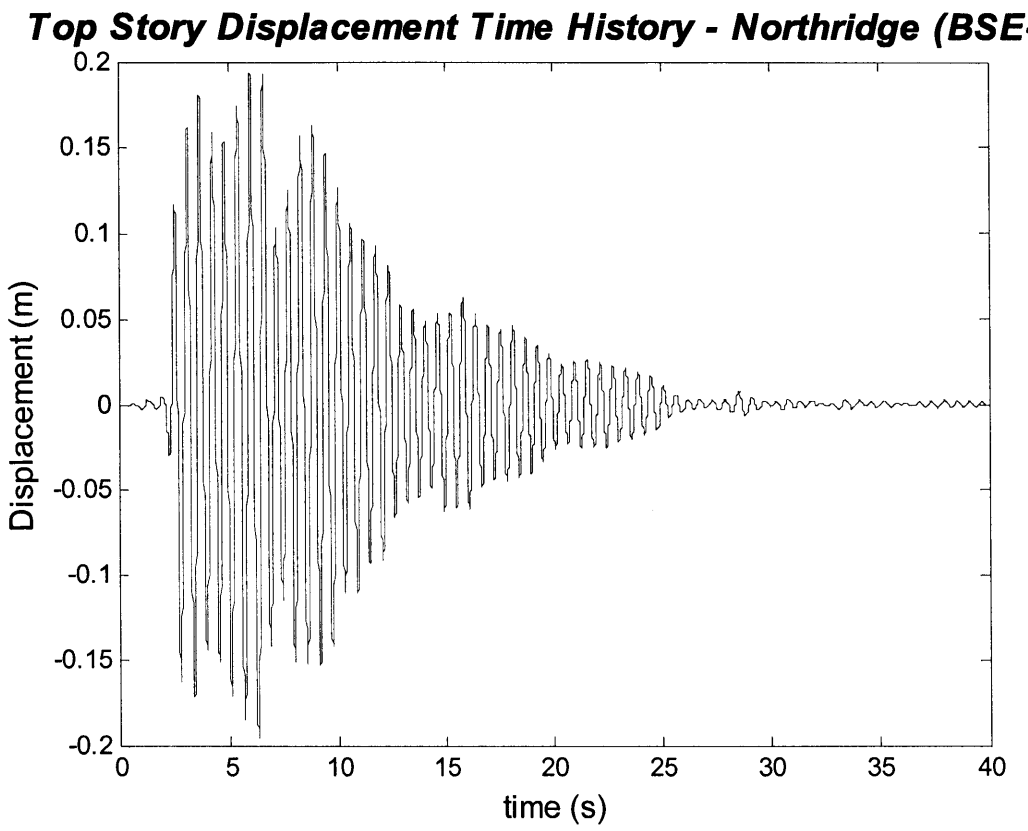

Figure 6.6 Response of the Calibrated System to Northridge (BSE-1) Earthquake

6.2.2 Yield Force and Stiffness Allocation Optimization

After calibrating the stiffness on each floor for BSE-1, the non-linear response of the system can be computed for varying *kratio* and *yratio* values. The specific domain searched for finding feasible solutions can be given as:

$$1 \leq yratio \leq 1.5 \tag{6.2}$$

$$0.5 \leq kratio \leq 1 \tag{6.3}$$

The specified range for *yratio* ensures linearity of the system in BSE-1 and allows yielding during BSE-2. Beyond these limits, the system either becomes non-linear in BSE-1 or doesn't yield at all in BSE-2.

The upper limit for *kratio* symbolizes a system without braces where all of the lateral stiffness is provided by the primary system. The lower limit is based on preliminary simulation runs. It was observed in these runs that the displacements and ductility demand from the braces rose sharply beyond this lower limit. This can be attributed to the low yielding point of the braces, which naturally increases the ductility ratio and deformation after yielding. Furthermore, the early yielding of the braces and their high contribution to the linear stiffness causes a sudden loss of stiffness to the system, which large accelerations and relative displacements. Both of these effects may be considered undesirable for both human comfort and safety considerations.

In summary, an optimal solution is sought after within the given domain. A feasible solution would be one that would satisfy the Collapse Prevention drift requirement given as %2 transient or permanent drift, which corresponds to 0.08m or inter-story displacement. On the other hand, an optimal solution would not only satisfy this criterion

but would also provide similar or better drift results when compared with a purely linear system.

From the graphs provided in Appendix C, the beneficial aspects of yielding braces are apparent. Although a system which stays linear at all times may have smaller deformations than a yielding one, it should be noted that keeping the primary load bearing linear at all times would be very costly. Hence, a solution that employs hysteretic dampers and has similar drift results with reasonable ductility demand from the braces would be preferable from an economic perspective.

Looking at the results obtained from the three earthquake records, one can say that there isn't a common clear trend in the variation with the yielding ratio. All of the results obtained within this domain are satisfactory from a Collapse Prevention perspective. Generally, a *yratio* value taken near 1 gives consistent results for all earthquakes considered. Interestingly, the results for the 1994 Northridge Earthquake resemble a horizontal line, suggesting that maximum inter-story drift is independent of the yielding point of the braces. This might be attributed to the impulsive nature of the earthquake. It is probable that at the time of the peak excitation, the drifts become maximal and energy dissipation capacity of the system doesn't influence the peak response significantly. In other words, the response in such a scenario is, to some extent, independent of the damping in the system. Consequently, for this case, we can say that designs employing hysteretic dampers will give similar, but not better results compared to a purely elastic system if drift is considered to be the only parameter of interest.

The change in response with stiffness allocation is the next important part that needs to be investigated. It is observed from the graphs that systems that have *yratio* equal to 1 and allocate 20-30% of the stiffness to the primary system have very good results compared to a purely elastic system. The inter-story displacements in these cases are approximately 0.03m., corresponding to .75% drift.

As a summary, we can say that an optimal solution from an economic and collapse prevention perspective would be to allocate ~25% of the global stiffness to the braces and design them such that they are on the verge of yielding for the BSE-1 earthquake.

Table 6.3 shows the characteristics of the selected system for calibration based on Imperial Valley Earthquake. In this table, kb and kp are brace and primary system stiffness respectively. Vy is the shear that causes yielding of the braces and c is the viscous damping coefficient of the structural system. Since most hysteretic dampers in the market have yield force values ranging from 500kN to 2000kN (100-500 kips), these yield values can be easily achieved by installing several braces on each floor.

Figure 6.7 shows the response of the system to BSE-1 and BSE-2 excitations. The effect of hysteretic damping after yielding is evident from these plots. Notice also the fact that some permanent plastic deformation has taken place in the system. The permanent drift corresponding to this deformation is within the limits specified for the Collapse Prevention Performance Level.

Floor	mass (kg)	kb (N/m)	kp (N/m)	c (Ns/m)	Vy (N)
1	5.00E+05	5.20E+08	1.56E+09	6.25E+06	1.04E+07
2	5.00E+05	5.13E+08	1.54E+09	6.15E+06	1.03E+07
3	5.00E+05	4.93E+08	1.48E+09	5.91E+06	9.86E+06
4	5.00E+05	4.62E+08	1.39E+09	5.54E+06	9.24E+06
5	5.00E+05	4.23E+08	1.27E+09	5.07E+06	8.45E+06
6	5.00E+05	3.78E+08	1.14E+09	4.54E+06	7.57E+06
7	5.00E+05	3.22E+08	9.67E+08	3.87E+06	6.45E+06
8	5.00E+05	2.55E+08	7.65E+08	3.06E+06	5.10E+06
9	5.00E+05	1.78E+08	5.34E+08	2.14E+06	3.56E+06
10	5.00E+05	9.50E+07	2.85E+08	1.14E+06	1.90E+06

Table 6.3 Spatial Distributions of Characteristics for the Selected System

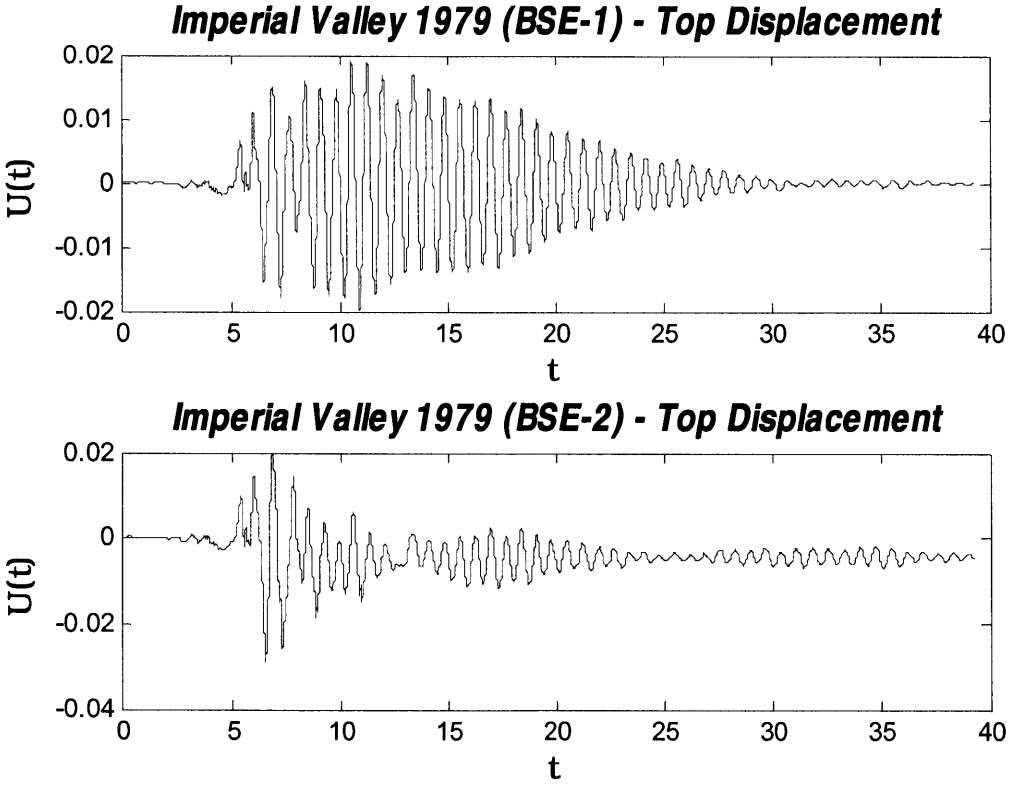

Figure 6.7 Response Time History of the Selected System

Since this result lies on the boundary of the solution domain provided for *yratio*, the next step would be to check whether better solutions exist beyond the limits specified at

the beginning of this section. The following section provides a brief discussion of brace stiffness and yielding configurations that allow the secondary system to perform inelastic deformation in BSE-1.

6.2.3 Alternative Solutions

In this section, the domain for the parametric study described in the previous section is extended to include brace configurations that would yield in the BSE-1 earthquake as well. The graphs provided in Appendix C for the 1979 Imperial Valley Earthquake suggest that expanding the solution domain reveals some very favorable results that would have been omitted otherwise. From the figures, it can be observed that a system with $yratio = 0.75$ and $kratio = 0.8$ can perform better than a purely elastic frame. Such a solution would perform highly and in the mean time would be very economical. The more recent research efforts seem to suggest that this approach is better than the one that has been adopted for this thesis [18].

On the other hand, allowing the bracing system to yield even in a moderate earthquake would increase the frequency of maintenance and repair, since even in a moderate earthquake the system would have some permanent inelastic deformations. From a reliability perspective, this would not be very desirable, since it cause partial down time for the building in every moderate earthquake.

More studies taking into account the permanent drift and plastic deformation of structural members would be required to validate the approach implemented in this section. Hence,

for the purposes of this thesis, the proposed ratios from the previous section are taken as the optimal calibration values.

Chapter 7

CONCLUDING REMARKS

The problem investigated in this thesis was the development of a robust design methodology for using hysteretic dampers to mitigate damage in structures. Despite the fact that a tremendous amount of theoretical and practical research has been conducted on the civil engineering applications of these devices, the implementation of this novel technology in the design and construction industry has been slow. Chapters 1 and 2 called attention to the economic significance of damage controlled structures and motion based design philosophy to give a clear view of the deficiencies in the current design practice and established building regulations. The purpose of this work was come up with simple rules of thumb that could be used in the preliminary design of mid-rise structural systems employing buckling restrained or equivalently unbonded braces. The established design values presented in Chapter 6 will hopefully be a useful stepping stone for future research and design practice in this field.

There are several shortcomings of the procedure presented in this methodology. Clearly, the analyses conducted are not exhaustive for all possible earthquakes and structural system configurations. It is highly probable that results presented are highly dependant on structural properties such as inherent damping, total height and spatial mass distribution. The same point is valid for the set of ground excitations used as well.

Another limitation could be the solution domains investigated in the problem. This was mentioned in the analysis section, and it was suggested that systems that are allowed to yield in moderate excitations may prove to be more effective in reducing total damage. Future studies on hysteretic dampers should shed light onto this issue.

A comprehensive study on this subject would also need to include different measures of damping efficiency, such as total energy dissipated, or equivalent damping of the system. A rather difficult aspect of the problem discussed herein is the quantification of total damage and the corresponding cost, which was a topic that was vaguely touched upon within the scope of this work. It is essential that future studies include a cost-benefit analysis for employing energy dissipation mechanisms in buildings.

As a final remark, the author would like to point out the fact that the application of new technologies such as hysteretic dampers to civil structures is highly influenced by public policy and the flexibility of existing regulations. Without the presence of a robust public policy that favors novel technologies, the aforementioned time delay in implementation can not be thoroughly eliminated. Overall, an all-encompassing strategy that promotes innovation in research and design is necessary for tackling the hazard mitigation issues of the 21st century.

REFERENCES

1. FEMA-273: NEHRP Guidelines for the Seismic Rehabilitation of Buildings, Technical Report, Federal Emergency Management Agency, 1997.
2. Çelikbaş, Ayşe. Economics of Damage Controlled Seismic Design; SM Thesis, Massachusetts Institute of Technology, Feb 1999
3. Connor J.J., Wada A., Iwata M., Huang, Y.H.. Damage-Controlled Structures I: Preliminary Design Methodology for Seismically Active Regions, Journal of Structural Engineering, April 1997
4. Khashaee, Payam. Damage-Based Seismic Design of Structures, Earthquake Spectra, May 2005
5. Connor, J.J. Introduction to Structural Motion Control, MIT Prentice Hall Series
6. www.taylordevices.com
7. www.gerb.com
8. www.fip-group.it
9. Housner, et al. Structural Control, Past Present and Future, Journal of Engineering Mechanics, September 1997
10. Black, C.J., Makris, N., Aiken I. D. Component Testing, Seismic Evaluation and Characterization of Buckling-Restrained Braces, Journal of Structural Engineering, June 2004
11. http://www0.nsc.co.jp/shinnihon_english/index.html
12. Fleming, Cody. A Design Methodology for Hysteretic Dampers in Buildings under Extreme Earthquakes, M. Eng. Thesis, Massachusetts Institute of Technology, June 2004

13. Aiken, I., Clark, P., Kazuhiko, K. , Ko, Eric, Kumura, Isao. Design Procedures for Buildings Incorporating Hysteretic Damping Devices, Proceedings 68th Annual Convention, Santa Barbara, California, Structural Engineers Association of California, October 1999
14. Skinner, R. I., Kelly, M. J., Heine, A. J. Hysteretic Dampers for Earthquake Resistant Structures, Earthquake Engineering and Structural Dynamics, 3, 287-296, 1975
15. www.arup.com
16. www.degenkolb.com
17. Mitchell, A. D., Parra, R. S., Heintz, J. A., Seismic Rehabilitation with FEMA 356: A Case Study, Structures, 2005
18. Huang, Y., Wada, A., Iwata, M., Mahin S. A., Connor, J. J. Design of Damage-Controlled Structures, Innovative Approaches to Earthquake Engineering, WIT Press 2002
19. Luş, H. System Identification in Structural Dynamics, Lecture Notes, Boğaziçi University
20. Kausel, E. Roesset, J. M. Advanced Structural Dynamics, Lecture Notes, Massachusetts Institute of Technology
21. FEMA-355C: Systems Performance of Steel Moment Frames Subject to Earthquake Ground Shaking, Technical Report, FEMA, 2001

APPENDIX A – EARTHQUAKE RECORDS

Earthquake Records as specified in [21]:

Table A.1: 50/50 Set of Records (72 years Return Period)

Designation	Record Info	Duration (sec)	Magnitude (Mw)	R (km)	Scale	PGA (in/sec^2)
LA41	Coyote Lake, 1979	39.38	5.7	8.8	2.28	227.7
LA42	Coyote Lake, 1979	39.38	5.7	8.8	2.28	128.7
LA43	Imperial Valley, 1979	39.08	6.5	1.2	0.40	55.4
LA44	Imperial Valley, 1979	39.08	6.5	1.2	0.40	43.1
LA45	Kern, 1952	78.60	7.7	107.0	2.92	55.7
LA46	Kern, 1952	78.60	7.7	107.0	2.92	61.4
LA47	Landers, 1992	79.98	7.3	64.0	2.63	130.4
LA48	Landers, 1992	79.98	7.3	64.0	2.63	118.8
LA49	Morgan Hill, 1984	59.98	6.2	15.0	2.35	123.0
LA50	Morgan Hill, 1984	59.98	6.2	15.0	2.35	211.0
LA51	Parkfield, 1966, Cholame 5W	43.92	6.1	3.7	1.81	301.4
LA52	Parkfield, 1966, Cholame 5W	43.92	6.1	3.7	1.81	243.8
LA53	Parkfield, 1966, Cholame 8W	26.14	6.1	8.0	2.92	267.7
LA54	Parkfield, 1966, Cholame 8W	26.14	6.1	8.0	2.92	305.1
LA55	North Palm Springs, 1986	59.98	6.0	9.6	2.75	199.8
LA56	North Palm Springs, 1986	59.98	6.0	9.6	2.75	146.3
LA57	San Fernando, 1971	79.46	6.5	1.0	1.30	97.7
LA58	San Fernando, 1971	79.46	6.5	1.0	1.30	89.2
LA59	Whittier, 1987	39.98	6.0	17.0	3.62	296.7
LA60	Whittier, 1987	39.98	6.0	17.0	3.62	184.7

Table A.2: 10/50 Set of Records (475 years Return Period).

Designation	Record Info	Duration (sec)	Magnitude (Mw)	R (km)	Scale	PGA (in/sec^2)
LA01	Imperial Valley, 1940	39.38	6.9	10.0	2.01	178.0
LA02	Imperial Valley, 1940	39.38	6.9	10.0	2.01	261.0
LA03	Imperial Valley, 1979	39.38	6.5	4.1	1.01	152.0
LA04	Imperial Valley, 1979	39.38	6.5	4.1	1.01	188.4
LA05	Imperial Valley, 1979	39.08	6.5	1.2	0.84	116.4
LA06	Imperial Valley, 1979	39.08	6.5	1.2	0.84	90.6
LA07	Landers, 1992	79.98	7.3	36.0	3.20	162.6
LA08	Landers, 1992	79.98	7.3	36.0	3.20	164.4
LA09	Landers, 1992	79.98	7.3	25.0	2.17	200.7
LA10	Landers, 1992	79.98	7.3	25.0	2.17	139.1
LA11	Loma Prieta, 1989	39.98	7.0	12.4	1.79	256.9
LA12	Loma Prieta, 1989	39.98	7.0	12.4	1.79	374.4
LA13	Northridge, 1994, Newhall	59.98	6.7	6.7	1.03	261.8
LA14	Northridge, 1994, Newhall	59.98	6.7	6.7	1.03	253.7
LA15	Northridge, 1994, Rinaldi	14.95	6.7	7.5	0.79	206.0
LA16	Northridge, 1994, Rinaldi	14.95	6.7	7.5	0.79	223.9
LA17	Northridge, 1994, Sylmar	59.98	6.7	6.4	0.99	219.9
LA18	Northridge, 1994, Sylmar	59.98	6.7	6.4	0.99	315.5
LA19	North Palm Springs, 1986	59.98	6.0	6.7	2.97	393.5
LA20	North Palm Springs, 1986	59.98	6.0	6.7	2.97	380.9

Table A.3: 2/50 Set of Records (2475 years Return Period).

Designation	Record Info	Duration (sec)	Magnitude (Mw)	R (km)	Scale	PGA (in/sec^2)
LA21	1995 Kobe	59.98	6.9	3.4	1.15	495.3
LA22	1995 Kobe	59.98	6.9	3.4	1.15	355.4
LA23	1989 Loma Prieta	24.99	7.0	3.5	0.82	161.4
LA24	1989 Loma Prieta	24.99	7.0	3.5	0.82	182.6
LA25	1994 Northridge	14.95	6.7	7.5	1.29	335.3
LA26	1994 Northridge	14.95	6.7	7.5	1.29	364.3
LA27	1994 Northridge	59.98	6.7	6.4	1.61	357.8
LA28	1994 Northridge	59.98	6.7	6.4	1.61	513.4
LA29	1974 Tabas	49.98	7.4	1.2	1.08	312.4
LA30	1974 Tabas	49.98	7.4	1.2	1.08	382.9
LA31	Elysian Park (simulated)	29.99	7.1	17.5	1.43	500.5
LA32	Elysian Park (simulated)	29.99	7.1	17.5	1.43	458.1
LA33	Elysian Park (simulated)	29.99	7.1	10.7	0.97	302.1
LA34	Elysian Park (simulated)	29.99	7.1	10.7	0.97	262.8
LA35	Elysian Park (simulated)	29.99	7.1	11.2	1.10	383.1
LA36	Elysian Park (simulated)	29.99	7.1	11.2	1.10	424.9
LA37	Palos Verdes (simulated)	59.98	7.1	1.5	0.90	274.7
LA38	Palos Verdes (simulated)	59.98	7.1	1.5	0.90	299.7
LA39	Palos Verdes (simulated)	59.98	7.1	1.5	0.88	193.1
LA40	Palos Verdes (simulated)	59.98	7.1	1.5	0.88	241.4

APPENDIX B – MATLAB CODES

MAIN CODE:

```
function [dd,ddi,dr,dri]=optima(kvec,yvec);

%EQN={'elcentro','impval','kern','loma','morgan','nridge',...
%    'npalm','park','sanfern','whittier'};
EQN={'impval','loma','nridge'};
ACC=[6.63 6.53 6.44];
N=10;
for eq=3; %1:length(EQN);
    eval(['load ', char(EQN(eq))])
    ag=ACC(eq)/max(abs(ag))*ag;
    for kc=1:length(kvec);
        ductdem=[];
        mdrift=[];
        skip=[];
        for yc=1:length(yvec);
            disp([upper(char(EQN(eq))),' k=',num2str(kvec(kc)),' & ',
'y=', num2str(yvec(yc))])
            if kc==1 & yc==1; kel=[];maxdrift=zeros(N,1); skip=0; else
kel=kel; , skip=1;end

[ag,t,maxdrift,mu,kb,kp,c,Vy,U1,V1,U2,V2,fbrace]=nlshbm(ag,dt,kvec(kc),
yvec(yc),skip,kel);
            kel=kp+kb;

%save([upper(char(EQN(eq))),'k',num2str(100*kvec(kc)),'y',num2str(100*y
vec(yc))])
                ductdem=[ductdem max(mu)];
                mdrift=[mdrift max(maxdrift)]
            end
            [dd,ddi]=max(ductdem);
            [dr,dri]=max(mdrift);
            figure (1)
            set(gcf,'units','normalized','outerposition',[0 0 1 1])
            subplot(2,1,1)
            plot(yvec,ductdem,'*')
            title([upper(char(EQN(eq))),' - Ductility Demand for
kratio=',num2str(kvec(kc))],'FontName','Arial
Narrow','FontSize',12,'FontWeight', 'demi')
            ylabel(['\mu'],'FontSize',18,'Rotation', 90)
            ylim([0 10])
            xlim([min(yvec) max(yvec)])
            xlabel('yratio','FontSize',16)
            hold on,
            subplot(2,1,2)
            plot(yvec,mdrift,'*')
            title([upper(char(EQN(eq))),' - Maximum Interstory Drift
for kratio=',num2str(kvec(kc))],'FontName','Arial
Narrow','FontSize',12,'FontWeight', 'demi')
            ylabel(['\Delta','u'],'FontSize',18)
            ylim([0 .1])
```

```
            xlim([min(yvec) max(yvec)])
            xlabel('yratio','FontSize',16)


saveas(gcf,[upper(char(EQN(eq))),'_k_',num2str(100*kvec(kc))],'fig')
        end
    end
end

SUBROUTINE:

function
[ag,t,maxdrift,mu,kb,kp,c,Vy,U1,V1,U2,V2,fbrace]=nlshbm(ag,dt,kratio,yr
atio,skip,kel);

%%%% SIMULATION PARAMETERS %%%%
%# of iterations for stiffness calibration based on BSE1
%EQN=1;          %# of the EQ, check list of EQ's.;
noit=15;
ag=6.63/max(abs(ag))*ag;
[ag, vg, dg] = baseline (ag, dt);
t=0:dt:dt*(length(ag)-1);
scale=1.5;      %scaling factor for BSE 2
alpha=1/2;      %NEWMARK BETA INTEGRATION PARAMETER
beta=1/4;       %NEWMARK BETA INTEGRATION PARAMETER
%%%% STRUCTURAL PROPERTIES:%%%%
N=10;
one=1:N;
one=one';%vector of node numbers for NDOF system
e=ones(N,1);    %vector of ones for NDOF system
nil=zeros(N);   %zeros matrix for NDOF system
mbase=500000;   %mass of a floor
kbase=3.5E9;    %base stiffness
alldrift=0.02;  %allowable drift for building


    %SKIPS BSE-1 ITERATIONS. FOR ANY EARTHQUAKE, BSE-1 ITERATIONS NEED
TO
    %BE DONE ONLY ONCE.
if skip==0;
    %   INITIAL STIFFNESS & YF DISTRIBUTION, PARABOLIC APPROXIMATION  %
    k=kbase*(1-((one-.5*e)/N).*(one-.5*e)/N);
    %   linear approximation for stiffness correction of the top 20
percent
    a=0.8*N;
    a=round(a);
    aa=N-a;
    for i=1:aa;
        k(a+i)=k(a)*(1-(.7*i)/aa);
        %    Vy(a+i)=Vy(a)*(1-(.7*i)/aa);
    end
    %%%%
    %ASSEMBLE GLOBAL MATRICES M,C,K
    K=nil; C=nil;
    M=mbase*eye(N);
    [K]=ccass(k,N);C=0.003*K;
```

```
    %%%%%%%%%%%%%%%%%%%%%%%%%%%%%%%%%%%%%%%%
    for i=1:noit;
        [U1,V1,k,fk] =
newmarkln(K,C,M,ag,dt,alpha,beta,k,alldrift,kratio);
        fk;k;
        [K]=ccass(k,N);C=0.003*K;
    end
    [U1,V1,k,fk] = newmarkln(K,C,M,ag,dt,alpha,beta,k,alldrift,kratio);
kel=k;
Klin=K;
Vy=yratio*(1-kratio)*kel*alldrift;
uy=alldrift*yratio;
Kp=kratio*Klin;
kb=(1-kratio)*kel;
kp=kratio*kel;
c=kel*0.003;
else
    U1=0;V1=0;
    M=mbase*eye(N);
    Klin=ccass(kel,N);
    C=0.003*Klin;
    Vy=yratio*(1-kratio)*kel*alldrift;
    uy=alldrift*yratio;
    Kp=kratio*Klin;
    kb=(1-kratio)*kel;
    kp=kratio*kel;
    c=kel*0.003;
end

%%%% HIT CALIBRATED SYSTEM WITH BSE 2, OBTAIN RESPONSE BY NL SIMULATION
ag=scale*ag;
[U2,V2,fbrace] = newmarknln(M,C,Kp,ag,dt,alpha,beta,Vy,kb,uy);
[mu,maxdrift]=ductdrift(U2,V2,alldrift,N,yratio)
 subplot(2,1,1)
        plot(t,U1(1,:))
        title('Imperial Valley 1979 (BSE-1) - Top
Displacement','FontName','Arial Narrow','FontSize',14,'FontWeight',
'demi')
        ylabel('U(t)','FontName','Bookman','FontSize',12,'FontWeight',
'demi')
        xlabel('t','FontName','Bookman','FontSize',12,'FontWeight',
'demi')
        hold on
 subplot(2,1,2)
        plot(t,U2(1,:))
        title('Imperial Valley 1979 (BSE-2) - Top
Displacement','FontName','Arial Narrow','FontSize',14,'FontWeight',
'demi')
        ylabel('U(t)','FontName','Bookman','FontSize',12,'FontWeight',
'demi')
        xlabel('t','FontName','Bookman','FontSize',12,'FontWeight',
'demi')
        hold on
%%%%%%%%%%%%%%%%%%%%%%%%%%%%%%END OF MAIN
CODE%%%%%%%%%%%%%%%%%%%%%%%%%%%%%%
function [u,v,k,fk] = newmarkln(K, C, M, ag, dt, alpha,
beta,k,alldrift,kratio);
```

```
[phi,omega]=eig(K,M);
T=2*pi./sqrt(diag(omega));
dtcrit=min(T)/pi;
if dt>dtcrit;
    disp('Interpolating...')
    t=0:dt:dt*(length(ag)-1);
    x=0:dtcrit:max(t);
    ag=interp1(t,ag,x,'linear');
end

[m,n] = size(M);
n1 = n+1;
n2 = 2*n;
me = M*ones(n,1);
dt2 = dt^2;
A11 = M+beta*dt2*K;
A12 = beta*dt2*C;
A21 = alpha*dt*K;
A22 = M+alpha*dt*C;
B11 = M-(0.5-beta)*dt2*K;
B12 = dt*(M-(0.5-beta)*dt*C);
B21 = -(1-alpha)*dt*K;
B22 = M-(1-alpha)*dt*C;
P11 = (0.5-beta)*dt2*eye(n);
P12 = beta*dt2*eye(n);
P21 = (1-alpha)*dt*eye(n);
P22 = alpha*dt*eye(n);
A = [A11,A12;A21,A22];
B = [B11,B12;B21,B22];
P = [P11,P12; P21,P22];
B = A\B;
P = A\P;

nt = length(ag);
u1 = zeros(n2,1);
u = u1;
drift=zeros(n,1);
for j=2:nt
    %size(B), size(P), size(u1)
    u2 =B*u1+ P*[-me*ag(j-1);-me*ag(j)];
    u = [u,u2];
    u1 = u2;
    drift(1,j)=u(1,j);
    for node=2:n;
        drift(node,j)=u(node,j)-u(node-1,j);
    end
end
for node=1:n;
    maxdrift(node)=max(abs(drift(node,:)));
    fk(node)=maxdrift(node)/alldrift;
    if fk>0.1;
        k(node)=fk(node)*k(node);
    end
end
v = u(n1:n2,:);
```

```
u = u(1:n,:);
return

%%%%%%%%%%%%%%%%%%%%%%%%%%%%%%%%%%%%%%%%%%%%%%%%%%%%%%%%%%%%%%%%%%%%%%%
%%%%
function [u,v,fbrace] = newmarknln(M, C, Kp, acc, dt, alpha,
beta,Vy,kb,uy);
% Integrates the equations of motion using the Newmark beta method
% (implicit version)
K=Kp;
tol = 0.01; % tolerance for iteration
alpha1 = (1-alpha)*dt;
alpha = alpha*dt;
beta1 = (0.5-beta)*dt^2;
beta = beta*dt^2;
n = length(K);
nt = length(acc);
u1 = zeros(n,1);
v1 = zeros(n,1);
e = M*ones(n,1);
u = zeros(n,nt);
v = zeros(n,nt);
up=0;
plastv=zeros(n,1);
unloadv=zeros(n,1);
driftprev=zeros(n,1);
upv=zeros(n,1);
V=zeros(n,1);
fb=zeros(n,nt);
M = inv(M);     % may need to change this for efficiency...
for j=1:nt-1
    j1 = j+1;

[fnl1,plastv,V,upv,unloadv,driftprev]=nlforce(plastv,unloadv,u1,driftpr
ev,upv,n,V,Vy,uy,kb);
    %fnl1=(K*u1);
    f1 = M*(e*acc(j)+C*v1+K*u1+fnl1');  % K*u1 may need to be
changed...
    % initial estimates
    f2 = f1;
    u2 = u1+v1*dt;
    v2 = v1;
    % non-iterated part of forward projection
    u0 = u1+v1*dt-beta1*f1;
    v0 = v1-alpha1*f1;
    iter = 0;
    err = 1;
    while iter<1 & err>tol
        iter = iter+1;

[fnl3,plastv,V,upv,unloadv,driftprev]=nlforce(plastv,unloadv,u2,driftpr
ev,upv,n,V,Vy,uy,kb);
        %fnl3=(K*u2);
        f3 = M*(e*acc(j1)+C*v2+K*u2+fnl3'); %K*u2 may need to be
changed...
        u3 = u0-beta*f3;
        v3 = v0-alpha*f3;
```

```
        erru = norm(u3-u2)/norm(u3+u2);
        errv = norm(v3-v2)/norm(v3+v2);
        errf = norm(f3-f2)/norm(f3+f2);
        err = max([erru,errv,errf]);
        u2 = u3;
        v2 = v3;
        f2 = f3;
    end
    u(:,j1) = u2;
    v(:,j1) = v2;
    u1 = u2;
    v1 = v2;
fbrace(:,j)=fnl3';
end
return

%%%%%%%%%%%%%%%%%%%%%%%%%%%%%%%%%%%%%%%%%%%%%%%%%%%%%%%%%%%%%%%%%%%%%%%%%
%%%%
function
[fnl,plastv,V,upv,unloadv,driftprev]=nlforce(plastv,unloadv,u,driftprev
,upv,n,V,Vy,uy,kb);
for node=1:n;
    if node==1
    drift(node)=u(node);
    else
    drift(node)=u(node)-u(node-1);
    end

[plastic,force,up,unload]=springforce(plastv(node),unloadv(node),V(node
),Vy(node),upv(node),drift(node),driftprev(node),uy,kb(node));
    V(node)=force;
    plastv(node)=plastic;
    upv(node)=up;
    unloadv(node)=unload;
    driftprev(node)=drift(node);
end
fnl(n)=V(n);
for node=1:n-1;
    fnl(node)=V(node)-V(node+1);
end
return

%%%%%%%%%%%%%%%%%%%%%%%%%%%%%%%%%%%%%%%%%%%%%%%%%%%%%%%%%%%%%%%%%%%%%%%%%
%%%%
function
[plastic,force,up,unload]=springforce(plastic,unload,force,fy,up,drift,
driftprev,uy,kb);

if plastic~=0
%%%%SPRING WAS FLOWING%%%%
    if plastic==1;        %L->R
        if drift <= driftprev;     %Stopped flowing?
            unload = -1;%Unloads R->L
            plastic=0;
            up=drift;
            force=fy;
```

```
        end
    elseif plastic==-1;  %R->L CASE
        if drift>=driftprev
            unload=1;
            plastic=0;
            up=drift;
            force=-fy;
        end
    end
elseif unload~=0
%%%%UNLOADING OR RELOADING%%%%
    du=drift-up;
    if unload<0;     %Was unloading?
        if du>0;     %Resumes flow L->R?
            plastic = 1;
            force = fy;
        elseif du <= -uy; %Exceeds yield limit in R->L direction
            up= up-uy;
            plastic=-1;
            force=-fy;
        else force=fy+kb*du; %Elastic unloading
        end
    elseif unload > 0               %Was it reloading?
        if du < 0           %Resumes flow R->L?
            plastic=-1;
            force = -fy;
        elseif du < uy;
            up = up + uy;
            plastic = 1;
            force = fy; %Exceeds yield limit in L->R direction
        else
            force= -fy +kb*du; %Elastic reloading, du > 0.
        end
    end
else
%%%%VIRGIN SPRING, NO INELASTIC DEFORMATION%%%%
    if drift>=uy;
        plastic=1;      %If limit exceeded, flows L->R
        up=uy;
        uy=2.*uy;
        force=fy;
    elseif drift<=-uy   %If limit exceeded, flows R->L
        plastic=-1;
        up=-uy;
        uy=2*uy;
        force=-fy;
    else
        force=drift*kb; %If spring is still elastic
    end
end

%%%%%%%%%%%%%%%%%%%%%%%%%%%%%%%%%%%%%%%%%%%%%%%%%%%%%%%%%%%%%%%%%%%%%%%%%%%%%%
%%%%
function [mu,maxdrift]=ductdrift(u,v,alldrift,N,yratio);
%COMPUTES THE DUCTILITY DEMAND AND MAXIMUM DRIFT BASED ON THE MAXIMUM
%VALUES OF THE TIME HISTORY OF THE SYSTEM
maxdrift=zeros(N,1);
```

```
for node=1:N;
    if node==1;
        drift(1,:)=u(1,:);
        gammadot(1,:)=v(1,:);
    else
        drift(node,:)=u(node,:)-u(node-1,:);
        gammadot(node,:)=v(node,:)-v(node-1,:);
    end
    maxdrift(node)=max(abs(drift(node,:)));
    mu(node)=maxdrift(node)/(alldrift*yratio);
end

%%%%%%%%%%%%%%%%%%%%%%%%%%%%%%%%%%%%%%%%%%%%%%%%%%%%%%%%%%%%%%%%%%%%%%%%%%
%%%%
function [K]=ccass(k,N);
%ASSEMBLES CLOSE COUPLED STIFFNESS OR DAMPING MATRIX FROM NODAL
PROPERTIES
%e.g. input stiffness of the ith floor and # of floors, get global K
for i=1:N-1;
    K(i,i)=k(i)+k(i+1);
    K(i,i+1)=-k(i+1);
    K(i+1,i)=-k(i+1);
end
K(N,N)=k(N);

%%%%%%%%%%%%%%%%%%%%%%%%%%%END OF
SUBROUTINES%%%%%%%%%%%%%%%%%%%%%%%%%%%%

function [acc, vg, dg] = baseline (acc, dt)
% Corrects the baseline of an earthquake record, and evaluates
% the velocity and displacement time histories
% Fits a parabolic baseline using the following criteria
%   a) zero initial and final velocity
%   b) zero initial and final displacement
%   c) minimum of integral of squared velocity
% Input arguments:
%   acc = acceleration record (cm/s^2)
%   dt  = time step (s)
% Returned arguments:
%   acc = baseline corrected record
%   vg  = ground velocity record
%   dg  = ground displacement record


% check shape of record etc
n = size(acc);
if n(1,1)==1, acc=acc'; end % make it a column vector
nn = length(acc);                    % original number of samples
n2 = nn; while n2>0 & acc(n2)==0, n2=n2-1; end  % remove trailing
zeroes
n1 = 1; while n1<=n2 & acc(n1)==0, n1=n1+1; end % remove leading zeroes
if n1>n2
    % record is empty, or filled with zeros
    acc=[]; vg=[]; d=[];
    return
else
```

```
    acc = acc(n1:n2);    % keep non-zero part
end

nt = length(acc);
N = nt-1;            % number of intervals
td = N*dt;           % duration

% First pass: eliminate average and linear components
k = [0:N]';
D = nt*(nt^2-1)/2;
A = sum(acc)/D;
B = sum(acc.*k)/D;
a =  N*(2*nt-1)*A-3*N*B;
b = -3*N*A+6*B;
acc = acc-a-b*k;
T = [0:dt:td]';
%plot(T,acc)
title('Corrected record, first pass')
%pause

% Second pass: minimize squared velocity using a
% parabolic baseline with vanishing 0-th and 1-st moments
v = cumsum(acc)/nt;
k = (0.5:nt-0.5)'/nt;
phi = k.*(1-k).*(1-2*k);
C = sum(phi.*v)/sum(phi.*phi);
acc = acc - C*(1-6*k.*(1-k));

% Restore leading and trailing zeroes, if any
if n1>1,  acc = [zeros(n1-1,1); acc]; end
if n2<nn, acc = [acc; zeros(nn-n2,1)]; end
td = (nn-1)*dt;

vg = dt*cumsum(acc);
dg = dt*cumsum(vg);
n1 = length(acc)-1;
vg = [0; vg(1:n1)];
dg = [0; dg(1:n1)];
a = dderiv(dg,dt);

% temporary statements: visualize baseline corrected record
T = [0:dt:td];
% plot(T,acc)
% hold on
% plot(T,a,'r');
% grid on;
% hold off;
% title('Corrected record vs. double derivative of displacement')
% pause;
% plot(T,vg)
% grid on;
% title('Corrected velocity')
% pause;
% plot(T,dg)
% grid on;
% title('Corrected displacement')
```

```
% pause;
close
return

function [a] = dderiv(x, dt)
% Computes the second derivative of [x] with respect to t using the
central
% difference method. dt is the time step
% Assumes x to be a column vector, with data at equal time intervals
n = length(x);
x0 = [0; 0; x];
x1 = [0; x; 0];
x2 = [x; 0; 0];
a = (x2-2*x1+x0)/dt^2;
a = a(2:n+1); % discard first and last point to match original size
a(1) = a(2);  % avoid artifacts at ends
a(n) = a(n-1);
return
```

APPENDIX C – MATLAB OUTPUTS

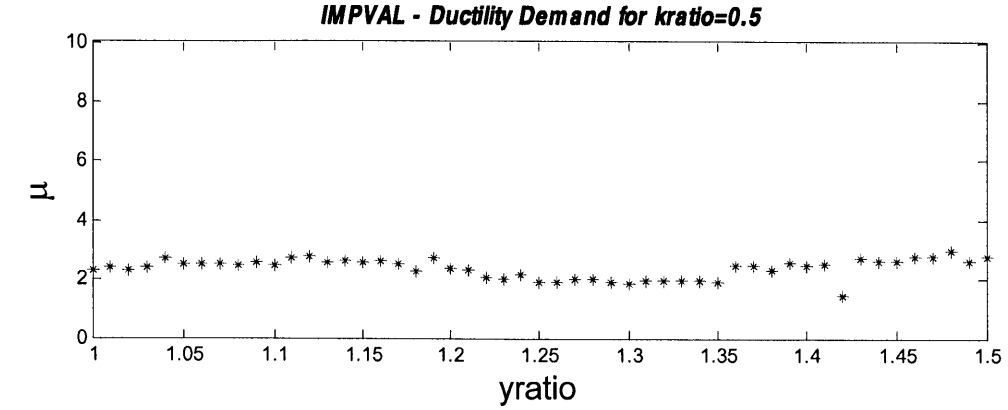
IMPVAL - Ductility Demand for kratio=0.5
μ
yratio

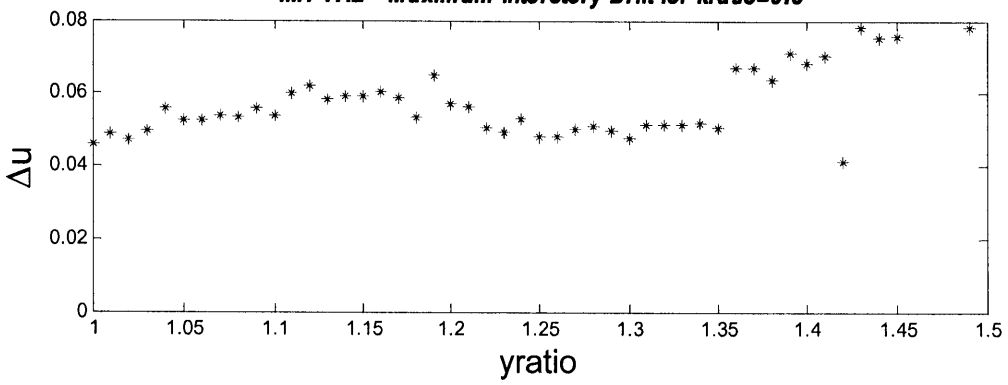
IMPVAL - Maximum Interstory Drift for kratio=0.5
Δu
yratio

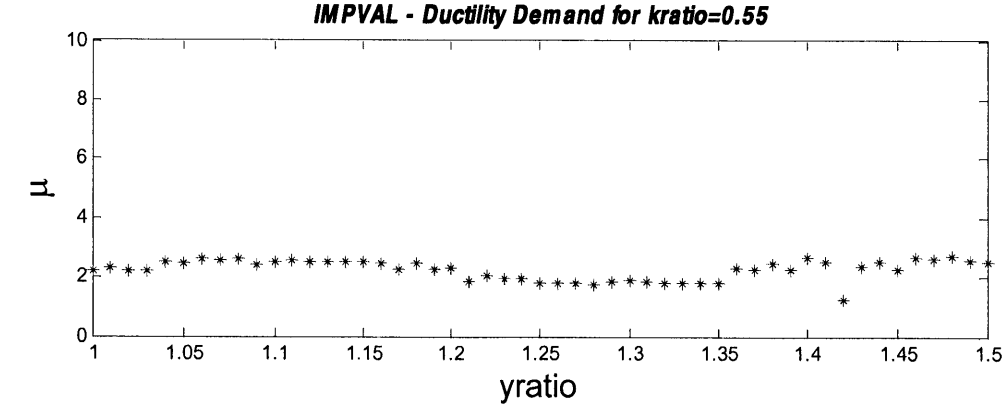
IMPVAL - Ductility Demand for kratio=0.55
μ
yratio

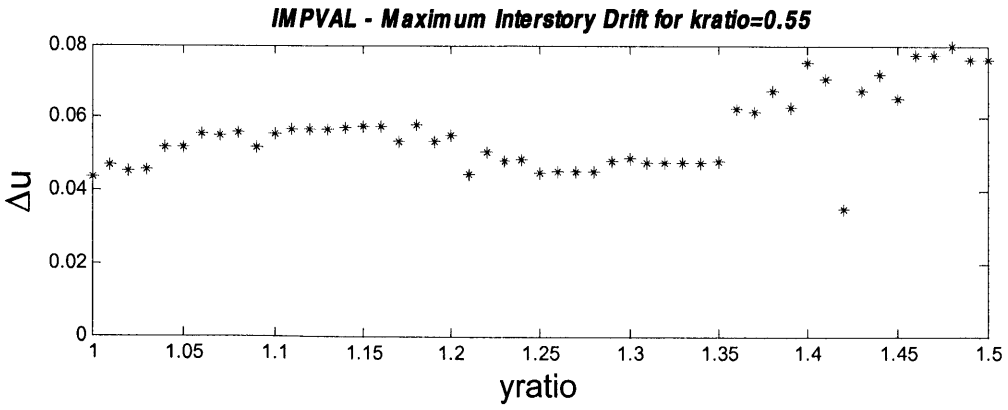
IMPVAL - Maximum Interstory Drift for kratio=0.55
Δu
yratio

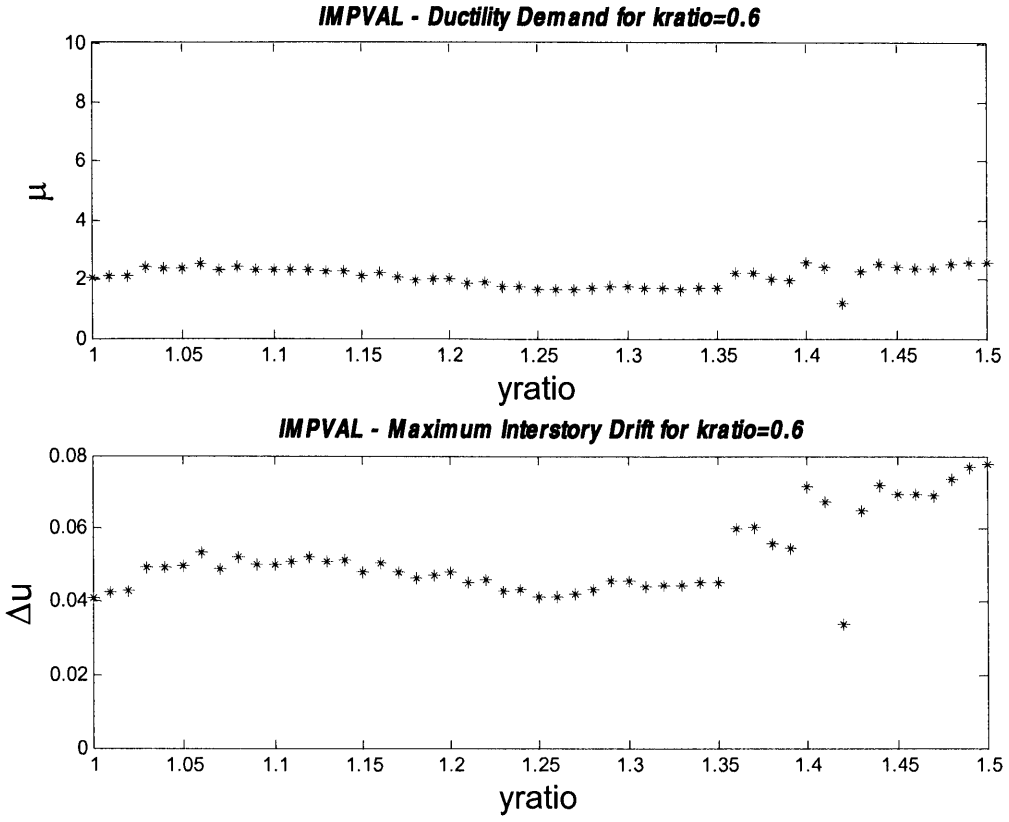
IMPVAL - Ductility Demand for kratio=0.6
μ
yratio
IMPVAL - Maximum Interstory Drift for kratio=0.6
Δu
yratio

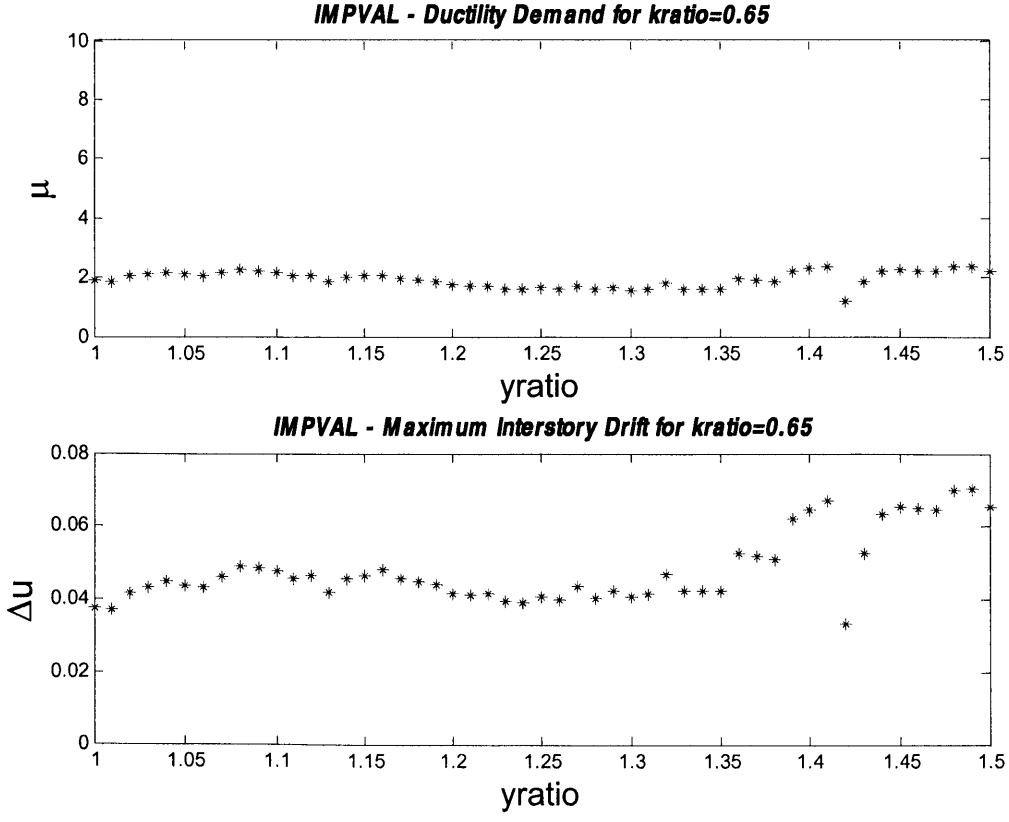
IMPVAL - Ductility Demand for kratio=0.65
μ
yratio
IMPVAL - Maximum Interstory Drift for kratio=0.65
Δu
yratio

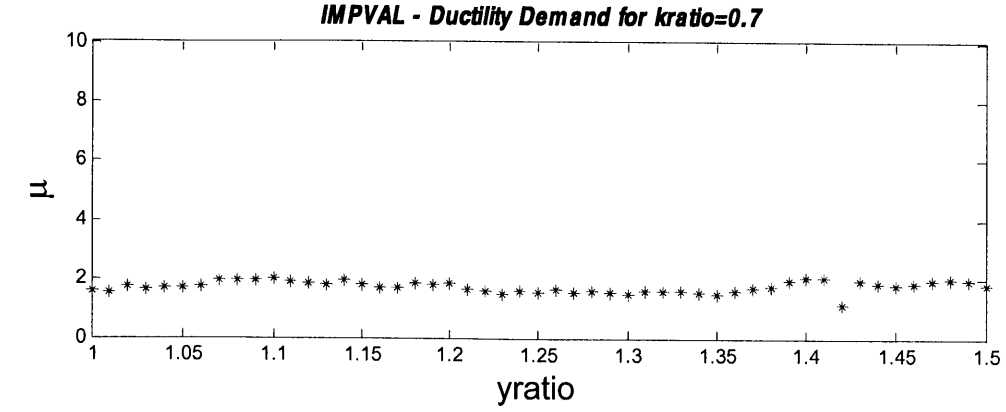
IMPVAL - Ductility Demand for kratio=0.7
μ
yratio

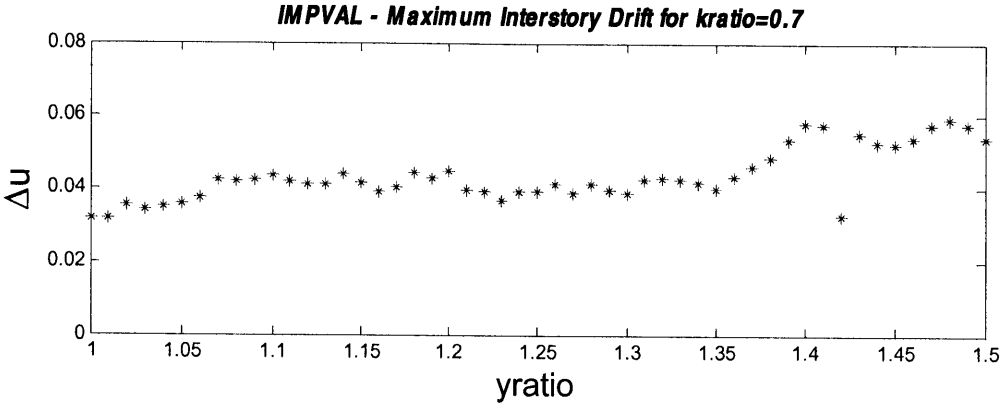
IMPVAL - Maximum Interstory Drift for kratio=0.7
Δu
yratio

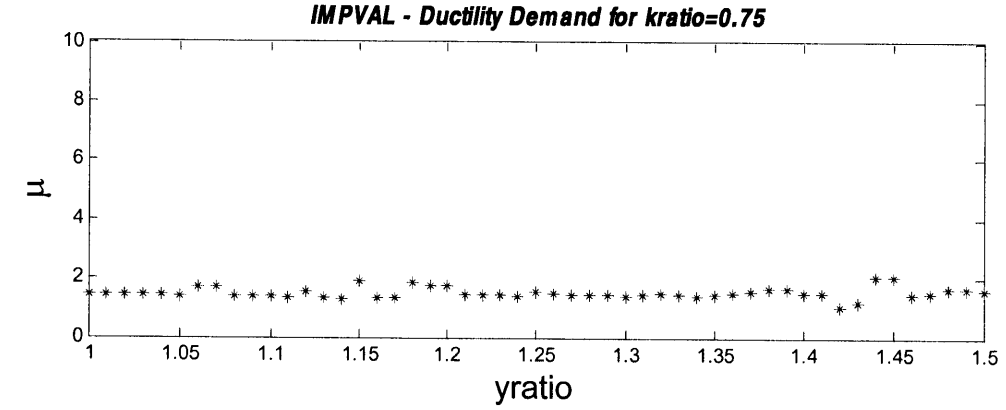
IMPVAL - Ductility Demand for kratio=0.75
μ
yratio

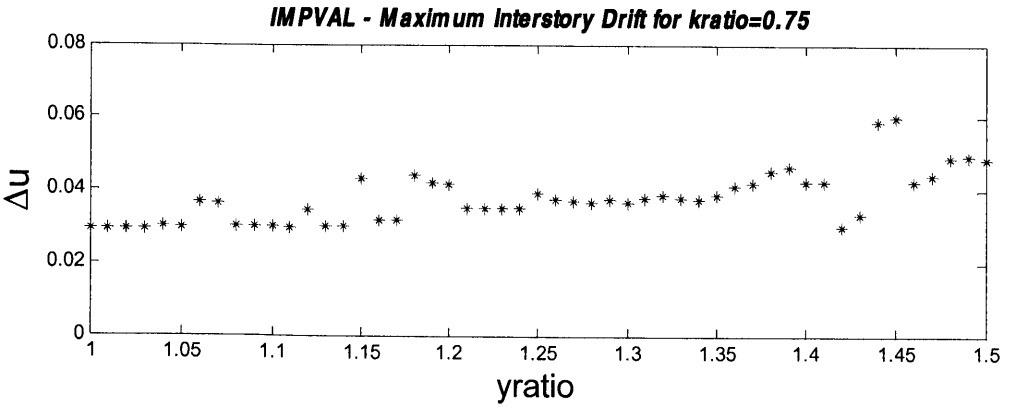
IMPVAL - Maximum Interstory Drift for kratio=0.75
Δu
yratio

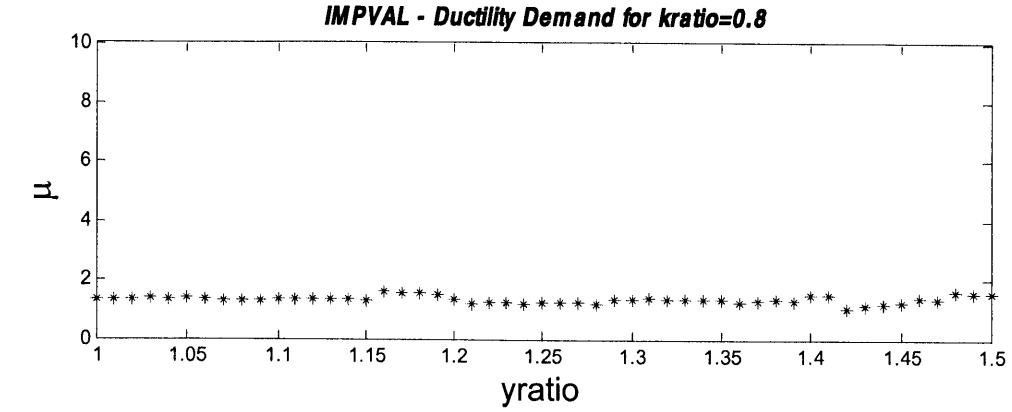
IMPVAL - Ductility Demand for kratio=0.8
μ
yratio

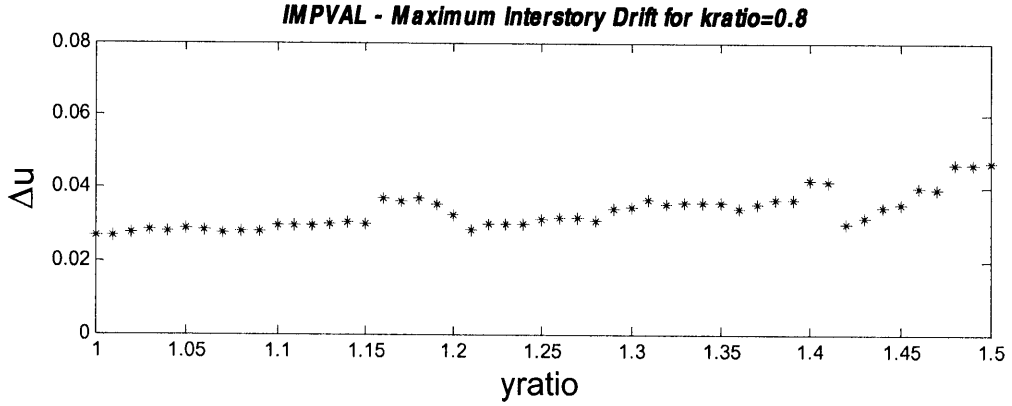
IMPVAL - Maximum Interstory Drift for kratio=0.8
Δu
yratio

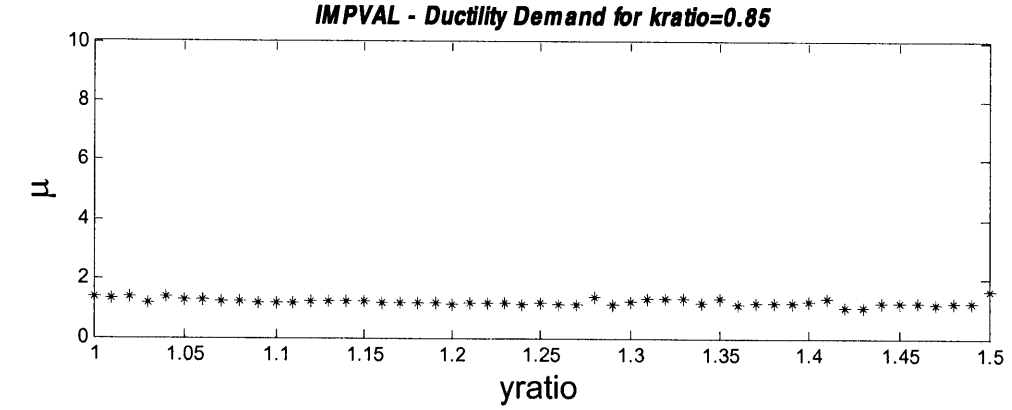
IMPVAL - Ductility Demand for kratio=0.85
μ
yratio

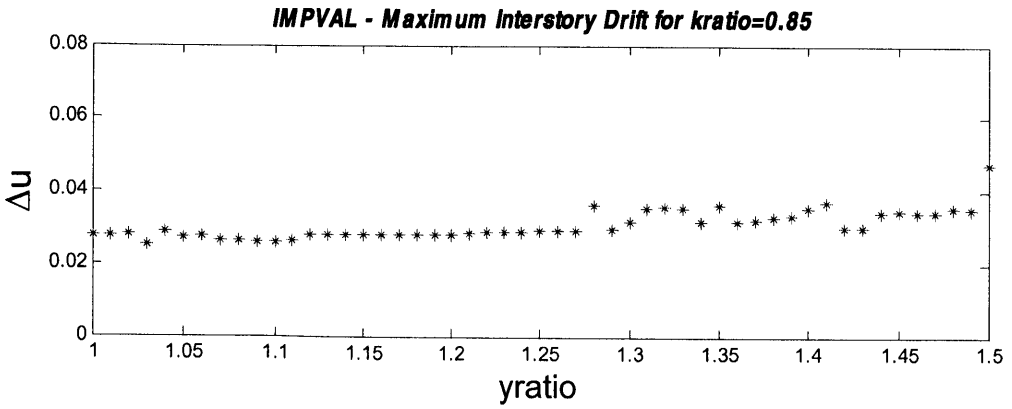
IMPVAL - Maximum Interstory Drift for kratio=0.85
Δu
yratio

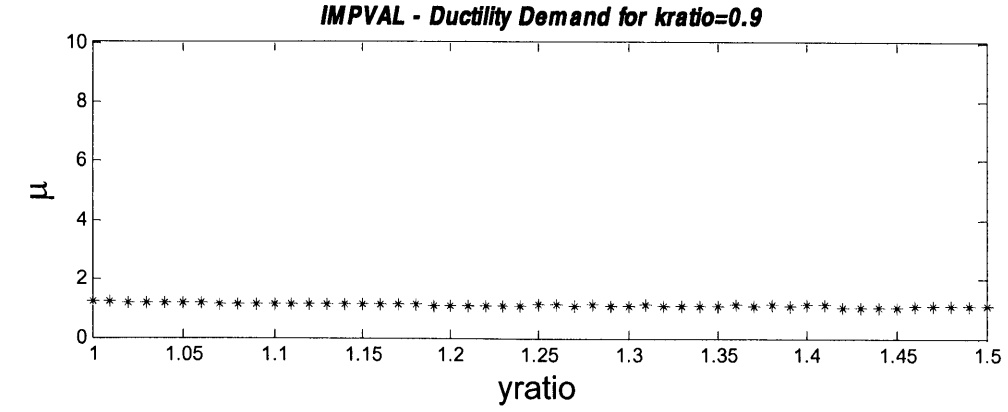
IMPVAL - Ductility Demand for kratio=0.9
μ
yratio
0
2
4
6
8
10
1
1.05
1.1
1.15
1.2
1.25
1.3
1.35
1.4
1.45
1.5

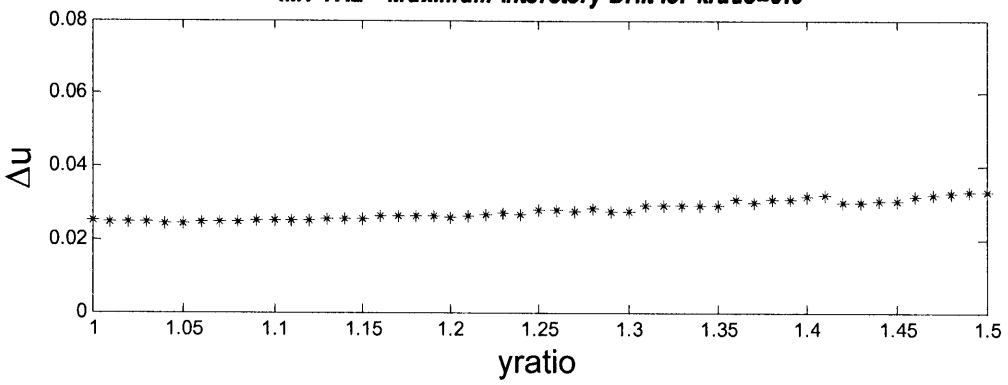
IMPVAL - Maximum Interstory Drift for kratio=0.9
Δu
yratio
0
0.02
0.04
0.06
0.08
1
1.05
1.1
1.15
1.2
1.25
1.3
1.35
1.4
1.45
1.5

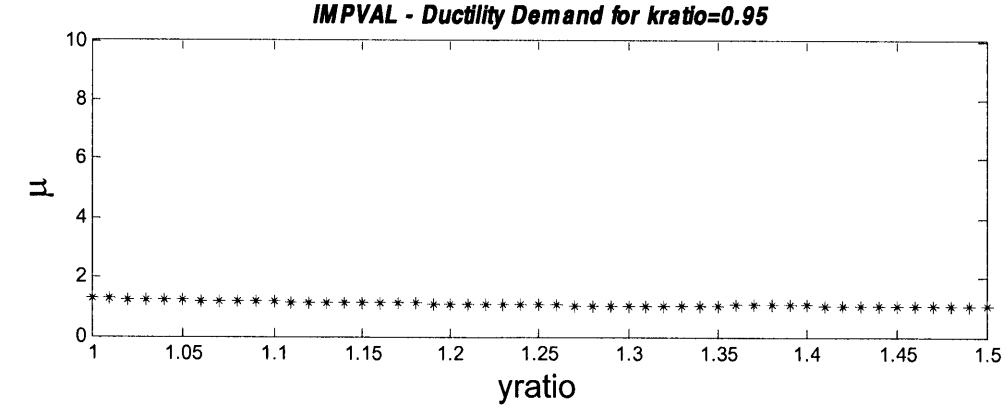
IMPVAL - Ductility Demand for kratio=0.95
μ
yratio
0
2
4
6
8
10
1
1.05
1.1
1.15
1.2
1.25
1.3
1.35
1.4
1.45
1.5

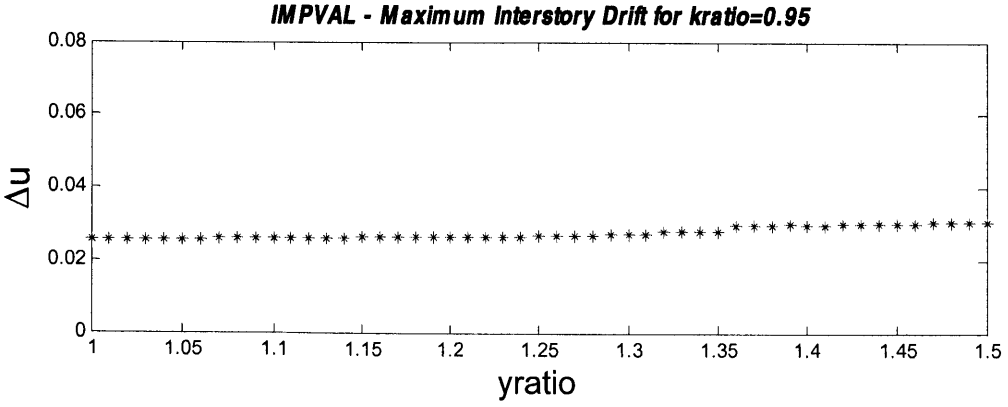
IMPVAL - Maximum Interstory Drift for kratio=0.95
Δu
yratio
0
0.02
0.04
0.06
0.08
1
1.05
1.1
1.15
1.2
1.25
1.3
1.35
1.4
1.45
1.5

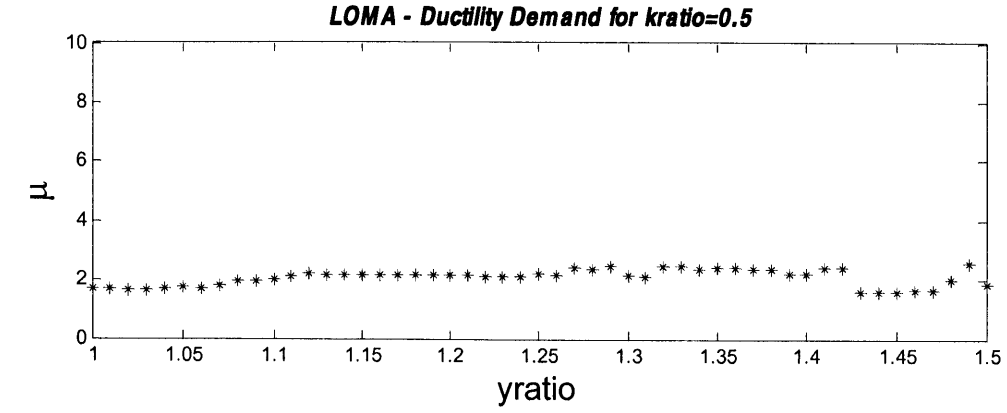
LOMA - Ductility Demand for kratio=0.5
μ
yratio

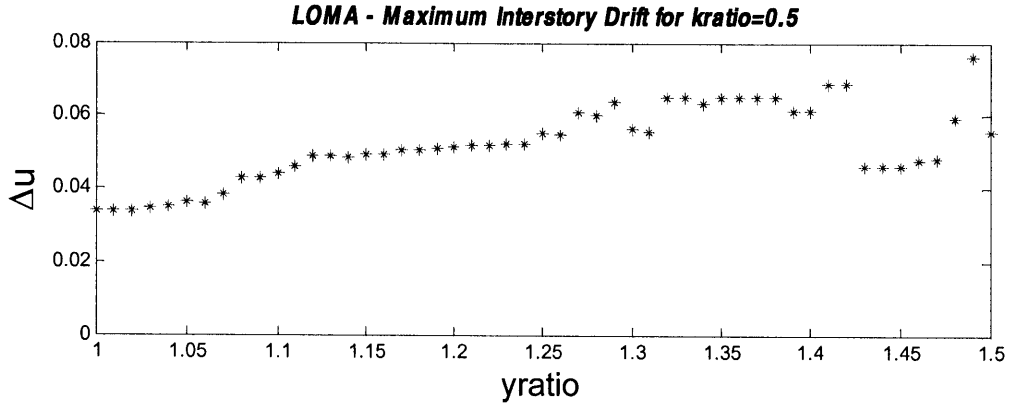
LOMA - Maximum Interstory Drift for kratio=0.5
Δu
yratio

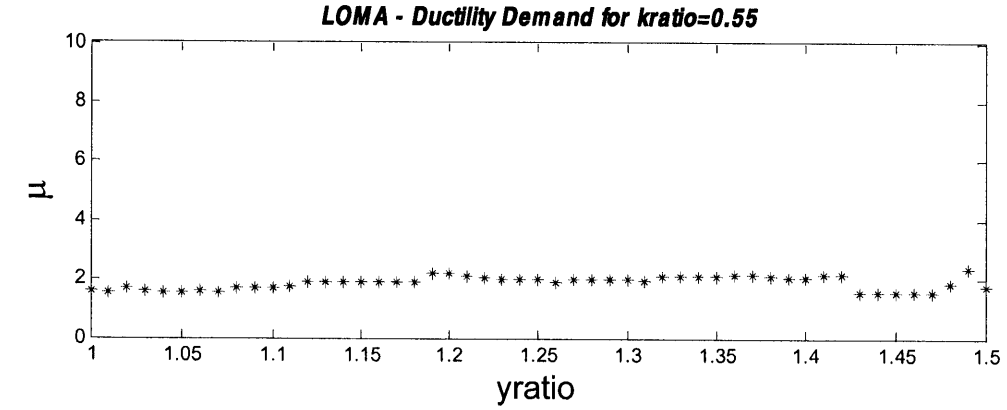
LOMA - Ductility Demand for kratio=0.55
μ
yratio

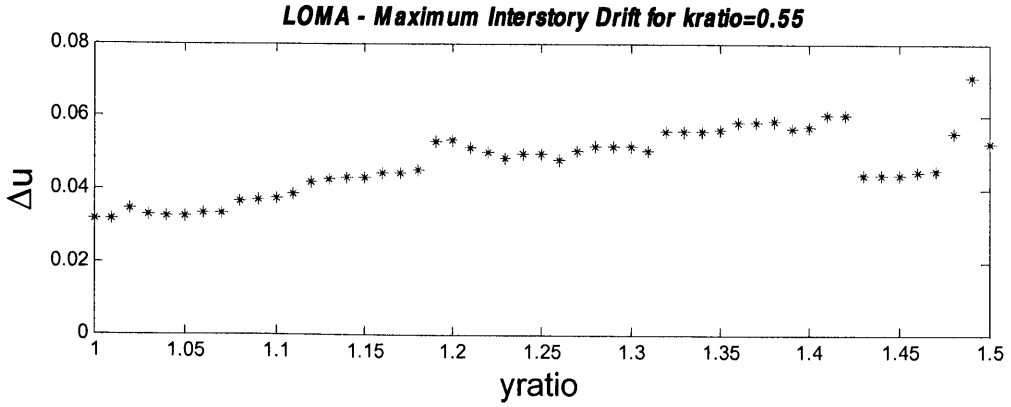
LOMA - Maximum Interstory Drift for kratio=0.55
Δu
yratio

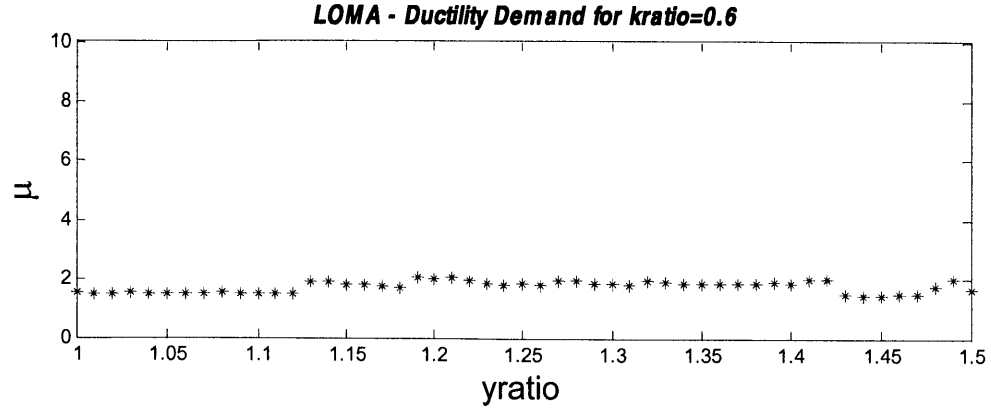
LOMA - Ductility Demand for kratio=0.6
μ
yratio

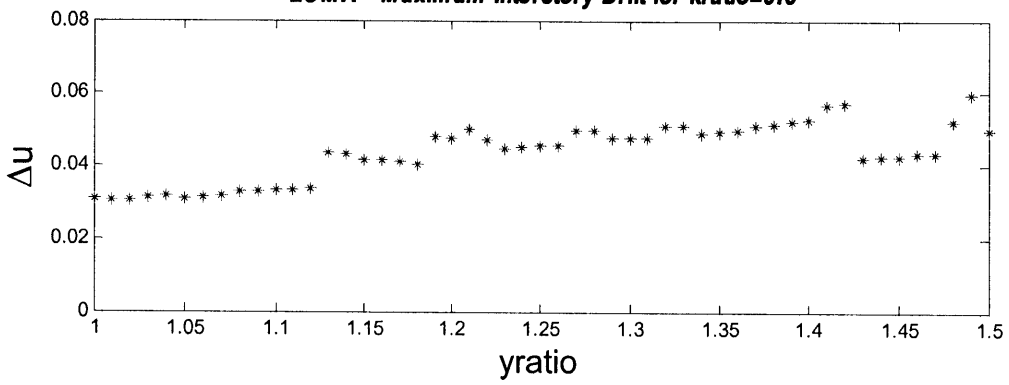
LOMA - Maximum Interstory Drift for kratio=0.6
Δu
yratio

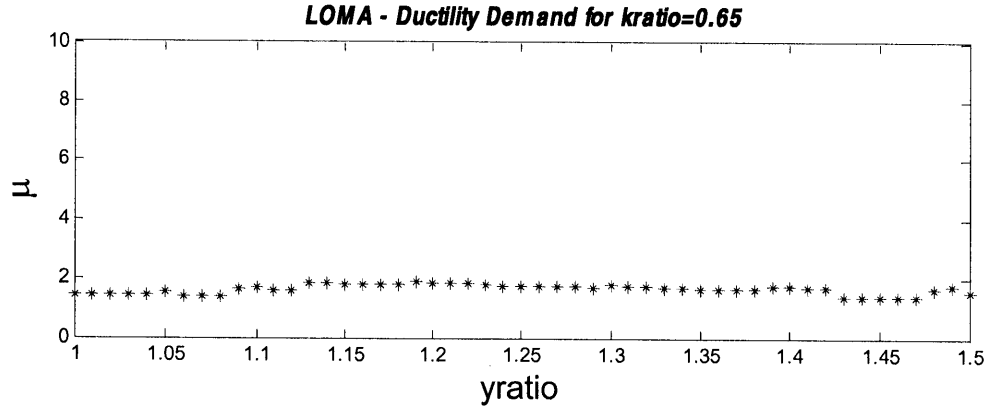
LOMA - Ductility Demand for kratio=0.65
μ
yratio

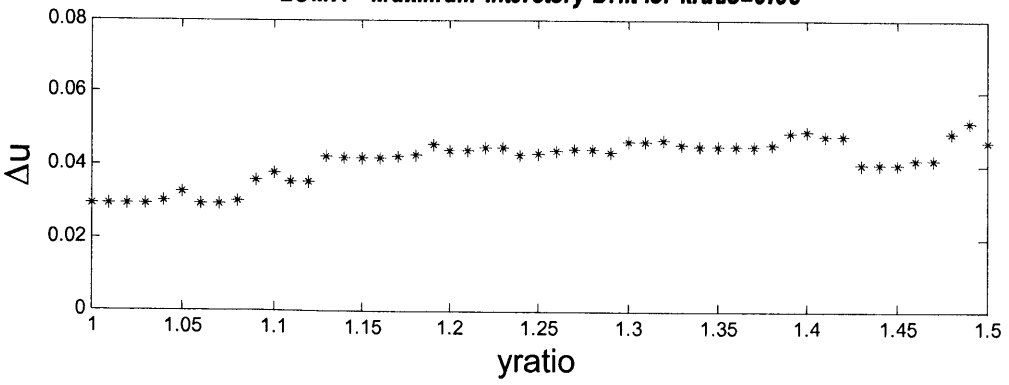
LOMA - Maximum Interstory Drift for kratio=0.65
Δu
yratio

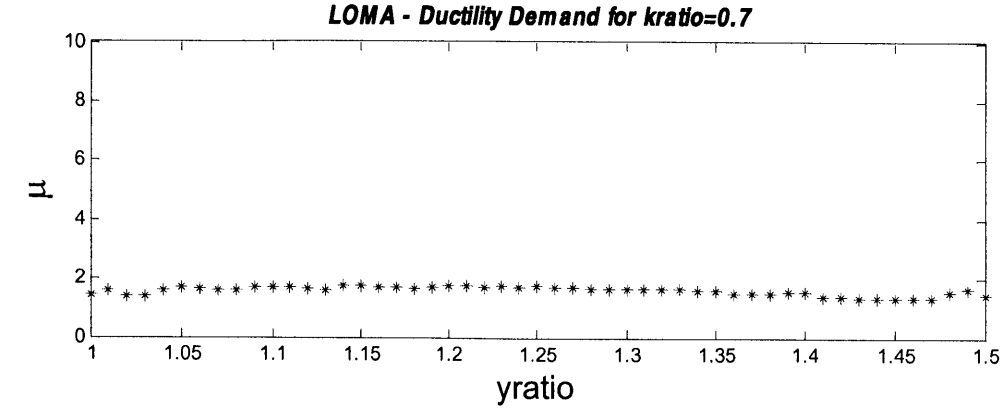
LOMA - Ductility Demand for kratio=0.7
μ
yratio
0
2
4
6
8
10
1
1.05
1.1
1.15
1.2
1.25
1.3
1.35
1.4
1.45
1.5

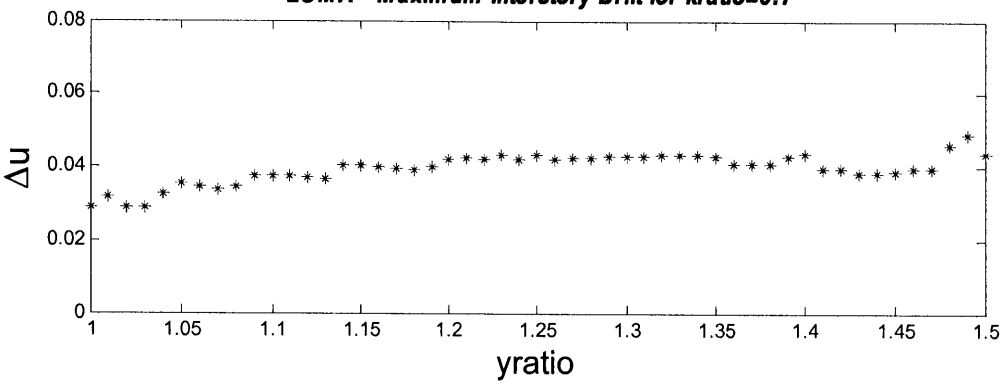
LOMA - Maximum Interstory Drift for kratio=0.7
Δu
yratio
0
0.02
0.04
0.06
0.08
1
1.05
1.1
1.15
1.2
1.25
1.3
1.35
1.4
1.45
1.5

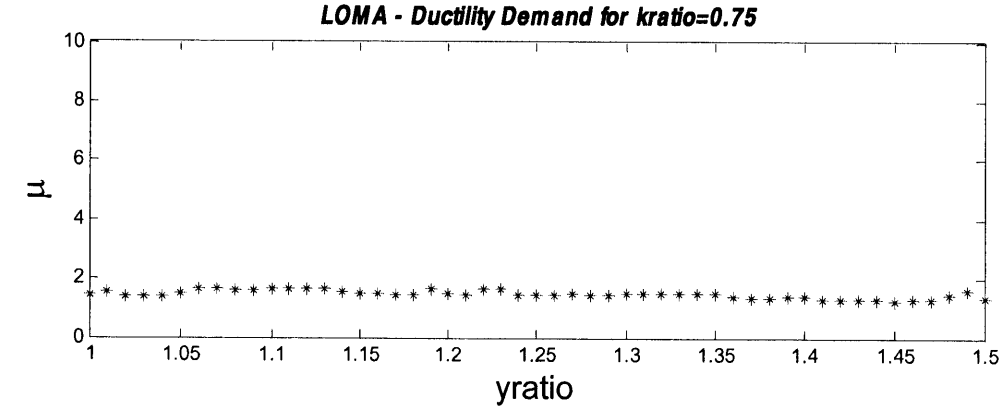
LOMA - Ductility Demand for kratio=0.75
μ
yratio
0
2
4
6
8
10
1
1.05
1.1
1.15
1.2
1.25
1.3
1.35
1.4
1.45
1.5

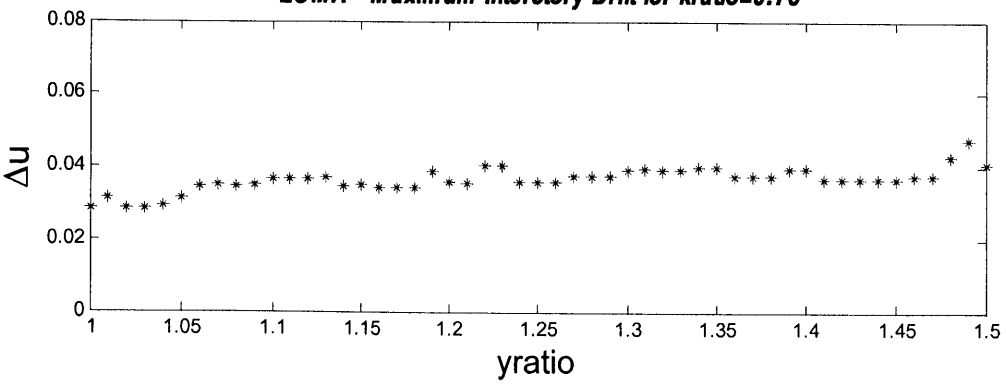
LOMA - Maximum Interstory Drift for kratio=0.75
Δu
yratio
0
0.02
0.04
0.06
0.08
1
1.05
1.1
1.15
1.2
1.25
1.3
1.35
1.4
1.45
1.5

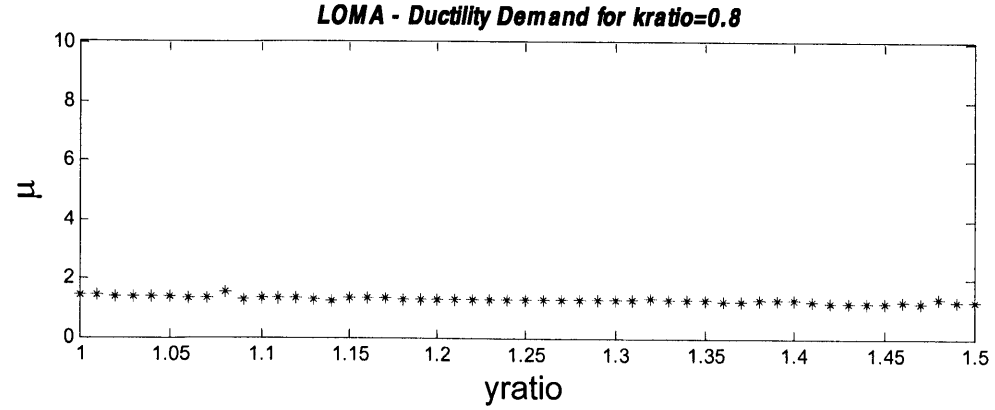
LOMA - Ductility Demand for kratio=0.8
μ
yratio

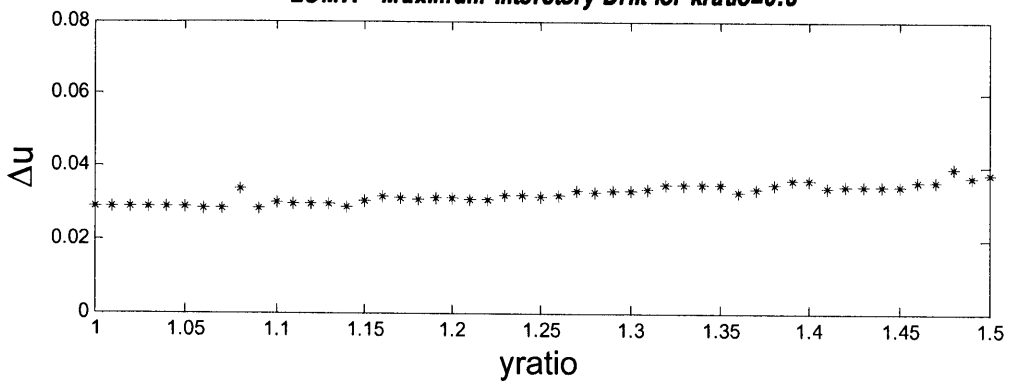
LOMA - Maximum Interstory Drift for kratio=0.8
Δu
yratio

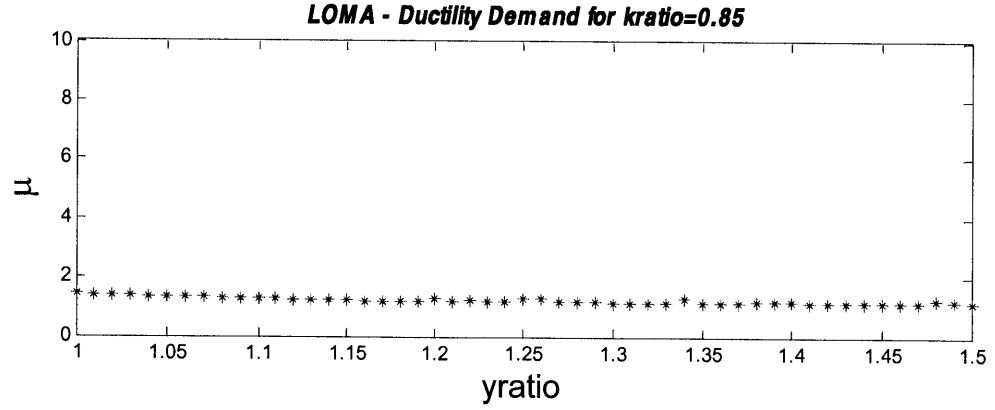
LOMA - Ductility Demand for kratio=0.85
μ
yratio

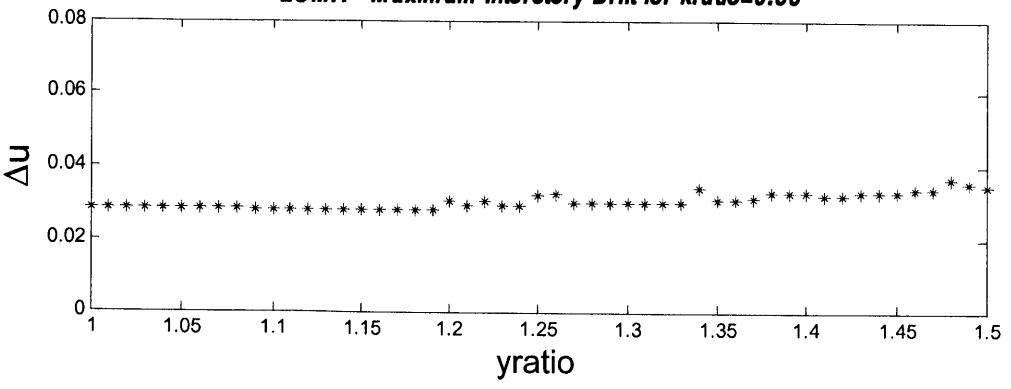
LOMA - Maximum Interstory Drift for kratio=0.85
Δu
yratio

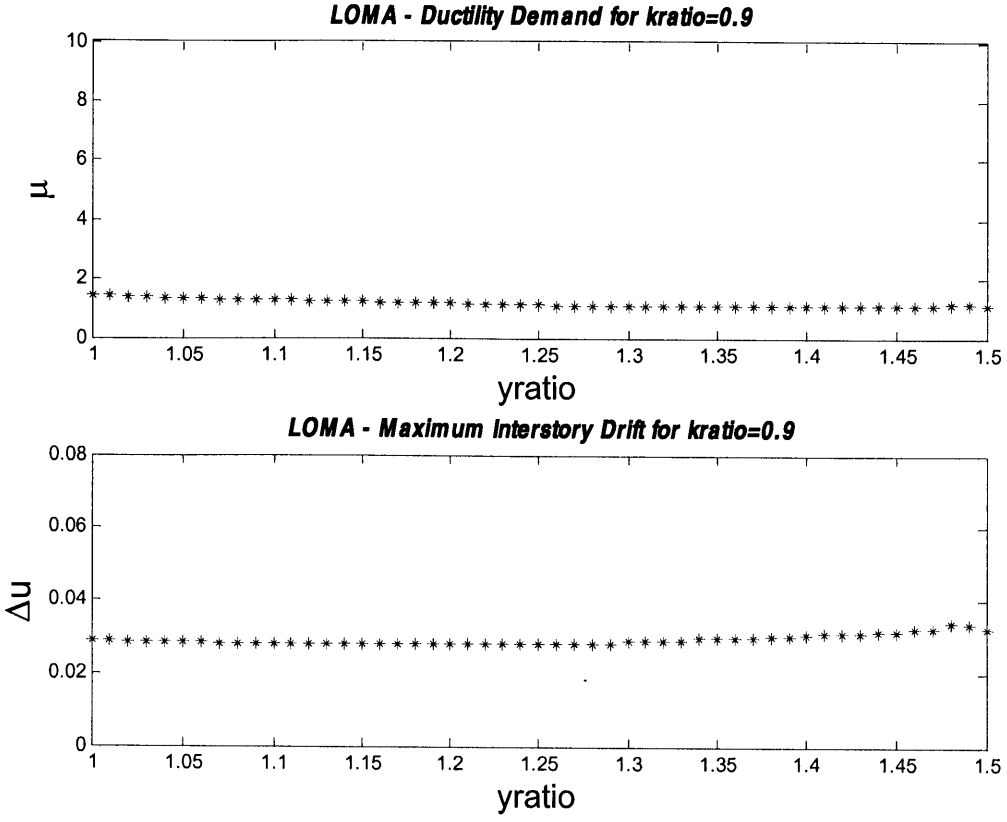
LOMA - Ductility Demand for kratio=0.9
μ
yratio
LOMA - Maximum Interstory Drift for kratio=0.9
Δu
yratio

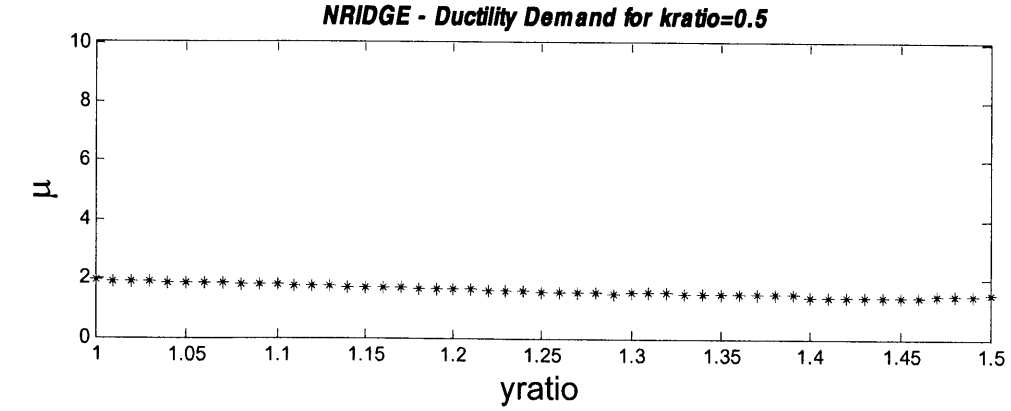
NRIDGE - Ductility Demand for kratio=0.5
μ
yratio
0
2
4
6
8
10
1
1.05
1.1
1.15
1.2
1.25
1.3
1.35
1.4
1.45
1.5

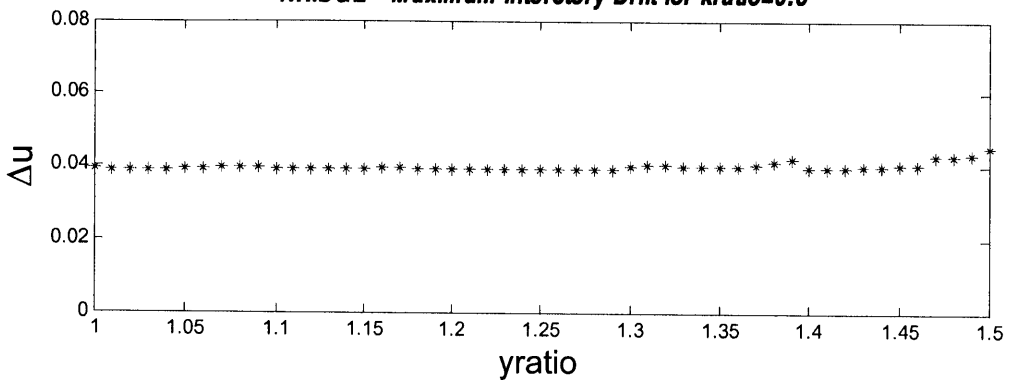
NRIDGE - Maximum Interstory Drift for kratio=0.5
Δu
yratio
0
0.02
0.04
0.06
0.08
1
1.05
1.1
1.15
1.2
1.25
1.3
1.35
1.4
1.45
1.5

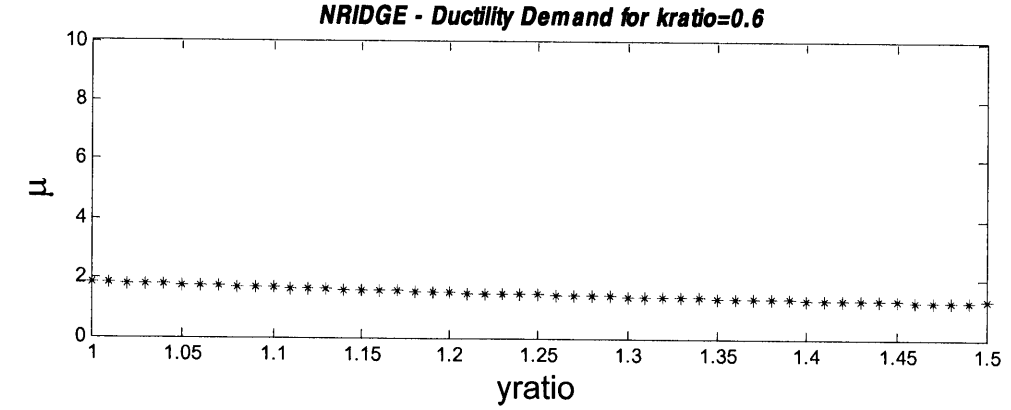
NRIDGE - Ductility Demand for kratio=0.6
μ
yratio
0
2
4
6
8
10
1
1.05
1.1
1.15
1.2
1.25
1.3
1.35
1.4
1.45
1.5

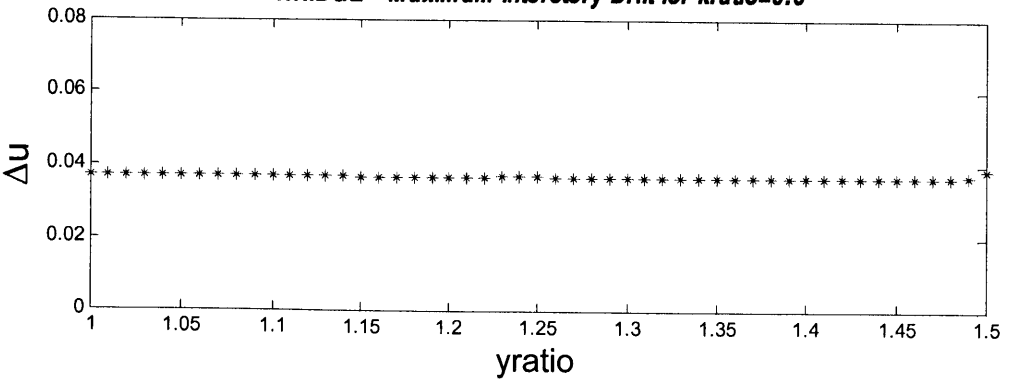
NRIDGE - Maximum Interstory Drift for kratio=0.6
Δu
yratio
0
0.02
0.04
0.06
0.08
1
1.05
1.1
1.15
1.2
1.25
1.3
1.35
1.4
1.45
1.5

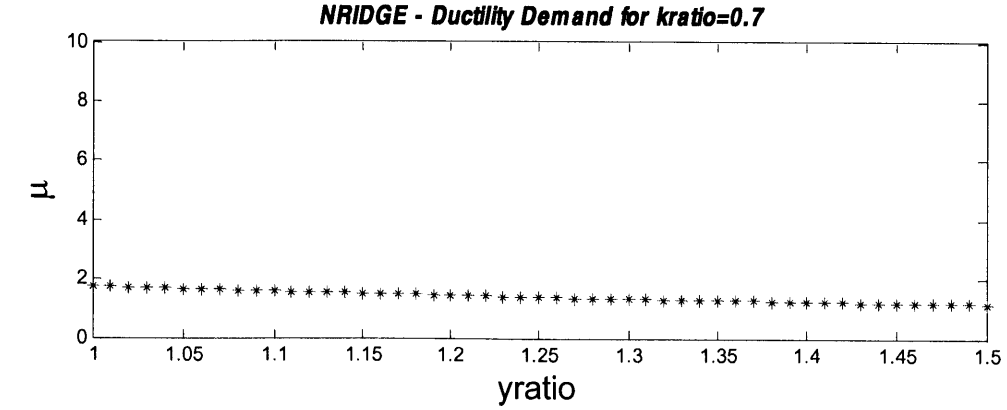
NRIDGE - Ductility Demand for kratio=0.7
μ
yratio
0
2
4
6
8
10
1
1.05
1.1
1.15
1.2
1.25
1.3
1.35
1.4
1.45
1.5

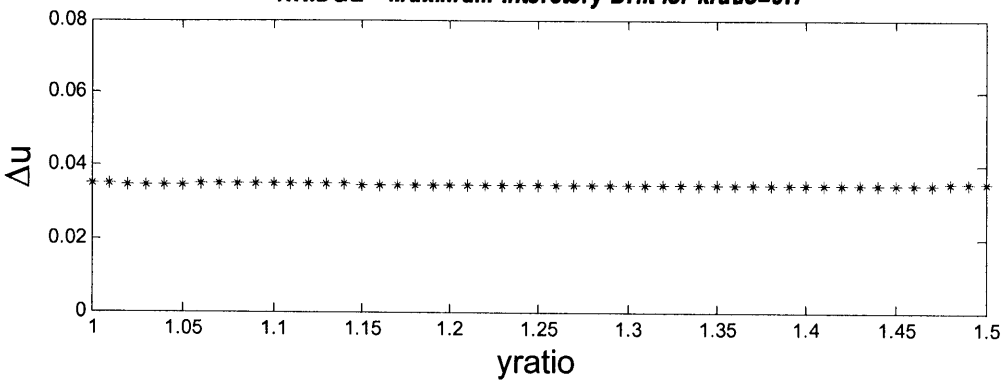
NRIDGE - Maximum Interstory Drift for kratio=0.7
Δu
yratio
0
0.02
0.04
0.06
0.08
1
1.05
1.1
1.15
1.2
1.25
1.3
1.35
1.4
1.45
1.5

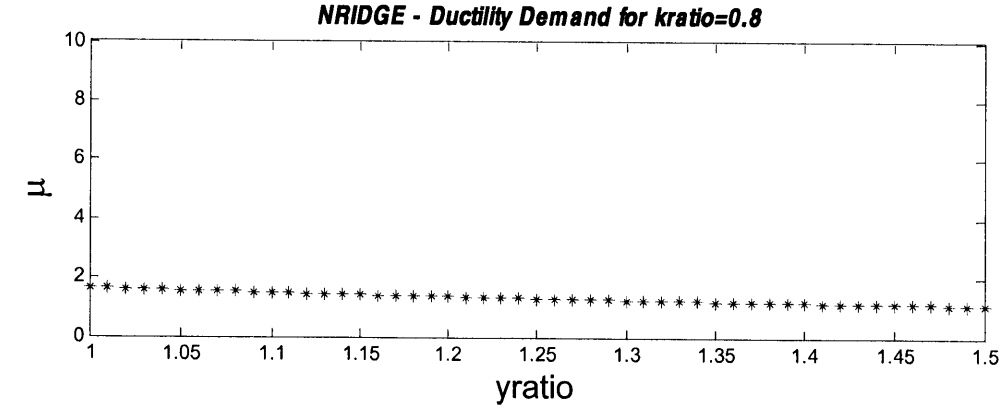
NRIDGE - Ductility Demand for kratio=0.8
μ
yratio
0
2
4
6
8
10
1
1.05
1.1
1.15
1.2
1.25
1.3
1.35
1.4
1.45
1.5

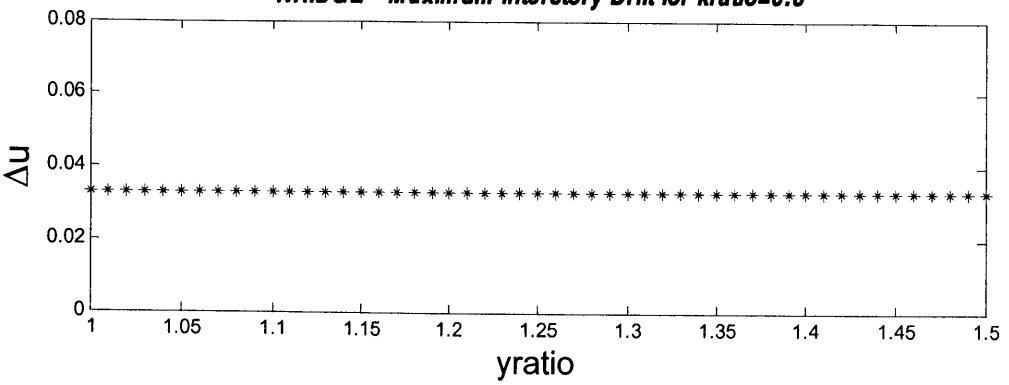
NRIDGE - Maximum Interstory Drift for kratio=0.8
Δu
yratio
0
0.02
0.04
0.06
0.08
1
1.05
1.1
1.15
1.2
1.25
1.3
1.35
1.4
1.45
1.5

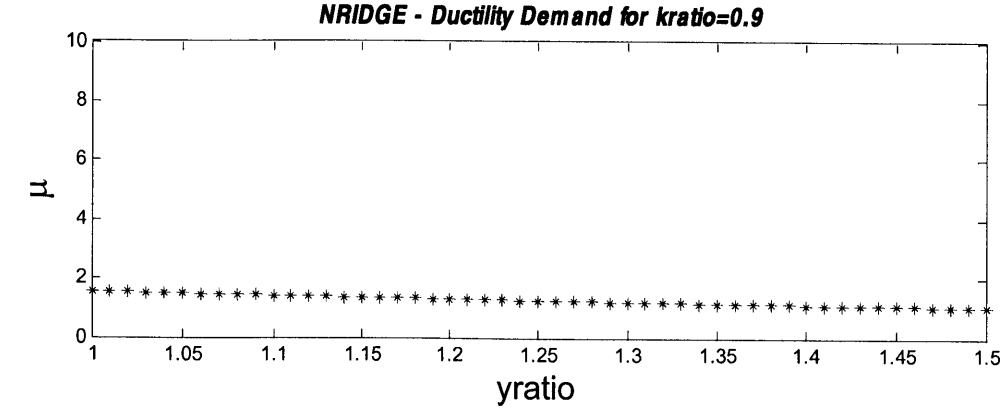
NRIDGE - Ductility Demand for kratio=0.9
μ
yratio
0
2
4
6
8
10
1
1.05
1.1
1.15
1.2
1.25
1.3
1.35
1.4
1.45
1.5

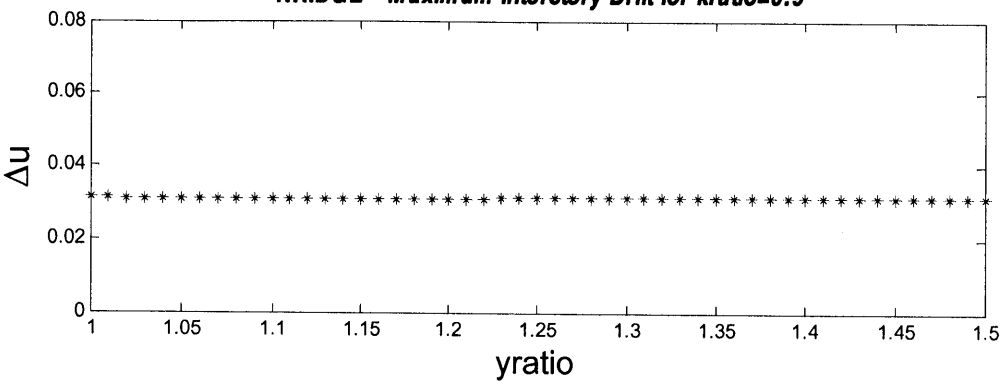
NRIDGE - Maximum Interstory Drift for kratio=0.9
Δu
yratio
0
0.02
0.04
0.06
0.08
1
1.05
1.1
1.15
1.2
1.25
1.3
1.35
1.4
1.45
1.5

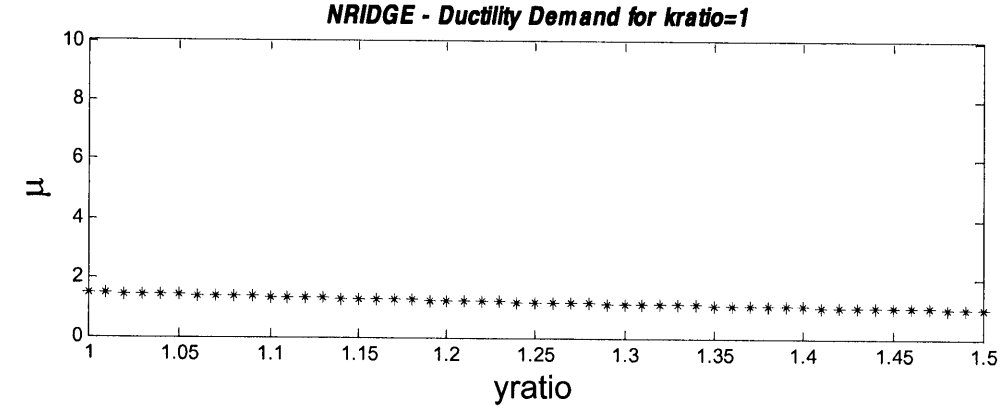
NRIDGE - Ductility Demand for kratio=1
μ
yratio
0
2
4
6
8
10
1
1.05
1.1
1.15
1.2
1.25
1.3
1.35
1.4
1.45
1.5

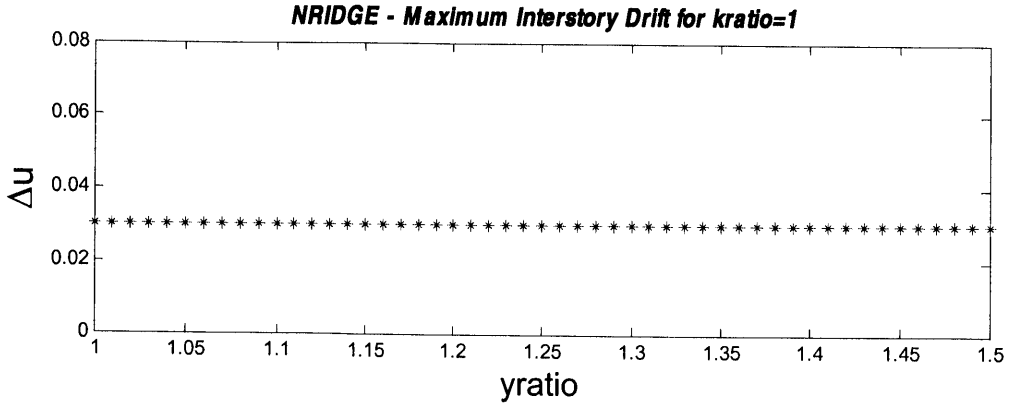
NRIDGE - Maximum Interstory Drift for kratio=1
Δu
yratio
0
0.02
0.04
0.06
0.08
1
1.05
1.1
1.15
1.2
1.25
1.3
1.35
1.4
1.45
1.5

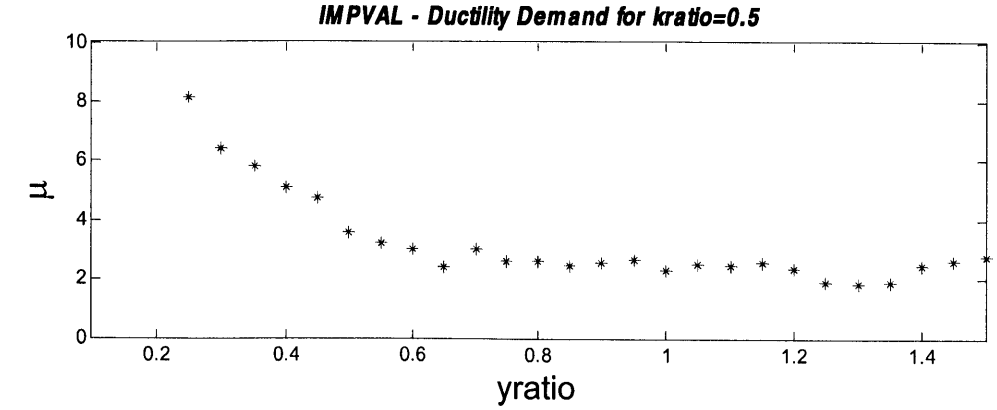
IMPVAL - Ductility Demand for kratio=0.5
μ
yratio
0
2
4
6
8
10
0.2
0.4
0.6
0.8
1
1.2
1.4

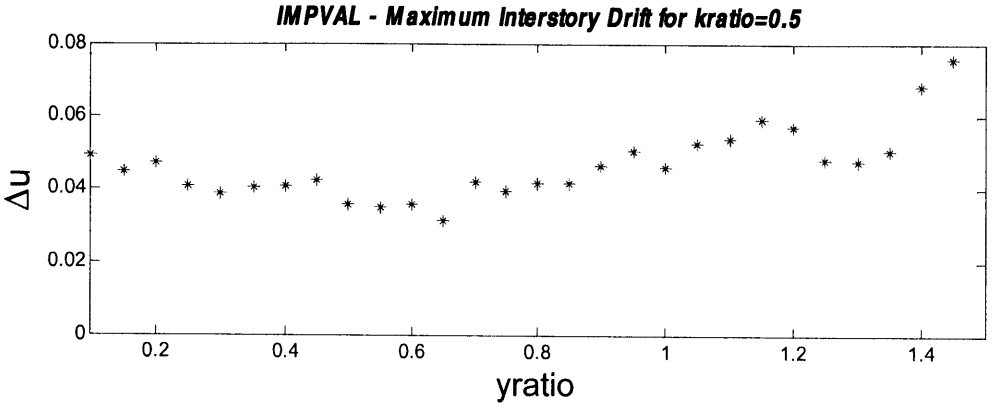
IMPVAL - Maximum Interstory Drift for kratio=0.5
Δu
yratio
0
0.02
0.04
0.06
0.08
0.2
0.4
0.6
0.8
1
1.2
1.4

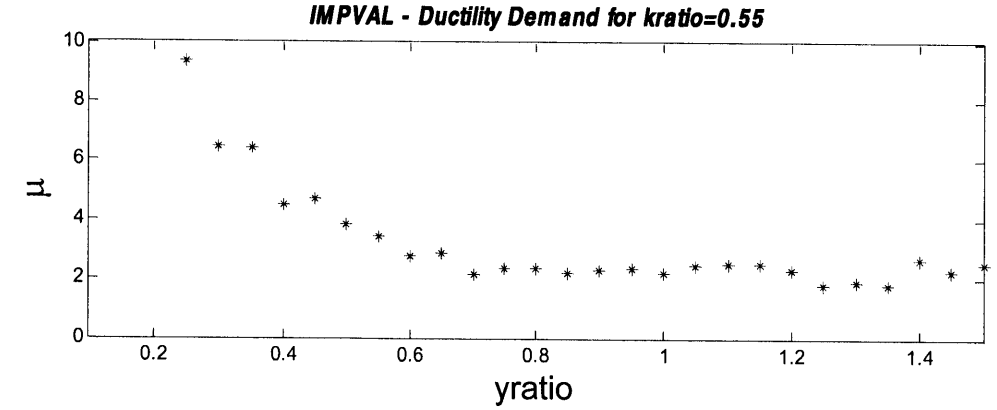
IMPVAL - Ductility Demand for kratio=0.55
μ
yratio
0
2
4
6
8
10
0.2
0.4
0.6
0.8
1
1.2
1.4

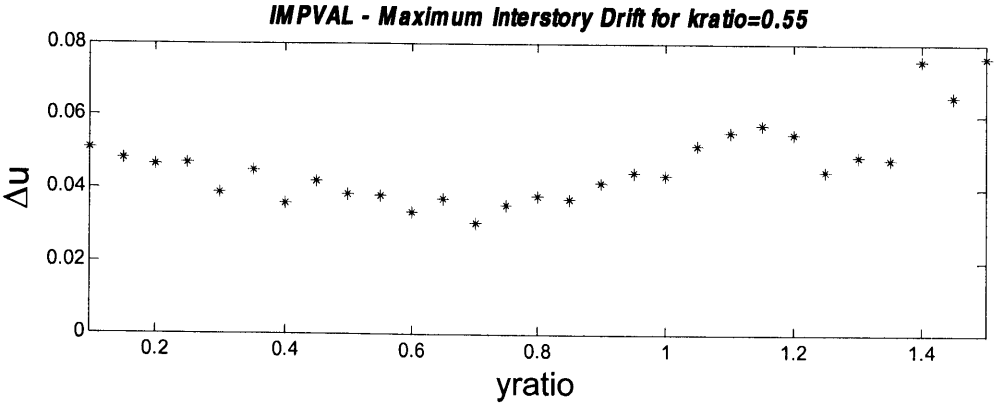
IMPVAL - Maximum Interstory Drift for kratio=0.55
Δu
yratio
0
0.02
0.04
0.06
0.08
0.2
0.4
0.6
0.8
1
1.2
1.4

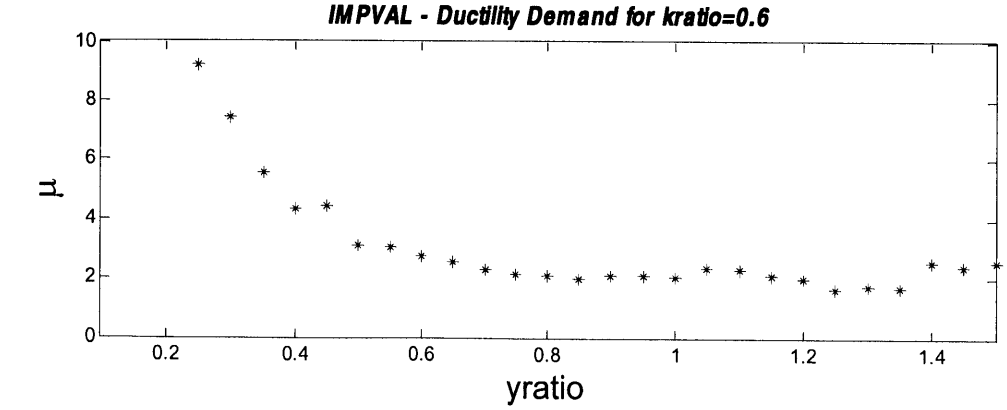
IMPVAL - Ductility Demand for kratio=0.6
μ
yratio

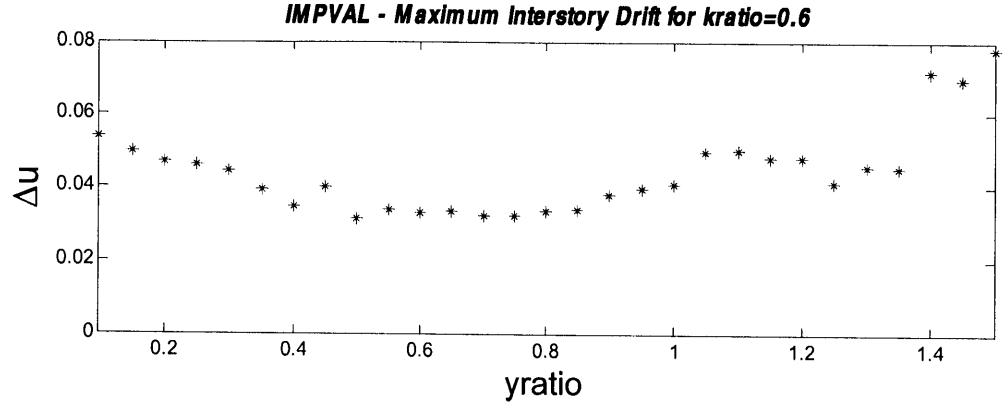
IMPVAL - Maximum Interstory Drift for kratio=0.6
Δu
yratio

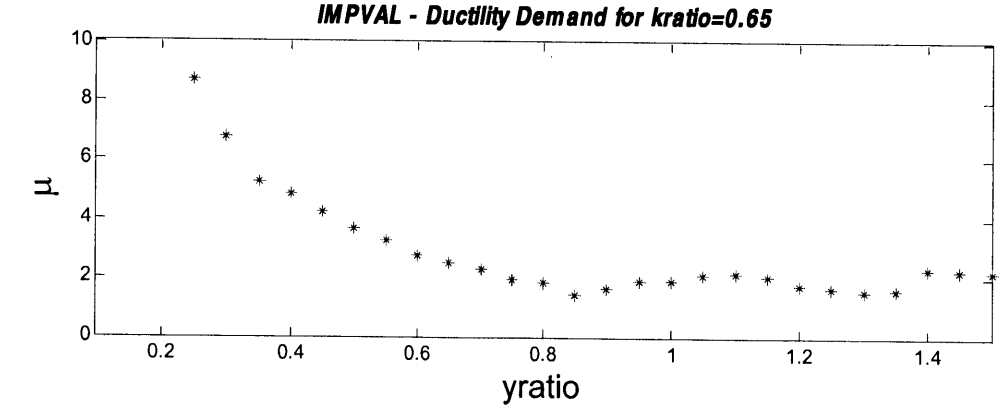
IMPVAL - Ductility Demand for kratio=0.65
μ
yratio

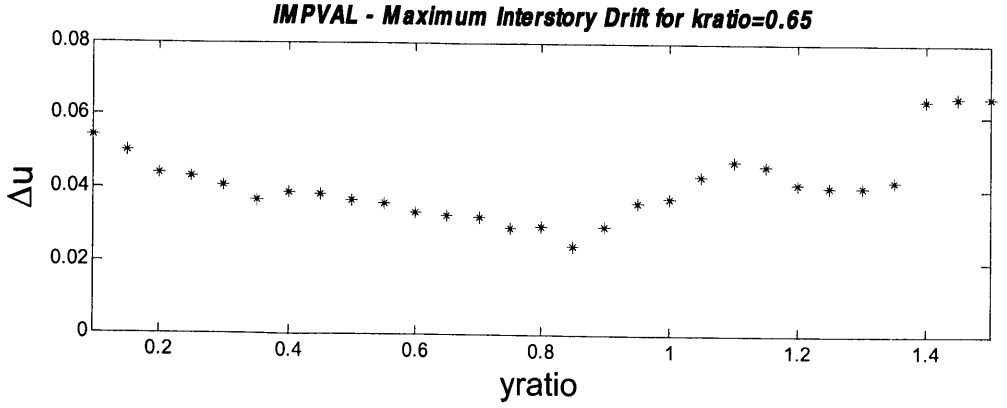
IMPVAL - Maximum Interstory Drift for kratio=0.65
Δu
yratio

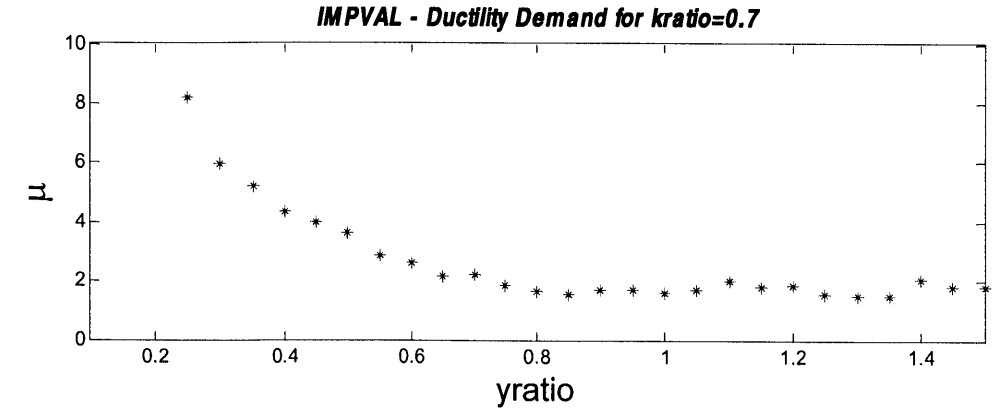
IMPVAL - Ductility Demand for kratio=0.7
μ
yratio

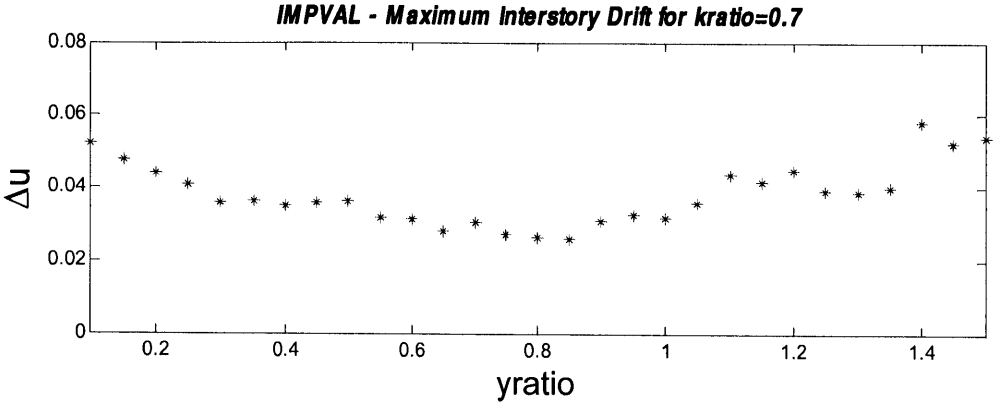
IMPVAL - Maximum Interstory Drift for kratio=0.7
Δu
yratio

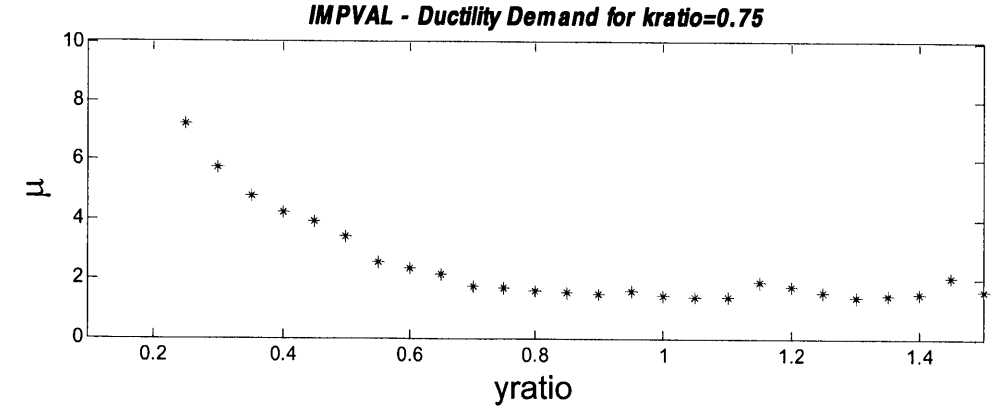
IMPVAL - Ductility Demand for kratio=0.75
μ
yratio

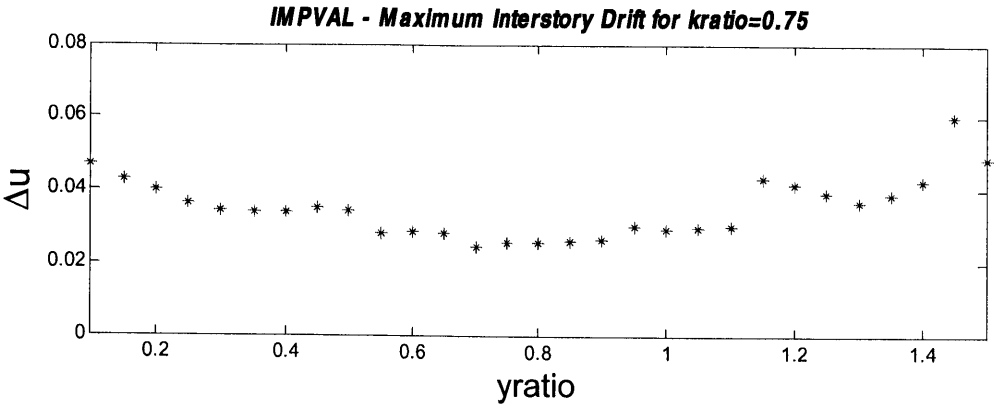
IMPVAL - Maximum Interstory Drift for kratio=0.75
Δu
yratio

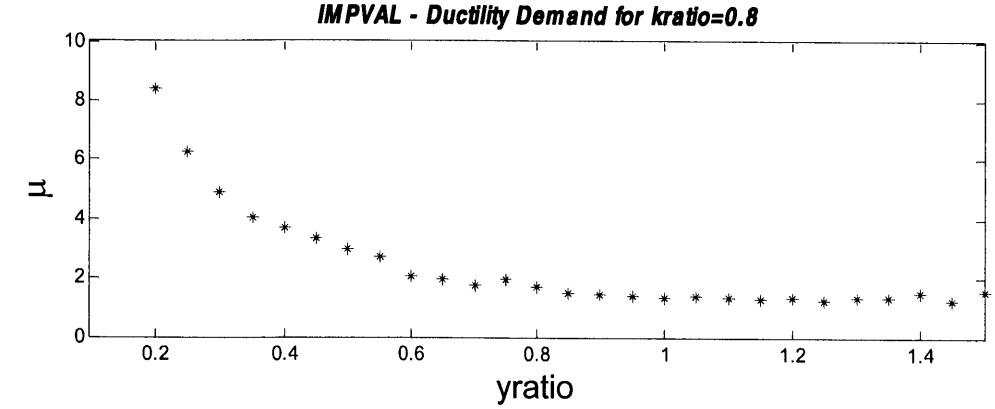
IMPVAL - Ductility Demand for kratio=0.8
μ
yratio

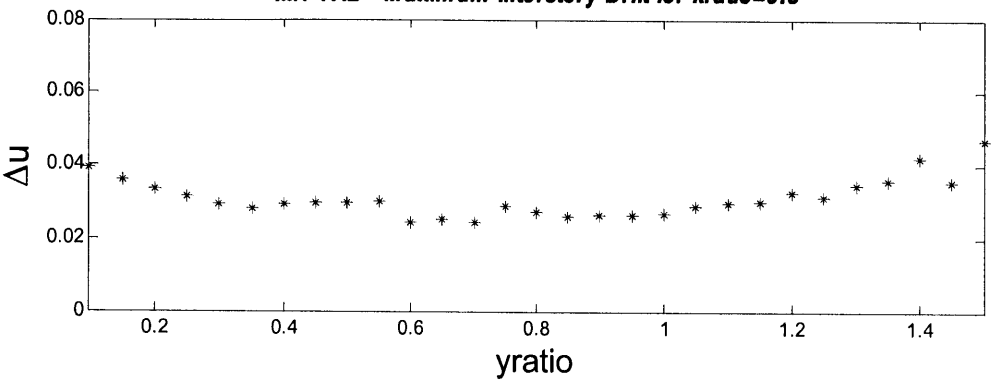
IMPVAL - Maximum Interstory Drift for kratio=0.8
Δu
yratio

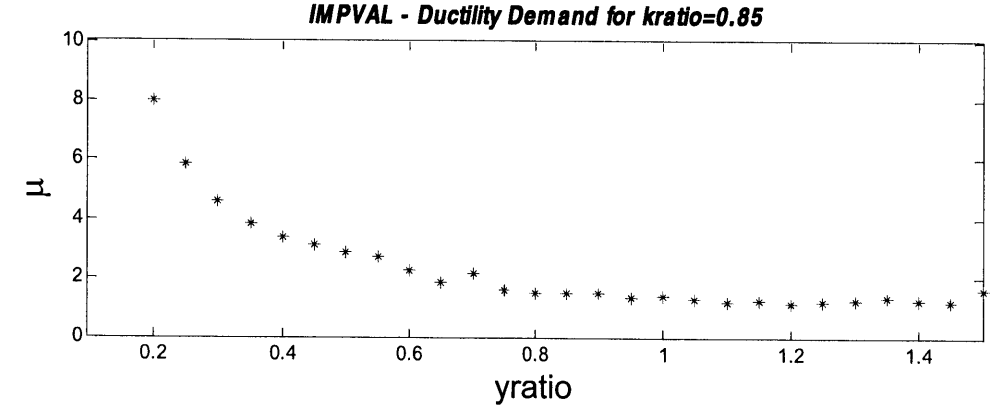
IMPVAL - Ductility Demand for kratio=0.85
μ
yratio

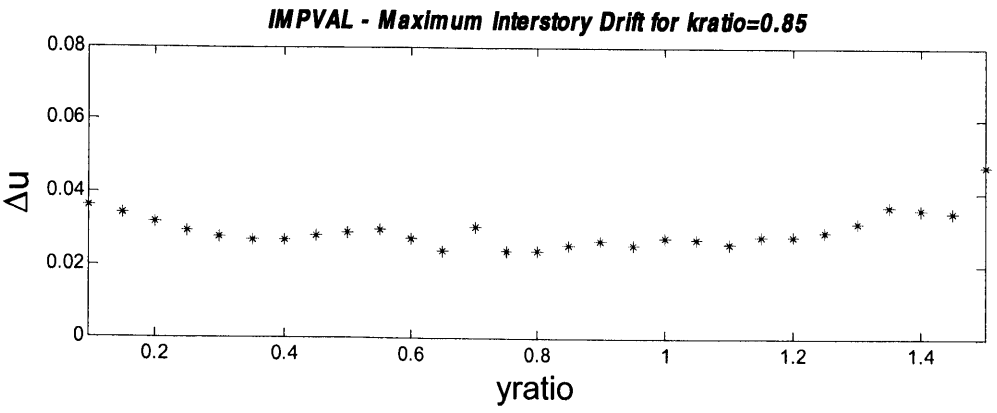
IMPVAL - Maximum Interstory Drift for kratio=0.85
Δu
yratio

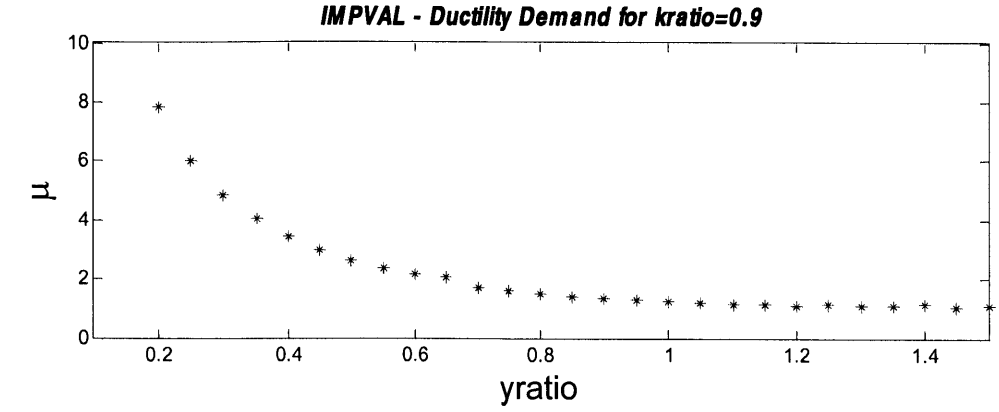
IMPVAL - Ductility Demand for kratio=0.9
μ
yratio

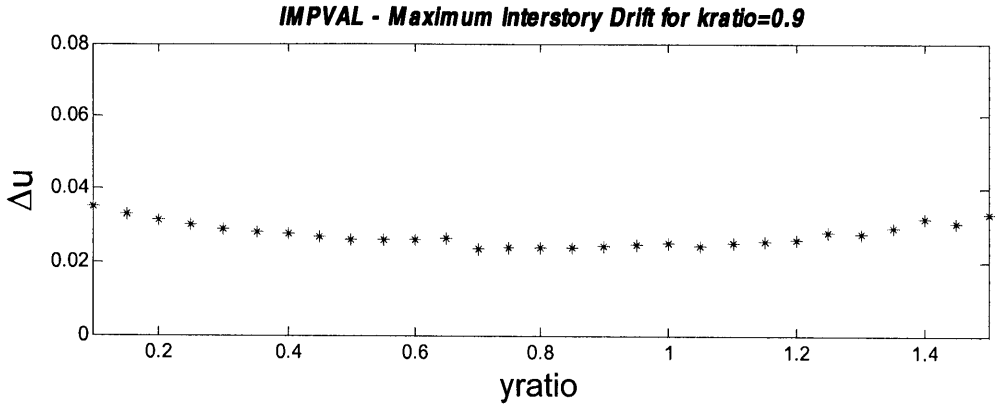
IMPVAL - Maximum Interstory Drift for kratio=0.9
Δu
yratio

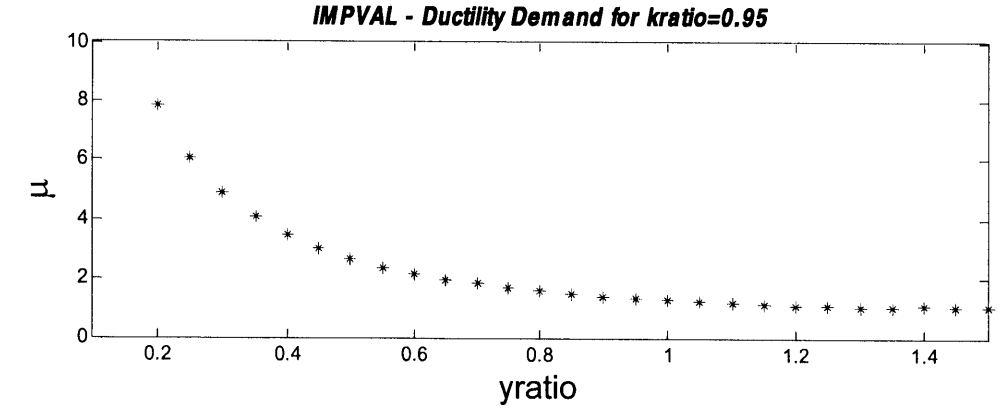
IMPVAL - Ductility Demand for kratio=0.95
μ
yratio

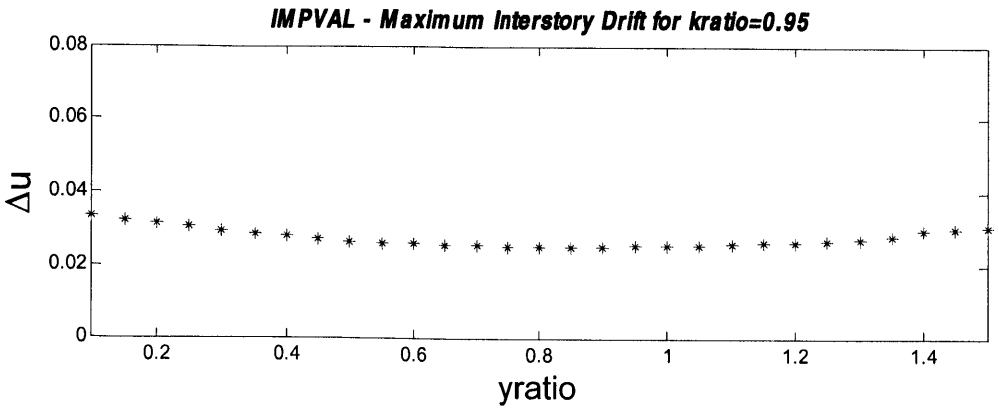
IMPVAL - Maximum Interstory Drift for kratio=0.95
Δu
yratio

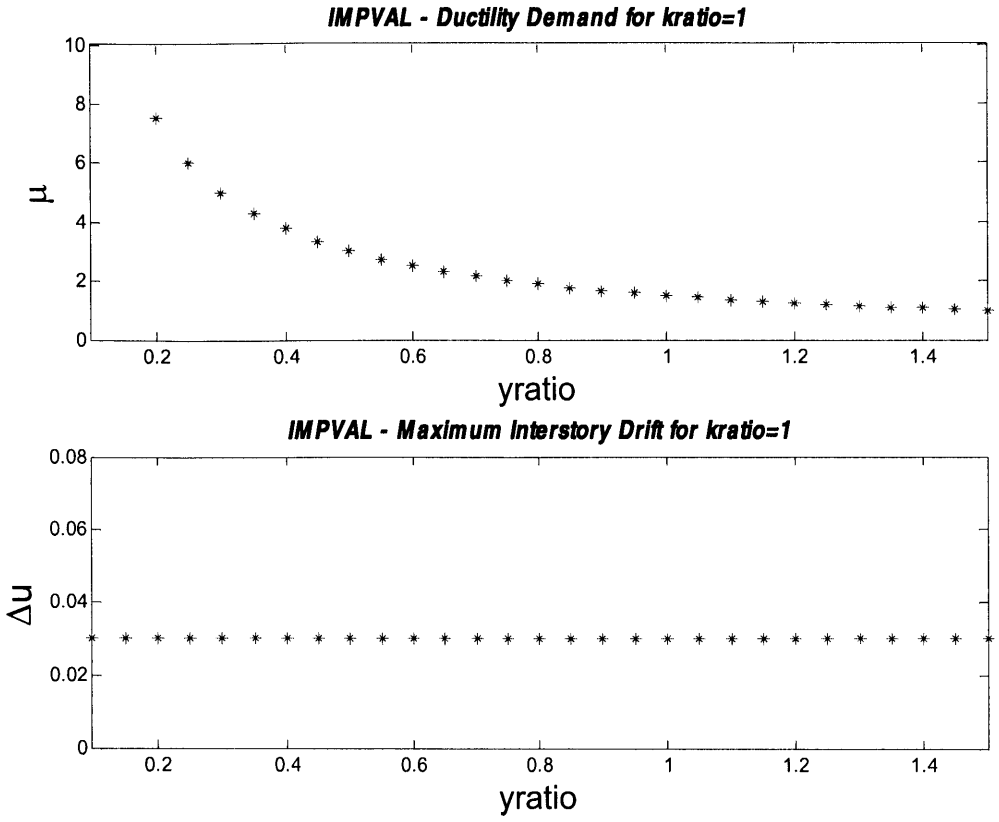
IMPVAL - Ductility Demand for kratio=1
μ
yratio
IMPVAL - Maximum Interstory Drift for kratio=1
Δu
yratio